Fraunhofer IGB

University of Stuttgart
Institute of Interfacial Process Engineering and Plasma Technology

Investigations and Technical Development of Adsorption Thermal Energy Storage Systems with Simulation and Different Control Strategies

Von der Fakultät Energie-, Verfahrens- und Biotechnik
der Universität Stuttgart
zur Erlangung der Würde eines Doktors der Ingenieurwissenschaften
(Dr. -Ing.) genehmigte Abhandlung

vorgelegt von

Mazen Abou Elfadil

aus

Sweida, Syrien

Hauptberichter: Prof. Dr. Thomas Hirth

Mitberichter: Prof. Dr. Alexander Sauer

Tag der mündlichen Prüfung: 07.07.2022

Institut für Grenzflächenverfahrenstechnik und Plasmatechnologie
der Universität Stuttgart

2021

Eidesstattliche Erklärung

Ich erkläre hiermit an Eides statt, dass ich die vorliegende Dissertation selbständig verfasst und nur die angegebenen Literaturquellen und Literaturverzeichnis verwendet habe.

Stuttgart, den 30.11.2021

Mazen Abou Elfadil

Unterschrift: .....

Declaration of authorship

I hereby declare that I have written this dissertation independently, using only the specified sources of literature and bibliography, which was properly and fully acknowledged.

Stuttgart, on 30.11.2021

Mazen Abou Elfadil

Signature: .....

Acknowledgements

I would like to thank everyone who supported me during the progress of this work in order to make it possible.

I would like to express my gratitude to Prof. Dr. Thomas Hirth for agreeing to be the doctoral supervisor for this work and giving me the opportunity to develop my PhD project in a topic of such extent at the Fraunhofer Institute for Interfacial Engineering and Biotechnology (IGB).

Special thanks to Dipl.-Ing. Siegfried Egner, Dr. Simone Mack and Dr.-Ing Antoine Dalibard for their continuous support, orientations and valuable suggestions, which provided me with great help and increased my knowledge.

Last but not least I would like to express my special thanks and love to my wife Nur, my parents (Kamal and Safaa) and my sister Catherine. Their love and support made a very important contribution to the preparation of this work.

Abstract

Thermal energy storage (TES) has been receiving an increasing worldwide attention, especially with the growing concerns about environmental problems caused by an inefficient utilization of energy. A major part of the energy consumption is considered as low temperature thermal energy. Thus, a better management of this energy by using thermal energy storage could provide a significant contribution to improve the overall efficiency of energy utilization in industrial processes and economies.

The thermal energy can be stored in different forms e.g. sensible heat, latent heat or thermo-chemical, allowing variety of choices depending on the application. While the sensible and latent heat storage technologies are standard products, the thermo-chemical energy storage is still under development. Based on the method used, thermo-chemical energy storage can be divided into absorptive and adsorptive thermal energy storage systems. The adsorptive thermal energy storage systems have a great potential in both daily (short term) and seasonal (long term) applications. However, their implementation is still limited due to their low degree of applicability caused by lack of scientific knowledge on the thermal analysis level, as well as the absence of knowledge on the level of system integration, which has prevented the heat storage systems from reaching their maximum potential and from being fully commercialized. Consequently, there is still a big necessity for research and development in this field [Salvatore Vasta, 2018].

The principle of the adsorption storage system is based on a gaseous working fluid (e.g. water resp. vapor) which gets adsorbed by a highly porous material (e.g. zeolite). This adsorption process is an exothermal one, thus heat is being released and can be transferred and used. In order to recharge the heat storage system, desorption of the working fluid is done by heating the porous material. The heat storage system consists mainly of a reactor (where the porous material is located), a condenser/evaporator and other auxiliary components (e.g. water tank, pumps, sensors…).

Efforts of development of the adsorptive TES were concentrated mainly on developing the adsorptive material, as the performance of the storage material has been the priority so far [Salvatore Vasta, 2018]. Little focus was put on heat power analysis and temperature behavior in the different system components, which have an impact on the overall system efficiency. Thus, system approach is still needed in order to combine and integrate this technology into industrial applications and products [Hauer, Andreas 2020] [Michelangelo Di Palo 2020].

With the aim of improving the heat storage efficiency (recovered heat to stored heat ratio), both numerical (simulations) and experimental (technical modifications) approaches were applied, which have enabled the system to achieve an optimal operational status in terms of energy utilization and efficiency. These approaches were later on used to define a fully automated control system assisting the adsorption TES to instantly react with the continuously varying parameters in such a way to assure an optimal performance.

Hence, in the first stage of this investigation, process-modeling and simulation of the whole heat storage system were carried out, so that the total performance of the heat storage system

can be predicted and evaluated for any future applications, including the possibility of combining different reactors or heat storage units. In the second stage, different experiments and technical modifications of the system were conducted. This includes testing various possibilities of TES setups (e.g. storage cascades), where the different pressure and temperature behavior in the reactor were evaluated. With the help of experiments, a detailed numerical 3D-model of the packed bed was created, giving an insight into the heat and mass transfer in the reactor during both adsorption and desorption. As a result, a new heat exchanger design was developed, which has improved the temperature distribution and the heating/cooling power. Additionally, the simulation's results suggested the separation between the evaporator and the condenser to achieve an enhanced water vapor transfer between the reactor and condenser.

On a parallel stage of this investigation, comprehensive heat power analysis during both adsorption and desorption processes was carried out, which has showed that the sensible heat left in the reactor, contributes to ca. 50% of the total stored heat. Consequently, multiple reactor concept was introduced, in order to enable the sensible heat recovery.

As a conclusion, process simulation enabled tests with different parameters to be performed within much shorter time than the real experimental time. Thus, it was possible to cover numerous application-scenarios and help improving the system overall efficiency. The experimental results have shown that the developed heat exchanger design has increased the maximum power of the heat exchanger about 74%. Moreover, by improving the fluid dynamics between the reactor and condenser, the efficiency of desorption η_d and overall efficiency η_o were increased by 32% and 9% respectively. Furthermore, about 36% of the sensible heat left in the reactor after desorption was recovered by using multiple reactors with sequential configuration, which has led to a reduction in the total invested heat by ca. 9%.

For future work it's recommended to investigate the possibility of controlling the amount of discharged heat from the system by regulating the water uptake during adsorption. In addition, trying a different approach to the reactor's design (e.g. moving bed reactor) could bring significant improvements to the system.

Kurzfassung

Die **T**hermische **E**nergie-**S**peicherung (TES) erfährt weltweit zunehmende Aufmerksamkeit, insbesondere angesichts der wachsenden Besorgnis über Umweltprobleme, die auch durch eine ineffiziente Energienutzung verursacht werden. Ein großer Teil des thermischen Energiebedarfs wird als thermische Energie bei niedrigen Temperaturen benötigt. Ein besseres Management dieser Energie durch den Einsatz von thermischen Energiespeichern könnte daher einen wesentlichen Beitrag zur Verbesserung der Gesamteffizienz der Energienutzung in industriellen Prozessen leisten.

Die thermische Energie kann in verschiedenen Formen gespeichert werden, z.B. in Form von fühlbarer Wärme, latenter Wärme oder thermochemischer Energie, so dass je nach Anwendung eine Vielzahl von Speichermöglichkeiten zur Verfügung steht. Während die Technologien zur Speicherung von fühlbarer und latenter Wärme Standardtechnologien sind, befindet sich die thermochemische Energiespeicherung noch weitgehend im Entwicklungsstadium. Je nach der verwendeten Methode kann die thermochemische Energiespeicherung in absorptive oder adsorptive thermische Energiespeichersysteme unterteilt werden. Die adsorptiven thermischen Energiespeichersysteme haben ein großes Potenzial sowohl für kurzfristige (tägliche) als auch für langfristige (saisonale) Anwendungen. Ihre Umsetzung ist jedoch immer noch begrenzt, da ihre Anwendbarkeit aufgrund nicht ausreichender wissenschaftlicher Kenntnisse auf der Ebene der thermischen Analyse sowie der Systemintegration gering ist, was verhindert, dass die Wärmespeichersysteme ihr maximales Potenzial erreichen. Folglich besteht in diesem Bereich noch ein großer Bedarf an Forschung und Entwicklung [Salvatore Vasta, 2018], welcher mit dieser Arbeit adressiert wurde.

Das Prinzip des Adsorptionsspeichers basiert auf einem gasförmigen Arbeitsmittel (z.B. Wasserdampf), das an einem hochporösen Material (z.B. Zeolith) adsorbiert wird. Dieser Adsorptionsprozess ist ein exothermer Prozess, d.h. Wärme wird freigesetzt und kann übertragen und genutzt werden. Um das Wärmespeichersystem wieder aufzuladen, erfolgt die Desorption des Arbeitsmittels durch Erwärmung des porösen Materials. Das Wärmespeichersystem besteht im Wesentlichen aus einem Reaktor (in dem sich das poröse Material befindet), einem Kondensator/Verdampfer und anderen Hilfskomponenten wie Wassertank, Pumpen und Sensoren.

Die Untersuchungen zur adsorptiven TES konzentrierten sich hauptsächlich auf die Entwicklung des adsorptiven Materials, da die Leistung des Speichermaterials bisher im Vordergrund stand [Salvatore Vasta, 2018]. Wenig Aufmerksamkeit wurde bisher auf die Analyse der Wärmeleistung und des Temperaturverhaltens in den verschiedenen Systemkomponenten gelegt, die sich auf die Effizienz des Gesamtsystems auswirken. Daher ist nach wie vor ein Systemansatz erforderlich, um diese Technologie in industrielle Anwendungen und Produkte einsetzen zu können [Hauer, Andreas 2020] [Michelangelo Di Palo 2020].

Mit dem Ziel, die Effizienz der Wärmespeicherung (Verhältnis von zurückgewonnener zu gespeicherter Wärme) zu verbessern, wurden sowohl numerische (Simulationen) als auch

experimentelle (technische Modifikationen) Ansätze verwendet, welche die Optimierung des Betriebszustands in Bezug auf Energienutzung und Wirkungsgrad ermöglichten. Diese Ansätze wurden im weiteren Verlauf der Arbeit verwendet, um ein vollautomatisches Steuersystem aufzusetzen, das das adsorptive thermische Energiespeichersystem dabei unterstützt, unmittelbar auf die sich ständig ändernden Parameter zu reagieren, um eine optimale Leistung zu gewährleisten.

Daher wurde in der ersten Phase dieser Untersuchung eine Prozessmodellierung und Simulation des gesamten Wärmespeichersystems durchgeführt, so dass die Gesamtleistung des Wärmespeichersystems vorhergesagt und für künftige Anwendungen bewertet werden kann, einschließlich der Möglichkeit, verschiedene Reaktoren oder Wärmespeichereinheiten zu kombinieren.

In der zweiten Phase wurden Experimente und technische Modifikationen des Systems untersucht und bewertet. Dazu gehörte das Testen verschiedener Möglichkeiten von TES-Setups (z.B. Speicherkaskaden), bei denen das unterschiedliche Druck- und Temperaturverhalten im Reaktor bewertet wurde. Aufbauend auf den Experimenten wurde ein detailliertes numerisches 3D-Modell des Schüttbettes erstellt, das einen Einblick in den Wärme- und Stoffübergang im Reaktor sowohl während der Adsorption als auch der Desorption gibt. Infolgedessen wurde ein neues Wärmetauscher-Design entwickelt, mit einer besseren Temperaturverteilung und Heizleistung. Darüber hinaus empfehlen die Simulationsergebnisse eine Trennung zwischen Verdampfer und Kondensator, um eine verbesserte Wasserdampfübertragung zwischen Reaktor und Kondensator zu erreichen.

Parallel zu dieser Untersuchung wurde eine umfassende Wärmeleistungsanalyse sowohl während der Adsorptions- als auch der Desorptionsprozesse durchgeführt, die gezeigt hat, dass die im Reaktor verbleibende fühlbare Wärme ca. 50 % der gesamten gespeicherten Wärme ausmacht. Folglich wurde ein Mehrfachreaktorkonzept eingeführt, um die Rückgewinnung eines höheren Anteils der fühlbaren Wärme zu ermöglichen.

Zusammenfassend lässt sich sagen, dass die Prozesssimulation es ermöglichte, Parameterstudien im Vergleich zu realen Experimenten in viel kürzerer Zeit durchzuführen. Dadurch war es innerhalb des zur Verfügung stehenden Zeitraums möglich, zahlreiche Anwendungsszenarien abzudecken und die Gesamteffizienz des Systems zu verbessern. Die experimentellen Ergebnisse haben gezeigt, dass das entwickelte Wärmetauscher-Konzept die maximale Leistung des Wärmetauschers um 74% erhöht. Darüber hinaus konnten durch die Verbesserung der Fluiddynamik zwischen Reaktor und Kondensator der Wirkungsgrad der Desorption η_d und der Gesamtwirkungsgrad η_o um 32% bzw. 9% gesteigert werden. Außerdem wurden etwa 36% der gebliebenen fühlbaren Wärmemenge (ca. 9% der investierten Gesamtwärme) durch den Einsatz mehrerer Reaktoren mit sequenzieller Konfiguration zurückgewonnen.

Für zukünftige Arbeiten wird empfohlen, die mögliche Steuerung der abgeführten Wärmemenge durch Regulierung der Wasseraufnahme während der Adsorption zu untersuchen. Zusätzlich könnte die Erprobung eines anderen Reaktordesigns (z.B. eines Wanderbett-Reaktors) erhebliche Verbesserungen für das System bringen.

Table of Contents

List of Figures

List of Tables

List of Symbols

Letter	Unit	Meaning
A	m^2	Cross-sectional area
Ã	m^2	Total surface area inside the container
a_m	%	Melted fraction
c	$mol \cdot m^{-3}$	Concentration
C_p	$J \cdot g^{-1} \cdot K^{-1}$	Specific heat capacity
C_{lp}	$J \cdot g^{-1} \cdot K^{-1}$	Average specific heat capacities for the liquid
C_{sp}	$J \cdot g^{-1} \cdot K^{-1}$	Average specific heat capacities for the solid
D	$m^2 \cdot s^{-1}$	Diffusion coefficient
e		Emissivity of the matter
ESD	$Wh \cdot kg^{-1}$	Energy storage densiy
ε	%	Porosity
h	$W \cdot m^{-1} \cdot °C^{-1}$	Convection heat transfer coefficient
Δh_m	$J \cdot kg^{-1}$	Heat of fusion per unit mass
ΔH_{ad}	J	Adsorption heat
ΔH_b	J	Binding heat
ΔH_v	J	Vaporization heat
J	$mol \cdot m^{-2} \cdot s^{-1}$	Diffusion flux
k	%	Permeability
K		Kozeny coefficient
λ	$W \cdot m^{-1} \cdot K^{-1}$	Thermal conductivity coefficient
m	kg	Mass
μ	$kg \cdot m^{-1} \cdot s^{-1}$	Fluid dynamic viscosity
P	$N \cdot m^{-2}$ or bar	Pressure
P’	$N \cdot m^{-2}$	Pressure for real gas

Q	W	Heat power
q	$W \cdot m^{-2}$	Heat flux
$\dot{Q}$	$J \cdot s^{-1}=W$	Heat flow
ρ	$kg \cdot m^{-3}$	Fluid density
ρ_b	$kg \cdot m^{-3}$	Bulk density
ρ_s	$kg \cdot m^{-3}$	Solid density
σ	$W \cdot m^{-2} \cdot K^{-4}$	Stefan-Boltzmann constant
S_v	$m^2 \cdot m^{-3}$	Specific surface area per unit volume
T	°C or K	Temperature
T_{abs}	K	Absolute temperature
η_{ad}		Storage efficiency for adsorption
η_d		Storage efficiency for desorption
η_o		Overall storage efficiency
U_0	$m \cdot s^{-1}$	Fluid velocity
V	m^3	Volume of the fluid
$\dot{V}$	$m^3 \cdot s^{-1}$	Volume flow
ΔX	m	Thickness of the wall
Z		Real gas compressibility factor

1. Introduction

One of the most important issues facing mankind is responding to the increasing demand on energy, and at the same time providing the future generations with sufficient sustainable sources of energy. This can be achieved by depending more on renewable sources of energy, and maximizing the utilization of each source, which includes reducing the energy losses to the minimum level.

A major part of the energy consumption is considered as low temperature thermal energy. Thus, a better management of this energy by thermal energy storage could provide a significant contribution to improve the overall efficiency in industrial economies.

The concept of **T**hermal **E**nergy **S**torage TES is not new, it has been used for a long time. The energy storage works on reducing the disparity between the production and demand, this is done by storing the excess energy during the low demand and providing it back when the demand peaks. Thus, it improves the energy utilization. [O. ErcanAtaer, 2006]

Different technologies in the field of thermal energy storage exist or are being developed, as sensible heat, latent heat or thermo-chemical energy storage, where the thermal energy (heat or cold) can be stored in a relatively wide range of temperatures from -40 to 400 °C. [IEA-ETSAP and IRENA, 2012]. Based on the method used, thermo-chemical energy storage can be divided into absorptive and adsorptive thermal energy storage systems (see Figure 2.2).

While the sensible and latent heat storage technologies are standard products, the thermo-chemical energy storage is still in the early stages of development. Despite their great potential in both daily (short term) and seasonal (long term) applications, the adsorptive thermal energy storage systems are not yet fully commercialized. However, some particular applications using adsorption TES principle have been introduced to the market. This limitation can be related to multiple obstacles on different system levels. Therefore, it is necessary to deepen the scientific knowledge as well as the technical understanding to be able to make these technologies usable for mankind in the future.

The main challenge facing the adsorptive TES technology is the low storage efficiency (ratio of the recovered energy to the total invested energy), which is standing in the way of introducing adsorptive thermal energy storage systems to the market. Among several aspects, poor heat and mass transfer in the reactor represents a major factor, which reduces the theoretically achievable heat storage density and efficiency. Therefore, numerous investigations have been performed in the past focusing on improving the thermal conductivity of the adsorbent materials by the help of highly conductive materials. However, there is still a lack in the system approach of the adsorptive TES with the focus on the whole heat storage system and not just the adsorbent materials.

Objectives of the work

This work focuses on filling some of the current scientific and technical gaps in system approach of the adsorptive TES, by concentrating on the following points:

- Conducting experiments and CFD simulations, in order to give an insight into the heat and mass transfer in the reactor during both adsorption and desorption. Thus, increasing the heat storage efficiency and improving the heat and mass transfer by developing better designs/arrangements of the key components of the storage system (e.g. Reactor, heat exchanger, condenser…)
- Analyzing thermal energy during both adsorption and desorption processes, for better understanding of the distribution of the heat shares and identifying the potential aspects of optimization.
- Creating a validated numerical 0D-model of the whole heat storage system, with the possibility to adjust all the operation parameters and predict the optimal system settings.
- Exploring different control strategies to increase the utilization of the stored heat.

In order to achieve this goal, the overall system was structured in 4 levels with regard to the components as shown in Figure 1.1. Depending on the system level different methods (numerical or experimental) were conducted.

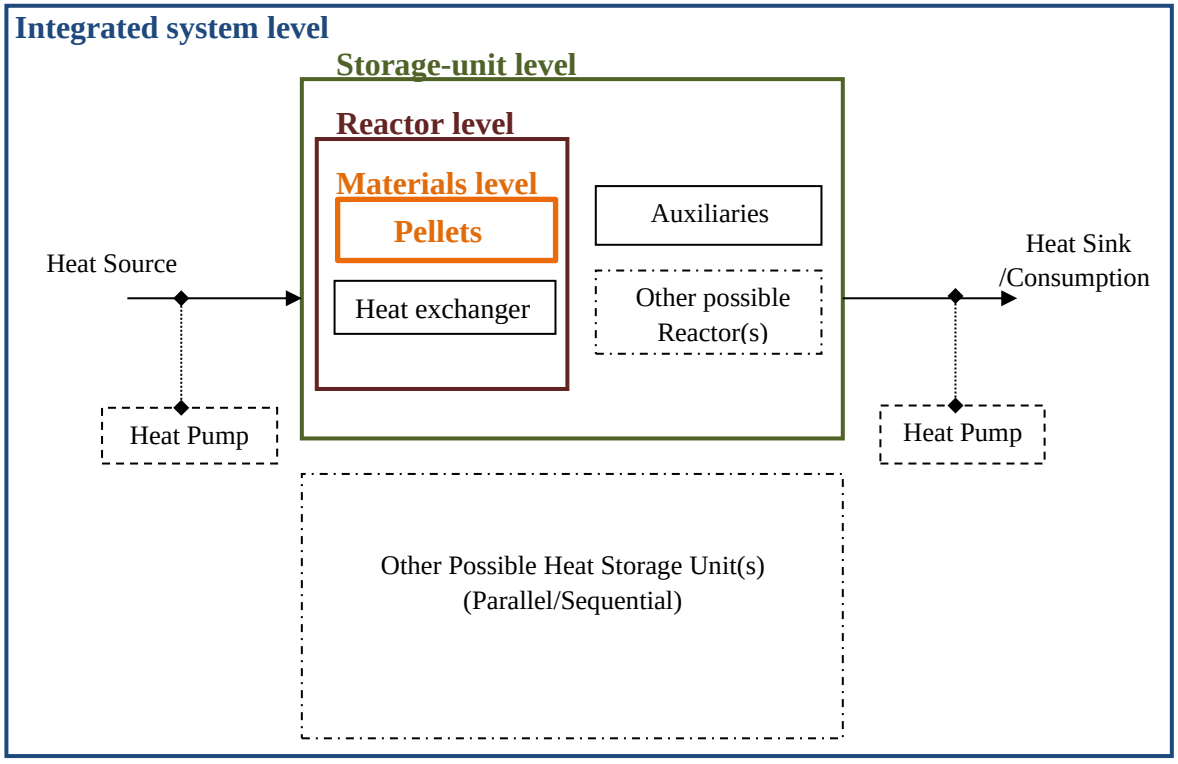

Figure 1.1 Overall adsorption TES system levels

These levels can be defined as the following:

- **Materials level**
  On this level, the materials used to store the heat are being investigated, in order to improve their storage heat capacity and thermal conductivity. Various types of materials

can be used in an adsorptive heat storage system. The most common working types of adsorbate / adsorbent pairs are: Ammonia, methanol and water as adsorbate, and activated carbon, silica-gel and zeolite as adsorbents. Investigations on this level were not the focus of this work.

- **Reactor level**
  The core of the heat storage is the reactor containing the storage material. On this level investigation regarding the optimization of e.g. heat and mass transfer as well as performance was done. Consequently, studying the influence of connecting reactors using different operational set-ups.

- **Storage-unit level**
  The heat storage unit represents the single storage system, which consists of the storage reactor containing the storage material (optional separated in multiple vessels), the evaporator/ condenser as well as various auxiliary components like vacuum pump, piping, instrumentation, etc. On this level control algorithms using simple sensors and controls were developed to improve the system and make it technically controllable for an optimal performance. The monitoring of the charging level and the status of the heat storage should be possible at any time.

- **Integrated system level - Overall heating and heat management system**

  This represents the real-life system application. Where on this level all connected units like heat sources, heat consumers, heat sinks as well as other optional units for heat storage (e.g. sensible storage) or heat pumps are included. The interfaces to the adsorption TES are needed to be defined and described. On this system level, simulation is used to investigate different system setups and find suitable configurations capable to increase the energy efficiency of the overall system. In this regard the parallel usage of heat pumps as well as the hybrid usage/storage of cold and heat was taken into account.

2. Theoretical Background

For a better understanding of the thermal energy storage systems, the state of the art and the theoretical background of the different types of heat storage are presented in this chapter. Furthermore, the heat and mass transfer in porous media is explained as it's essential for creating a numerical module of the system.

2.1. Thermal energy storage TES

Since the energy forms vary a lot (chemical, potential...) there are different technologies to store the energy (electrical, thermal...), however this thesis concentrates only on the thermal energy storage.
Thermal Energy Storage (TES) can be categorized in different ways depending on the criteria used in this classification. Taking the temperature level of the stored thermal energy as a criterion, the TES can be divided into "Heat Storage" and "Cold Storage", while if the looking perspective is the storage period then it can be divided into two different categories "Short Term Storage" and "Long Term Storage". Finally, by taking the type of the energy storing method as a criterion then the TES is being classified as "Sensible Heat Storage", "Latent Heat Storage" and "Thermo-chemical Heat Storage". Figure 2.1 shows the different categories by different criteria.

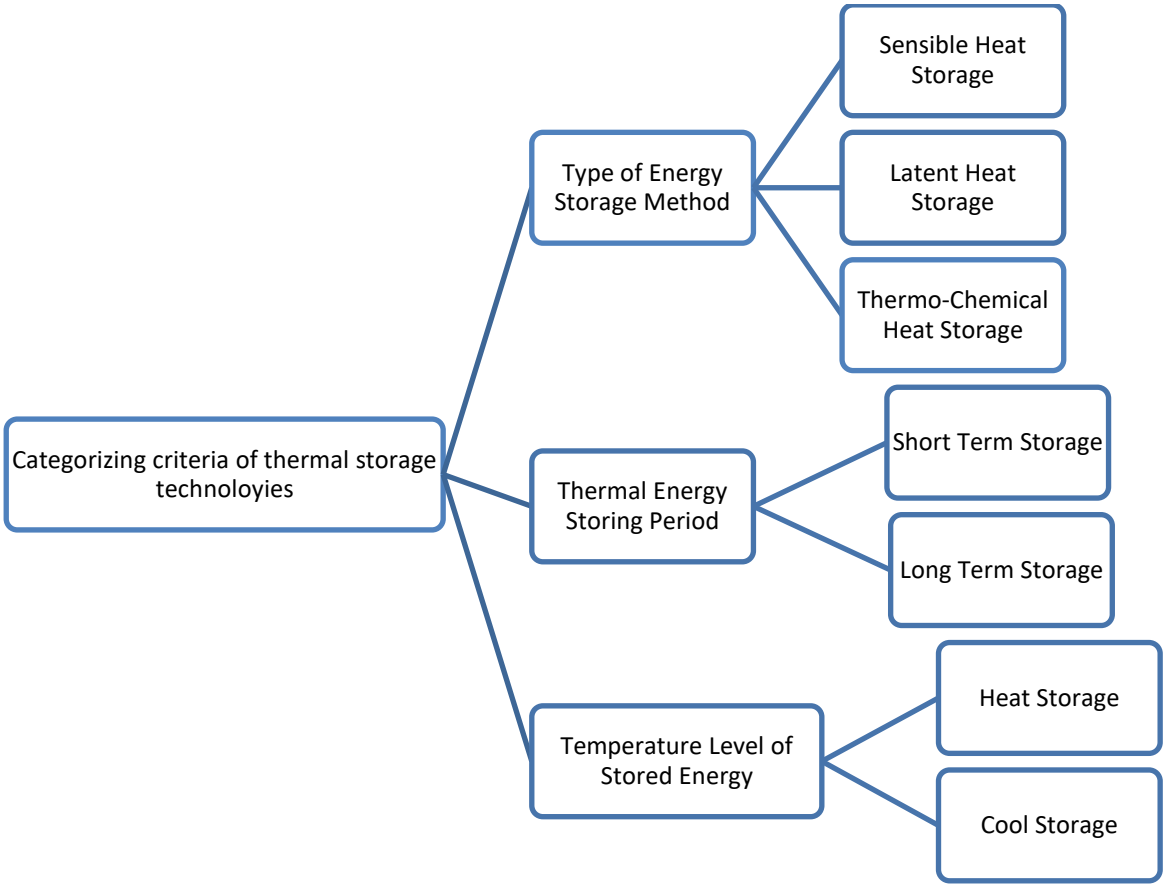

Figure 2.1 Categories of Thermal Energy Storage

The exact field which this thesis is concerned about is the thermo-chemical heat storage, which in its turn can be divided into “Sorption Storage” and “Chemical Storage”. From the sorption storage two basic technologies can be distinguished, adsorption and absorption storage. The process is called adsorption when the substance is accumulated at the surface of a solid or a liquid. Whereas, the process is called absorption when the substance is assimilated within the bulk of a solid or liquid. For this thesis the specific topic of investigation is the adsorption storage, as explained in Figure 2.2

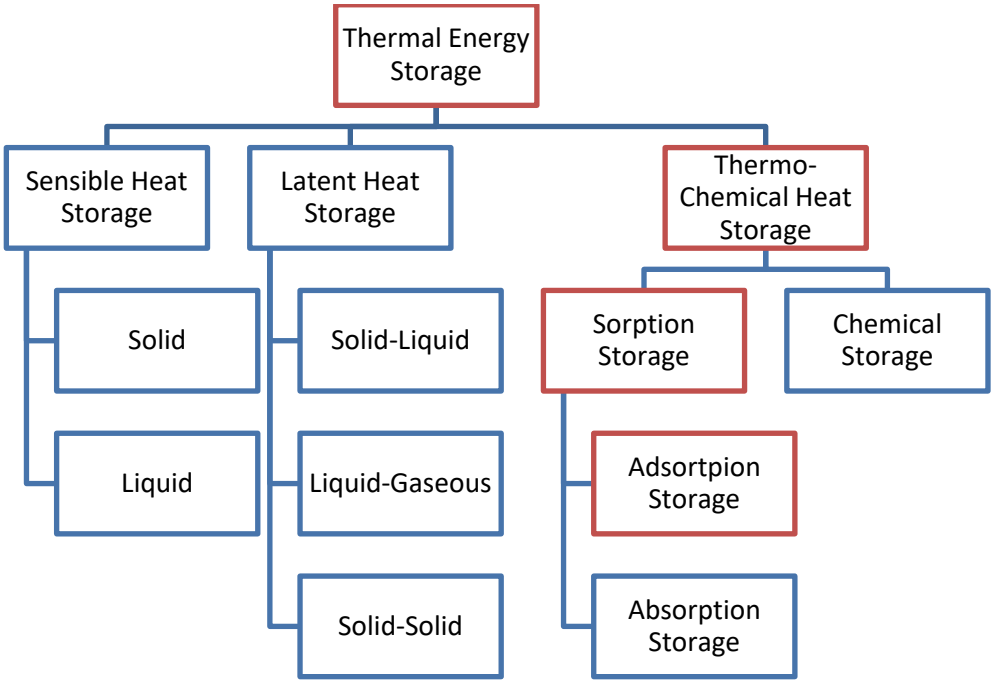

Figure 2.2 Categories of Thermal Energy Storage according to the type of the storage method

2.1.1. Sensible heat storage

The main principle of sensible heat storage method SHS is that the storing material undergoes temperature changes while it maintains the same physical state, where no phase changes should take place. Therefore, the temperature is being increased during the heat storage phase, and decreased again when the heat is being recovered.

The amount of stored heat is related to the temperature differences through the following formula.

$$Q = \int_{T_1}^{T_2} m\, C_p\, dT \qquad \text{Equation 2.1}$$

Where:

Q: the amount of heat in [J]

T_1 and T_2 are the initial and final temperature of the storing material in [K]

m: the mass of the storing material in [g]

C_p: specific heat capacity in [J/(g*K)], which is a function of the temperature

Considering that the temperature difference between T_1 and T_2 is small, the equation 2.1 can be written as:

$$Q = m\, C_{p,avg}(T_1 - T_2) = m\, c_{p,avg}\Delta T \qquad \text{Equation 2.2}$$

Where $C_{p,avg}$ is the average specific heat capacity in the range between T_1 and T_2.

As it was represented in Figure 2.2 the sensible heat storage medium could be solid, liquid or gaseous, nevertheless it is recommended that the medium used has all or some of the following properties:

- high value of the specific heat capacity
- low cost
- stabile under thermal cycling for a long term
- shows a good compatibility with its containment

The storage materials which are commonly used are cheap ones like rocks, water, sand, pebbles etc.

Disadvantages of this method can be the large volume needed to store the energy (low storage capacity) and the short-term heat storage due to the relatively big heat losses. Some of the sensible heat storage media however may have a relatively high capacity, but it is limited to a certain extent, especially if the temperature range is small.

2.1.2. Latent heat storage

A second possibility of thermal energy storage is latent heat storage LHS. This method can be used instead of the sensible one, where on the contrary of sensible heat storage, latent heat storage experiences a phase change during the heat storing or recovering process. In the case of heat storage, this phase change can in principle be from solid to liquid, from liquid to gas or from solid to solid (no physical phase change takes place but by changing the crystalline formation), while in the case of heat release, a reverse phase change will take place. (Practically liquid/gas phase changes are not relevant due to the very high storage volume required for the gas).
The amount of stored heat is related to both the temperature differences before and after the phase change, and the amount of heat need for the phase transformation. The following formula represents the heat storage capacity in case of solid-liquid transformation (most common case)

$$Q = \int_{T_i}^{T_m} m \cdot C_p \cdot dT + m \cdot a_m \cdot \Delta h_m + \int_{T_m}^{T_f} m \cdot C_p \cdot dT \qquad \text{Equation 2.3}$$

Where T_i, T_m and T_f are the initial, melting and final temperatures respectively, m is the mass of the heat storage material, C_p is the specific heat capacity, a_m is the fraction melted and Δh_m is the heat of fusion per mass unit (J/kg). [J. Carrasco Portaspana, 2011]

Considering the temperature differences between (T_i, T_m) and also (T_m, T_f) are small, an average specific heat capacity can be used, and the following formula can be concluded

$$Q = m\,[\,C_{sp}\,(T_m - T_i) + a_m \cdot \Delta h_m + C_{lp}\,(T_f - T_m)] \qquad \text{Equation 2.4}$$

Where C_{sp} and C_{lp} are the average specific heat capacities for the solid and liquid phases respectively.

As shown in equation 2.4, the stored heat can be divided into two types, sensible heat which is acting on rising the temperature from the initial to the melting temperature, and from the melting to the final temperature. The second type is the latent heat which is responsible for transforming the material from the solid to the liquid phase.

Since the heat of evaporation or fusion is much higher than the specific heat, the energy storage capacity per unit of volume for the latent storage materials can be much higher than the capacity for the sensible storage materials. High storage capacities compared to sensible storage systems are especially achieved if the temperature span between T_i and T_f are relatively small. In case of a wide range sensible heat storage systems may still have a higher capacity due to their usually larger specific heat storage capacity.

Hence smaller storage volume is often required for the latent heat storage compared to the sensible one, when storing the same amount of heat. Another advantage of the latent heat storage is that both of the heat storage and recovery take place at a constant temperature. Therefore, it is much easier to choose the storage material for each specific application. However, in the case of a system which has a fluctuating temperature level (e.g. solar heating system), then this advantage could have a negative effect on the heat storage process. A disadvantage of this method is the poor heat conduction of PCMs, especially in the solid state. This usually results in a low volume specific heat power.

The phase change materials which are used in the latent heat storage can be categorized as shown in Figure 2.3 into three groups: organic, inorganic and eutectic materials.

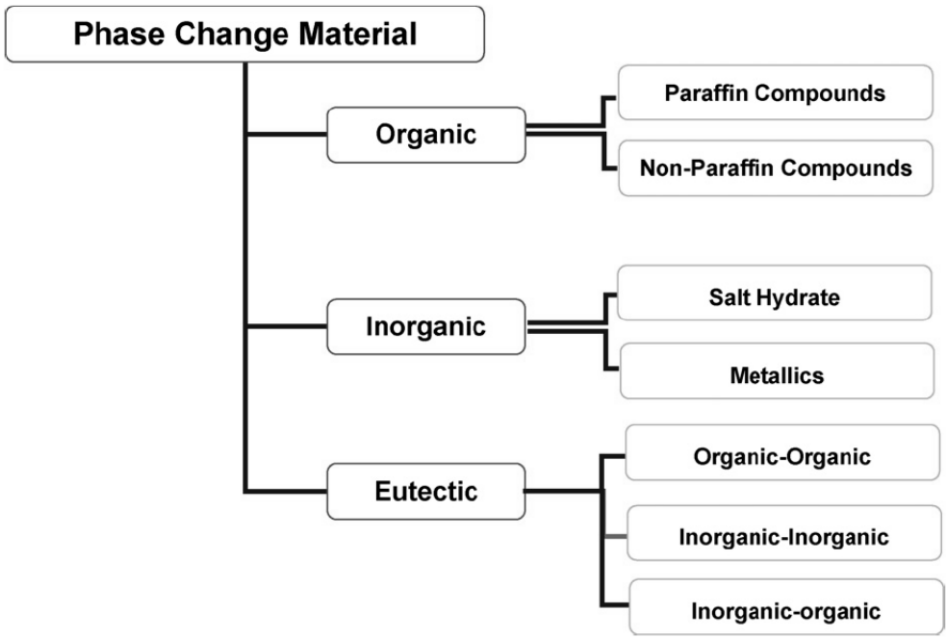

Figure 2.3 Classifications of PCMs [Atul Sharma, 2007]

In order to use the PCMs materials in the design of the heat storage systems, they should possess some specific thermophysical, kinetic and chemical properties as listed in Table 2-1 [Atul Sharma, 2007]

Table 2-1 Desired PCMs properties

Thermal Properties	▪ Suitable phase change temperature ▪ High melting enthalpy, in order to have the minimum possible storage volume ▪ Good thermal conductivity
Physical Properties	▪ High density, and thus less volume is needed ▪ Small volume change during the phase changing process ▪ Low vapor pressure
Chemical Properties	▪ Long term chemical stability ▪ Compatibility with its containment ▪ Nontoxic ▪ No fire risks
Kinetic Properties	▪ Sufficient crystallization rate ▪ No or limited supercooling which hinder the heat recovery
Economics	▪ Abundant ▪ Cost effective

2.1.3. Thermo-chemical heat storage

The main principle for the thermo-chemical heat storage is using reversible chemical reactions. The following equations represent the basic mechanism of this method [Cao Sunliang, 2010]

Endothermic reaction: $AB + \dot{Q} \rightarrow A + B$

Exothermic reaction: $A + B \rightarrow AB + \dot{Q}$

The endothermic reaction is when the heat storage takes place, where a compound reactant AB uses the heat, in order to decompose into two resultants A and B. This certain amount of thermal energy is being absorbed under a relatively high temperature condition. In reverse the exothermic reaction is responsible for the heat recovery, where A and B react with each other forming again the compound AB, and on the same time releasing a certain amount of thermal energy.

In order to assure that these two reactions will not occur simultaneously, a separation between the resultants A and B is needed. In case of A and B have different phase forms (e.g. gas and solid), the separation process will be easier, and thus the application of such materials is more advisable.

As long as these two reactants are separated, then in theory there should be no heat losses. This feature makes the thermo-chemical method attractive for a medium to long-term heat storage. Since the heat is not stored as a sensible heat, heat losses do not occur and therefore the storage efficiency can be very high. In addition, no or just few thermal insulations are required, which is another plus for the cost efficiency.
Another advantage for this method is that the enthalpy of the reaction is significantly larger than the specific heat (in SHS) or the heat of fusion (in LHS). This means that the heat storage density can be much higher than in the other two methods.
There are different chemical compounds and material pairs which can be used in the thermo-chemical heat storage method. However, in order to achieve desirable performance, these compounds should possess some properties. [J. Carrasco Portaspana, 2011]

- **Reversibility:** The reaction must go to completion; no side reactions or changes in reaction rate with time should occur.
- **Reaction rates:** Both forward and reverse reactions must be rapid enough to absorb all the available energy or release it promptly. The reaction rates must not decrease with cycling. Such a decrease can be observed, if structural changes of the storage medium occur (e.g., crushing of particles into powder).
- **Controllability:** The reactions must be controllable because they have to be turned on and off when required. Controllability is achieved by product separation, by controlling the temperature and pressure, or by catalysts.
- **Ease of storage:** The reaction products have to be easily separable prior to storage. Reactions must not occur at ambient temperature.
- **Safety:** Toxicity, inflammability, and corrosiveness of the reaction products may pose unacceptable safety hazards.
- **Cost:** Their cost should be low; this requires materials which are readily available.

Adsorption heat storage

In this heat storage method, a material in the gas or liquid phase is attached to another material's surface (solid or liquid). This mechanism is called "adsorption", where the molecules which are bond to the surface are called adsorbate, and the material holding these molecules is known as adsorbent. The adsorption process has a reverse process called desorption, where the adsorbed molecules are being released back from the surface into their original fluid phase.
Depending on the type of the acting forces, the adsorption can be divided into two types chemical or physical. In the chemical adsorption, the adsorbate molecules form bonds with the surface atoms of the adsorbent, by sharing electrons. This type of adsorption can also be referred to as "chemisorption". Due to the type of the bonds in the chemisorption, very high temperatures are needed in order to make the adsorbate be desorbed. This has limited the applications of the chemisorption.
The other type of adsorption is known as physical adsorption or "physisorption". In this type the adsorbate molecules are attached to the adsorbent surface by electrostatic and van der Waals forces, where no electrons sharing takes place.
When the adsorbate is being adsorbed, an adsorption heat will be released, this heat equals to the adsorbate-adsorbent binding energy. However, in the case of gaseous adsorbate phase, then

the adsorption heat will be equal to the sum of the binding energy and the condensation one [schawe, 2001]

$$\Delta h_{ad} = \Delta h_{condensation} + \Delta h_{binding} \qquad \text{Equation 2.5}$$

This sum is represented by the total area under the differential heat of adsorption curve as shown in Figure 2.4

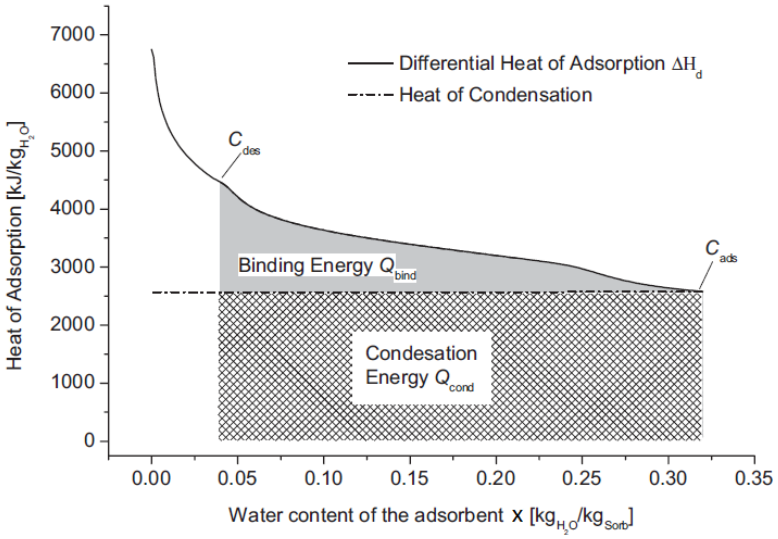

Figure 2.4 Binding and condensation enthalpy for adsorption of water on yeolite NaX [Hauer, 2002]

The materials which are used as adsorbents should provide large surface area in order to increase the adsorption capacity. On the other hand, it is always preferable to have small volumes (for better heat storage density). Therefore, to have this high surface/volume ratio, the material should have pores. Table 2-2 represents the classification of pores by the International Union of Pure and Applied Chemistry (IUPAC).

Table 2-2 IUPAC classification of pore sizes [Douglas Levan, Carta et al. 2008]

Type	**Pore Width [nm]**	**Characteristic**	**Example**
Micropore	< 2	Superimposed adsorption potential	Zeolites, silica gels, activated carbon
Mesopore	2 – 50	Capillary Condensation	Silica gels, M41S-materials, carbon nano tubes
Macropore	> 50	Effectively flat walled up to saturation pressure of the gas phase	Porous glasses, activated carbon

The adsorbents used in heat storage unit of this investigation are pellets and granular zeolite. The zeolites are crystalline hydrated aluminosilicates which have pore diameter range of 0.3 to 2 nm. They are naturally occurring minerals; however, the artificially produced zeolites can be reliable for heat storage, due to their defined pore diameter unlike the natural ones, in addition

to their ability of hydrate and dehydrate without changing their original structure. However, the zeolite can also be manufactured to suit the different industrial applications such as catalyst, ion exchanger, adsorbent and molecular sieve. Usually the zeolite powder is shaped by the help of binders, which include in general alumina, silica and natural clays [Storch, Reichenauer 2008].

Adsorption and desorption processes

Figure 2.5 shows the heat storage cycle for a closed adsorption system, which represents the case of the heat storage unit used in Fraunhofer IGB.

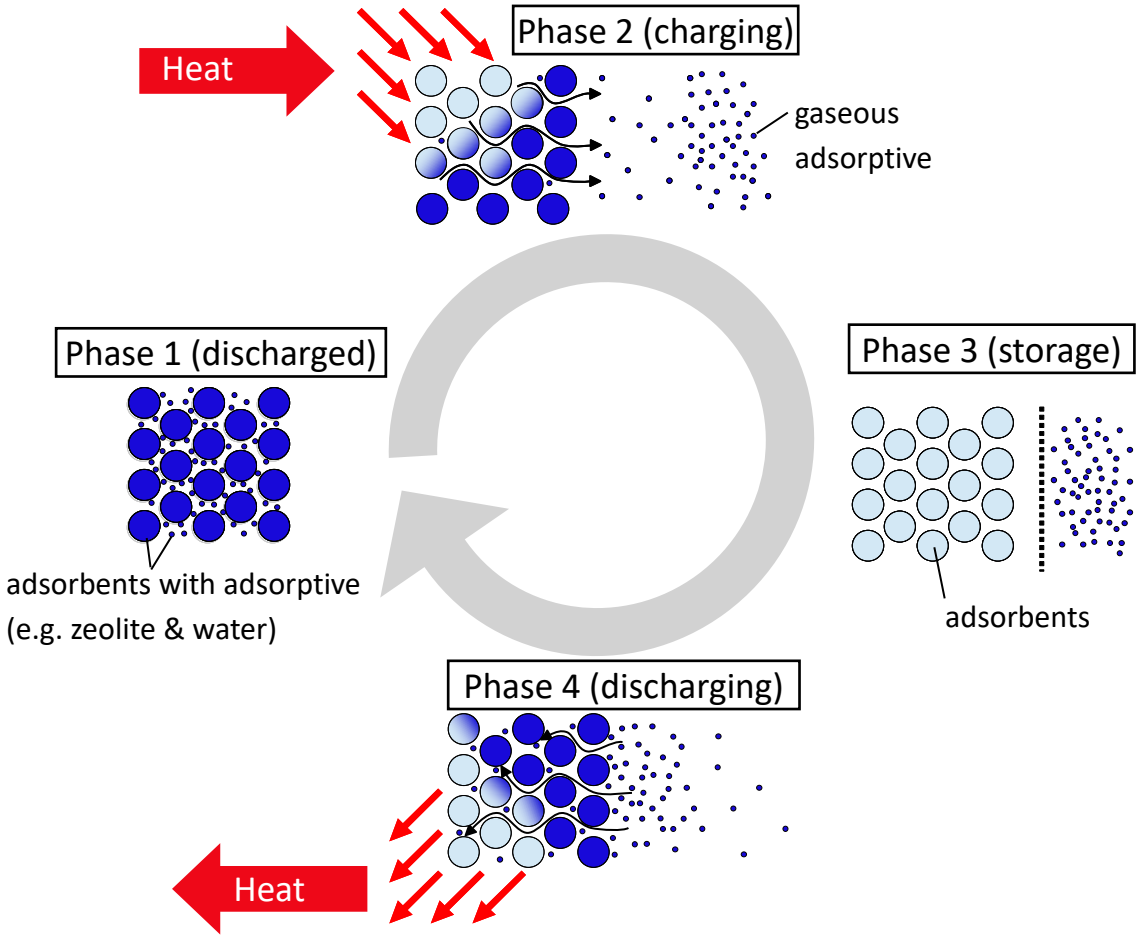

Figure 2.5 Adsorptive heat storage cycle [Source: S.Biehler (Fraunhofer IGB)]

The cycle can be divided into 4 phases:

Phase 1 (Discharged): the system is in a discharged state, where the adsorbent is fully loaded with the adsorbate. In this investigation case, the zeolite will have a maximum loading of water.
Phase 2 (Charging): heat is being given to the adsorbent packed bed, causing the adsorbate (e.g. water) to be desorbed from the pores.
Phase 3 (Storage): in this phase, the adsorbent has a minimum loading of the adsorbate, and as long as they are kept separated, then the heat should stay in theory stored.
Phase 4 (Discharging): the adsorbate is being introduced to the adsorbent packed bed, where it binds with the adsorbent's surface, causing the adsorption heat to be released.

2.2. State of the art

Adsorption thermal energy storage technology has a great potential in both daily (short term) and seasonal (long term) applications. However, the commercial applications are still limited due to the relatively higher costs and the absence of sufficient technical knowledge on the system level. In order to fill this gap between theory and technical application more research and system development are required.

The current state of research and know-how in this area can be divided into three levels: Materials, components and systems.

2.2.1. Adsorbent materials

The most common working pairs (adsorbate / adsorbent) are: Ammonia, methanol and water as adsorbate, and activated carbon, silica-gel and zeolite as adsorbents. Table 2-3 shows the adsorption parameters for some pair's combinations, in comparison to a sensible heat storage using water.

Table 2-3 Adsorption parameters for some adsorbent/adsorbate pairs [Wang, 2014]

Adsorption pair	Maximum theoretical stored heat [MJ/kg]	Maximum theoretical heat storage capacity [kWh/kg]	Min. T_{Des} [C°]	Max. T_{Des} [C°]	Advantages	Disadvantages	Heat storage capacity to water	Storage volume for 100 kWh [m3]	materials density [kg/l]	water uptake %
Silica gel / Water	2.5	0.694	>50	120	Low T_{Des}	Only for T>0	8.50	0.51	0.7	40
Synthetic zeolite / Water	4.2	1.167	120	>200	Adsorption Heat	Only for T>0	14.29	0.43	0.66	30
Natural zeolite / Water	3.3	0.917	120	>200	Adsorption Heat	Only for T>0	11.22	0.55	0.66	30
Activated carbon / Methanol	1.8	0.500	80-100	120	Low T_{Des}	Vacuum, T>150 → Methanol → Dimethyl	6.12	1.11	0.45	40
Activated carbon / Ammonia	0.942	0.262	>150	>200	High pressure ($T_{cond.}$ 40°C at 16 bars)	Odor, toxicity, incompatibility with copper	3.20	2.12	0.45	40
Activated carbon / Ethanol	0.944	0.262	90-100	150	Low T_{Des}	Low adsorption at high temperatures	3.21	2.12	0.45	40
Activated alumina / Water	3	0.833	160	>200	Adsorption Heat	Only for T>0	10.20	0.25	0.8	60
Water Δt=70°C	0.294	0.082	-	-	Low cost and simplicity	Only for T>0 and heat losses	1.00	1.22	1	-

The theoretical heat storage density of an adsorbent is directly dependent on the temperatures of adsorption (discharging) and desorption (charging). Figure 2.6 shows the theoretically calculated heat storage density at different charging/discharging temperatures for multiple materials compared to water heat storage system as a reference. As silica gel and zeolite use the adsorption TES technology, the sodium acetate trihydrate uses the latent heat storage method (with a melting temperature of 58°C). The heat storage capacities were calculated in Fraunhofer IGB using characteristic curves of adsorption provided by Zeosys GmbH.

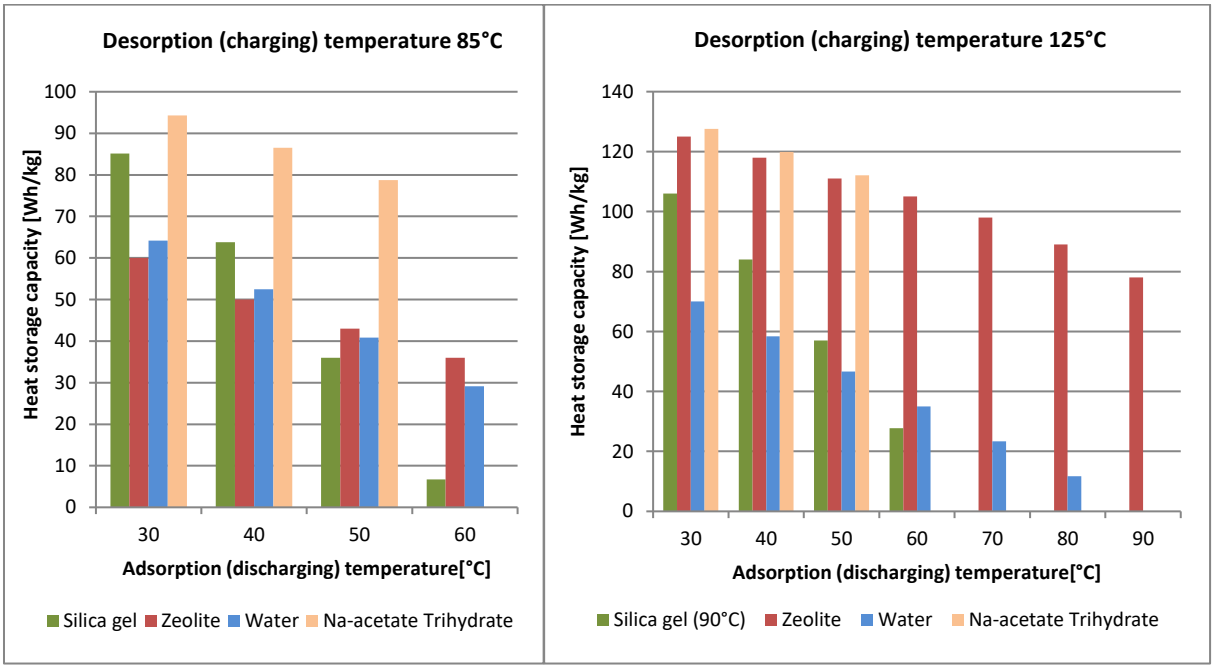

Figure 2.6 Theoretical heat storage capacity for different materials [source: M.Elfadil (Fraunhofer IGB)]

2.2.1.1. Silica gels

Silica gels have been one of the most used adsorbent materials for water vapor. Due to their low costs, they are widely used as a dehumidifier. In addition, they are considered a less expensive option for adsorption TES for applications with heat sources at temperatures lower than 100°C. In spite of their competitive cost and abundance, silica gels have low heat storage capacity, this has given water TES systems an advantage over them and left silica gels as a possible option for long-term heat storage only. It's worth mentioning, that the porous structure of silica gels differs between open adsorption TES and closed systems. Furthermore, the partial pressure for a closed adsorption/desorption process is limited to a range between 0.1 and 0.3 p/p_0. Therefore, the employed silica gels should have a highly microporous structures.

2.2.1.2. Zeolites

Zeolites (aluminosilicates) have a high specific surface to volume ratio (abou 800 m^2/g), this structure has made zeolites highly hydrophilic and perfectly suitable for adsorption of water vapor. Due to its high affinity for water, the bond between zeolite's surface and water is strong,

and thus, it requires a higher temperature to broken compared to silica gels (i.e. higher than 120°C). The common synthetic types of zeolites used in adsorption TES are: Type A, 13X, NaX, and Y.

Thanks to zeolite's structure, they can generate a higher hydrothermal stability compared to silica gels, which gives zeolites an advantage when several adsorption and desorption cycles are required. As a result of their high regeneration temperatures, they are more suitable for industrial waste heat recovery and storage [Yu, N.;Wang, 2013].

The binderless zeolite (Köstrolith NaMSX) material in the form of spheres (2.5mm-3.5mm) as shown in Figure 2.7 and water are used as an adsorbent-adsorptive pair during this work. Molecular sieve NaMSX is a synthetic crystalline aluminosilicate with a regular micro-pore structure.

Figure 2.7 Köstrolith NaMSX spheres [Source: Fraunhofer IGB]

The chemical formula of NaMSX zeolite is

$$Na_2O \cdot Al_2O_3 \cdot mSiO_2 \cdot nH_2O$$

Where, m ≤ 2.35 and n is the number of water molecules adsorbed.

All the relevant physical properties of NaMSX are listed in Table 2-4.

Table 2-4 Physical properties of Köstrolith NAMSX [ZeoSys GmbH]

Property	***Value***
Beads size Range [nominal, mm]	2.5-3.5
Pore size [nm]	0.9
Specific heat capacity [kJ/kg K]	0.88
Thermal conductivity [packed bed ,W/m K]	0.07
Bulk Density [compacted, g/l]	655-700
Attrition [%wt]	max. 0.2
Crush Strength	min.25

2.2.1.3. Activated carbons

Activated carbons are obtained from various precursors (e.g. wood, coal, coconut shells…). They possess a high specific surface volume ratio (ca. 1200 m^2/g) and represent potential to be used for adsorption TES as adsorbents of alcohols or ammonia. Nonetheless, there are still no examples in the literature of TES applications using these materials.

2.2.2. Storage-unit level

So far, all the development of closed adsorption TES units was generally concentrated on the reactor (materials and heat exchanger) [Salvatore Vasta, 2018]. Due to the low thermal conductivity of adsorbent materials, it's not possible to fully achieve the theoretical specific storage density. Hence, research activities have been focusing on improving the heat and mass transfer inside the reactor, mainly by exploring new heat exchanger designs or by adding to the adsorbent packed bed other materials with high thermal conductivity (e.g. copper wires, metal coating for the granulates) [Demir, H. 2008].

Other investigations aimed to improve the thermal conductivity by using the in-situ crystallization technique, which allows adsorbents (e.g. zeolites or zeo-like materials) to be synthesized over the metallic substrate of the heat exchanger directly [Bauer J. 2009].

2.2.3. System level

As mentioned before, the current state of research has not covered yet the development of adsorption TES on system level, leaving a great potential for optimizations on this level.

Hence, intensive investigations are required to overcome the barriers, which are preventing the adsorption TES technology to be present in the market as a dedicated heat storage system.

In spite of some commercially introduced applications, which are using the adsorption TES principle (e.g. a dishwasher from Bosch, a "self-cooling" beer barrel…). The main purpose of these applications was not to store the heat, but rather to utilize the adsorption TES as a secondary function or to improve the efficiency of these products.

2.3. Heat and mass transfer

Due to the important influence of the heat and mass transfer on a thermal energy storage system, a theoretical background about these two phenomena is included in this section.

2.3.1. Mass transfer through porous media

The flow resistance of a fluid through porous media is dependent on the number of particles which exist, or the volume concentration, however the bed porosity terms are usually used. On the extreme of which the bed is full of solids (zero porosity) the resistance in this case will be infinite. While on the other hand if the bed does not contain any solids and the porosity is 100%, then the superficial and interstitial velocities will be the same. Figure 2.8 gives an illustration of the fluid flow through a porous medium with consideration to the existing volume fraction.

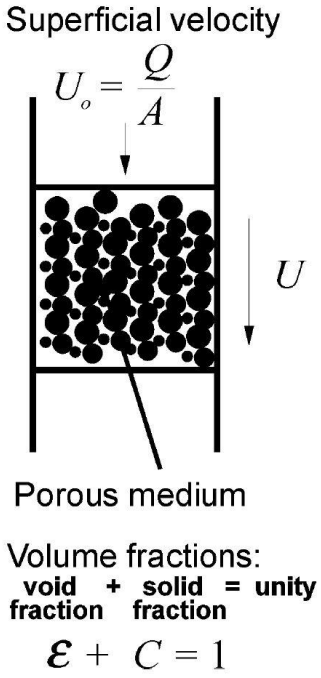

Figure 2.8 Fluid flow through a porous medium [Richard G. Holdich, 2002]

This fluid flow resistance causes the pressure drop in the fluid Δp to increase. This pressure drop is related to the distance L, where the pressure-drop increases in the direction of the fluid velocity, and thus the pressure gradient should be (-Δp/L). Nonetheless, the term pressure difference will be adopted and therefore no negative symbol will be used in the following.

Depending on the nature of the material's particles and the packing way of the materials in the packed bed, the porosity will change accordingly. For example, the porosity can range from about 45% for an uncompressed glass beads, to a value of 90% or higher for biological material such as yeast cells. [Richard G. Holdich, 2002]

The porosity can be calculated from the following formula

$$\rho_b = (1-\varepsilon)\rho_s + \varepsilon\,\rho \qquad \text{Equation 2.6}$$

Where ρ_b, ρ_s and ρ are the bulk, solid and fluid densities respectively in [kg/m^3], and since the fluid is gas, then its density can be neglected in comparison to the bulk density, and thus:

$$\varepsilon = 1 - \frac{\rho_b}{\rho_s} \qquad \text{Equation 2.7}$$

In the case of this investigation, the gas flow through the packed bed is assumed to be laminar flow, since just natural convection is the driving force. In fluid flow, high fluid viscosity (μ) and low bed permeability provide high flow resistance. The following formula represents Darcy's law which describes the relation between the pressure drop and the other flow parameters.

$$\frac{\Delta p}{L} = \frac{\mu}{k}\frac{dV}{dt}\frac{1}{A} \qquad \text{Equation 2.8}$$

Where k is the permeability and V is the volume of the fluid flowing in time t.

The permeability can be calculated from the following equation [Richard G. Holdich, 2002]:

$$k = \frac{\varepsilon^3}{K(1-\varepsilon)^2 S_v^2} \qquad \text{Equation 2.9}$$

Where S_v is the specific surface area per unit volume [m^2/m^3], and K is the Kozeny constant which is often 5, however much experimental evidence suggests that K = f(ε)

In the case of fixed bed length, the pressure drop rises linearly in relation to the volume flow rate, or the fluid velocity which can be calculated by the following formula. [Richard G. Holdich, 2002]

$$U_0 = \frac{\dot{V}}{A} = \frac{dV}{dt}\frac{1}{A} \qquad \text{Equation 2.10}$$

Figure 2.9 represent Darcy's law graphically, where the permeability can be measured by using the gradient from the plot. In this case the particles in the packed bed are assumed to be uniformed and therefore the permeability is constant as well.

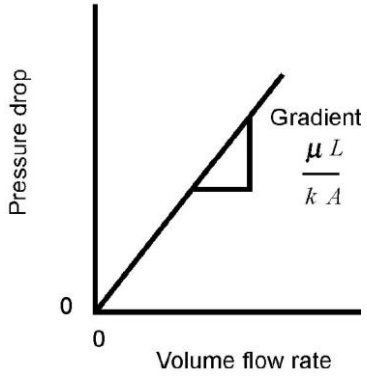

Figure 2.9 Graphical representation of Darcy's law for bed with a fixed overall length

Vapor pressure drop due to surface adsorption

Gas pressure in a container with a volume V is calculated by applying the real gas law

$$P' = ZRT \cdot \frac{n}{V}$$ Equation 2.11

Where Z is a factor for real gas compressibility which expresses the deviation from the behavior of an ideal gas when compressed, this factor is a variable dependent on the gas and the pressure.

The previous formula however neglects the interaction between the gas molecules and the solid molecules. Still this interaction can be included in the formula in order to calculate the exact pressure, as the following [Chih-Hang Hsieh, 1980]

$$P = ZRTd_1 = P' - \frac{\tilde{A}.\delta_s}{V}(d_2 - d_1) \cdot ZRT$$ Equation 2.12

Where:

P is the pressure in the container in [Pa]

P' is the pressure calculated by applying real gas law

$\tilde{A}$ is the total surface area inside the container in [m^2]

δ_s is the range of surface forces in [m]

d_1 [mol/m^3] is the density of gas molecules not affected by surface forces

d_2 [mol/m^3] is the average density of gas molecules which are affected by surface forces

Equation 2.12 shows that the exact pressure P is smaller than the one from the real gas law P'. However, in most cases this difference between P and P' can be neglected in comparison to the value of P. This is due to the relatively very small value of δ_s (in angstrom) when it is compared to the value of $V/\tilde{A}$ (in centimeters).

Nevertheless, in the case of porous media, where the surface area is large and the volume of the pore is small, then the difference between P and P' cannot be neglected anymore, since the term $\frac{\tilde{A}.\delta_s}{V}$ is relatively big now. Hence the vapor pressure in porous medium is considerably lower than the one calculated by the real gas law [Chih-Hang Hsieh, 1980]. This is the case in adsorption heat storage systems, where this pressure difference is the driving force for the adsorption process.

From what has been mentioned before, it appears that the surface adsorption plays an important role in the vapor pressure drop through porous medium.

2.3.2. Mass transfer in small pores

The mass transfer has an influence on the sorption rate of porous sorbents; hence a theoretical background of mass transfer is presented.

In the case of pure water vapor, the mass transfer in a zeolite crystal can be divided into three phases.

- At the beginning the vapor is transported to the zeolite layer or particles e.g. by a flow through the bulk (chapter 2.2.1).
- Then it passes through the intercrystalline macropores and the system of micropores.
- Finally, it reaches the sodalite cages, where the adsorption takes place.

For example, in the sorption heat storage the driving force in the first part of mass transfer is the pressure difference between the adsorber and the evaporator, while in the other two parts the structure of the zeolite layer has the influence on this mass transfer. [R. Lang, 1995]

Thermal motion and subsequent collision of the molecules cause diffusion, this diffusion can be divided into two types: transport diffusion caused by concentration gradient, and self-diffusion which occurs in system at equilibrium. [Danny Schuring, 2002]

Fick's first law of diffusion describes the flux due to transport diffusion

$$\vec{J} = -D \cdot \nabla c \qquad \text{Equation 2.13}$$

Where D is the diffusion constant and c is the concentration.

In the case of self-diffusion, it is usually expressed with self-diffusion constant D_c. these coefficients for transport and self-diffusion are different, in spite of that these two types of diffusion occur generally by the same microscopic principle.

Diffusion in zeolite is not the same as ordinary diffusion, because the molecules have to move through channels of molecular dimensions, therefore the zeolite framework interact constantly with the diffusing molecules, and thus the molecular motion is strongly dependent on the exact size and shape of these channels instead of only the concentration and temperature. [Danny Schuring, 2002]

Intercrystalline diffusion

- **Diffusion from gas to micropores**
  As mentioned before the diffusion through the zeolite pores are significantly different from the one in the gas. Whereas the diffusion in gas is driven by the collision between the molecules due to their thermal motion, the diffusion in pores on the other hand is dependent on the pore size and can therefore be divided into different regimes as shown in Figure 2.10.

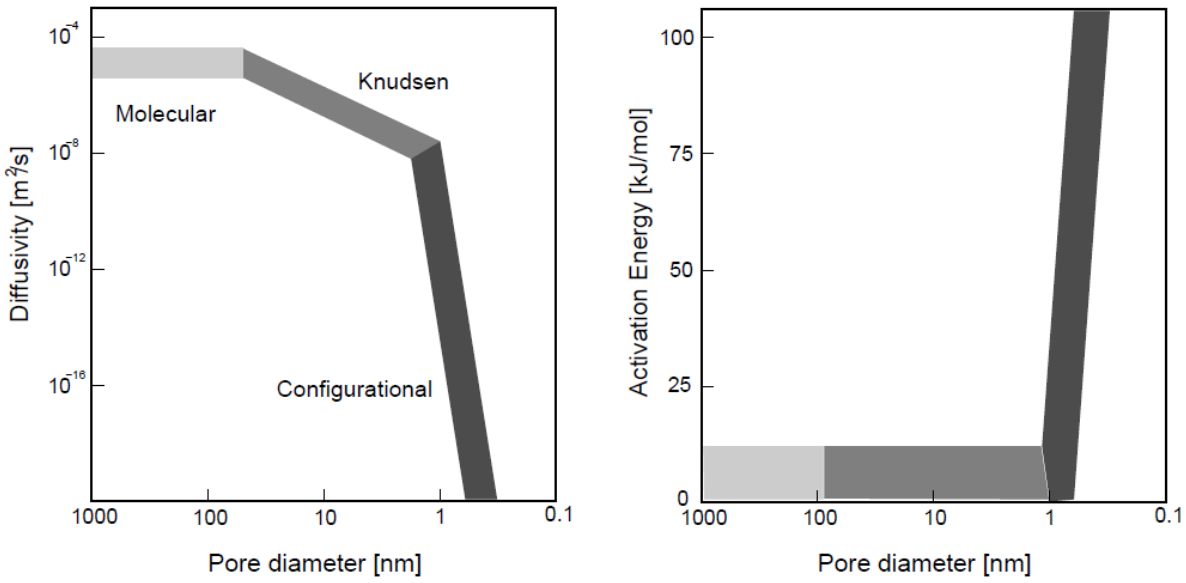

Figure 2.10 Pore size effect on the diffusivity and activation energy of diffusion [M.F.M. Post, 1991]

In case of large pore diameters (or macropores), the dominant mechanism will be the molecular diffusion, because the probability of the molecules to collide with each other is higher than the one of the collisions between the molecules and the pore walls. The smaller the pore diameter is the higher the number of collisions between the molecules and the wall gets. At the point when the pore diameter has a lower value of the mean free path of the gas molecules, then Knudsen diffusion takes place, which means the mobility of the molecules is depending on the size of the pore. Nevertheless, when the size of the pore is very small with the same range of the size of the molecules, then the interaction between the molecules and the wall will be continuous, and this is usually the case of the diffusion in the zeolite micropores, this regime is called configurational diffusion.

- **Diffusion in zeolite**
  Since the pore size of the zeolite is very small, it makes the molecules very close to the pore's wall. This causes the molecules to be more or less physically bonded to the wall. Hence the configurational regime can be in this case comparable to the surface diffusion. Many different parameters can influence the diffusivity in this regime, such as: pore diameter, interaction between the diffusing molecules and the surface atoms, the

structure of the pore wall, the shape of the diffusing molecules and the way the channels are connected. Therefore, it is very difficult to derive generalized equations in order to relate the mentioned properties to the diffusion coefficient.
The diffusivity of the molecules in the zeolite channels in comparison with the one in the gas phase is significantly reduced, and it is often observed to be strongly temperature dependent.

2.3.3. Heat transfer

There are many different mechanisms with which the heat can transfer, however the main mechanisms are considered to be conduction, convection and radiation. Other mechanisms which are related to one or combination of these mechanisms are condensation and boiling.
In comparison with the other different heat transfer mechanisms, the radiation mechanism is taken into consideration only at high temperatures (above 500-700 °C) [Dr. K. J. Bell, Dr. A. C. Mueller, 2001].
Therefore, it can be neglected in the temperature range of the sorption heat storage system, which is the content of this thesis. This section will focus on the mechanisms of the transfer processes and will introduce few basic equations.

- **Conduction**

  Heat conduction occurs due to the collision of the molecules in liquids and gases during their random movement, or the vibration of the molecules and electrons in solids. The electrons or molecules in the hotter part have a higher kinetic energy level than the ones in the colder part. This difference in the energy levels will drive them to give some of their kinetic energy to the other electrons or molecules in the cold part, the energy transmit is caused by collision.
  Which distinguish the conduction from other transport mechanisms is that no motion of the medium is taking place.

  The amount of heat transferred by conduction in the case of a steady heat flow across a plane wall as shown in Figure 2.11, can be given by Fourier's equation

$$\frac{\dot{Q}}{A} = q = \lambda\left(\frac{T_1 - T_2}{X_1 - X_2}\right) = \lambda\frac{\Delta T}{\Delta X} \qquad \text{Equation 2.14}$$

  Where q is the heat flux or the heat flow $\dot{Q}$ over the surface area A, T_1 and T_2 are the temperatures of the surfaces ($T_1 > T_2$), ΔX is the thickness of the wall and λ is the thermal conductivity coefficient, which its value is experimentally measured for each material.

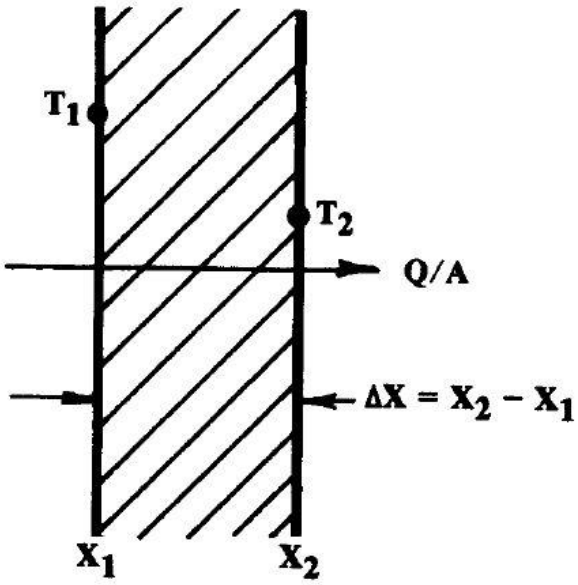

Figure 2.11 Heat conduction through a plane wall [Dr. K. J. Bell, Dr. A. C. Mueller, 2001]

- **Convection**

  Convection occurs in a single phase (liquid or gas), where the heat transfer takes place because of the microscopic or macroscopic motion of the fluid, where the heat is being carried as an internal energy, and thus when a hot material flows into a cold material, it will heat up the region and vice versa.
  The flow can be driven by the density of pressure differences between the two points, or by an external driving source (e.g. pumps, fans…etc.). In this case, the transport mechanism will be called a forced convection.
  If the flow of the liquid or gas is laminar, the heat is being transferred between the layers of the flow by conduction. Nevertheless, when the flow is turbulent, eddy transport becomes more dominant.
  It was found for many convection heat transfer processes, that the heat flux is proportional to the temperature differences of the two points where the convection is taking place in between. Thus, the flowing formula can be concluded

$$\frac{Q}{A} = h\,(T_2 - T_1) \qquad \text{Equation 2.15}$$

  Where h is the convection heat transfer coefficient [w/(m^2*K)] and T_1, T_2 are the temperatures of the two points.

  In the case of two phases of material (solid-gas) then the heat transfer will be a combination between convection and conduction.

- **Radiation**

  Energy is being emitted by radiation form all matter in the form of electromagnetic waves, this amount of emitted energy is mainly dependent on the temperature of the matter, however it could be also related to the nature of the surface of the matter.
  The basic law of radiation was derived by Stefan and Boltzmann, which can be written as the following:

$$\frac{Q}{A} = \sigma \, e \, T_{abs}^4 \qquad \text{Equation 2.16}$$

  Where:

  σ is Stefan-Boltzmann constant (5.67×10^{-8} W/m^2*K^4)
  T_{abs} is the absolute temperature [K]
  e is the emissivity of the matter, it has a value between 0 and 1, whereas 0 means a perfectly reflecting body, 1 means a perfect emitter (so called "black body")

  Compared to the other heat transfer mechanisms, heat transfer by radiation is relatively unimportant at low temperatures, and it becomes important to be taken into consideration at temperatures higher than 500°C.

- **Condensation**

  Condensation is the mechanism by which the vapor is changed into liquid. This process occurs by removing the latent heat of condensation form the vapor. Four different mechanisms of condensation are recognized in general: dropwise, filmwise, direct contact and homogeneous condensation.

a. Dropwise condensation

In this condensation mechanism, the vapor starts to form liquid drops on the solid surface at specific favored locations, these locations are called "nucleation sites". These sites could be scratches, pits or any surface irregularity and in few square centimeters there may be many thousands of them. The drops then start to grow because of the continuous condensation of the vapor on one hand, and the agglomeration of adjacent drops whenever they come in contact with each other on the other hand. The dropwise condensation takes place when the solid surface on which the condensation is occurring is not strongly wetted by the liquid, so that the formed drops do not spread out over the whole surface, but they grow in their place until they are large enough that they run off.

b. Filmwise condensation

In the filmwise condensation mechanism, the formation of the drops occurs relatively fast causing them to merge with each other, and thus a continuous liquid film is being produced on the solid surface, where the heat should also be transferred through this film. The heat transfer mechanism in this case will be quite complex since it is subjected into two-phase flow (gas-liquid), involving the quantities, properties and fluid mechanics of both phases.

The other two condensation mechanisms do not apply for this investigation; therefore, their mechanisms are not included in detail.

- **Vaporization**

  There are different cases and mechanisms by which vaporization may take place (e.g. pool boiling, vaporization during flow…), nevertheless in this thesis only the pool boiling mechanism is in concern.
  When the heated surface is submerged in a container filled with liquid where there is no motion except for that induced by the boiling process. This process is called pool boiling. Conversely, if the liquid boils because it is forced over the heated surface, then it is called forced convection boiling. [ME 4331, 2010]
  Pool boiling can occur in many different mechanisms depending in the first place on the temperature difference between the wall and the liquid. Figure 2.12 represents the relation between the heat flux and the temperature difference between walls temperature and liquid saturation temperature.

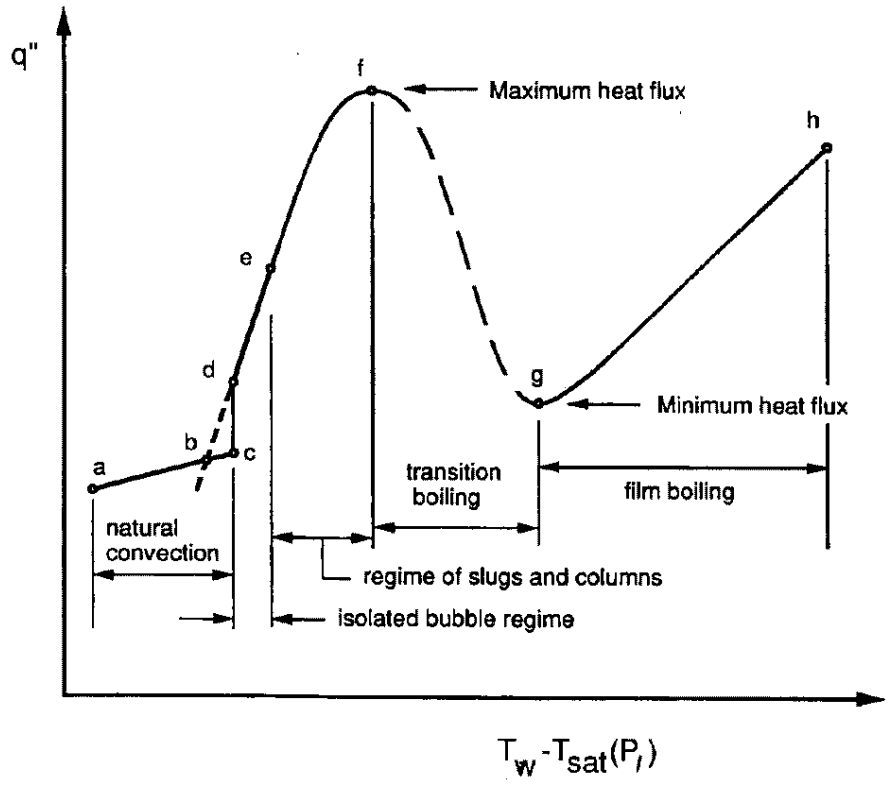

Figure 2.12 Saturated pool boiling curve [ME 4331, 2010]

From Figure 2.12 it is clear that the behavior of the heat flux can be divided into many different regimes, however it can be simplified as the following:

Natural convection regime (ac)

The liquid in contact with the hot surface is heated and then it rises up. The heat is being transferred mainly by single-phase convection. In this regime no vapor bubbles are being formed.

Nucleate boiling regime (cf)

In this regime vapor bubbles start to be formed from the favored nucleation sites, in the first part (ce) the bubbles are formed separated from each other, while in the other part (ef) and due to the increase of the bubbles formation, the bubbles start to interfere with each other forming vapor columns. The point f represents the maximum achievable heat flux.

Transition boiling (fg)

An unstable vapor film is formed near the hot surface during this regime, the film keeps collapsing and reforming again. The film decreases the heat flux again due to the smaller heat transfer properties of the gas.

Film boiling (gh)

In this region the vapor film between the hot surface and the liquid becomes stable, this case usually occurs when the temperature difference between the hot surface and the liquid exceeds 600 °C.

Conclusion

While the sensible and latent heat storage technologies are standard products, the thermo-chemical energy storage is still under development. The adsorption heat storage system has not been introduced as a commercial product yet. Therefore, it is necessary to intensify the scientific knowledge as well as the technical understanding to be able to make these technologies usable for mankind in the future [Salvatore Vasta, 2018].

3. Methodology

In this chapter all different aspects, which were used in the investigation, are going to be described in detail. This includes: simulations, technical modifications, experiments and thermal energy analysis.

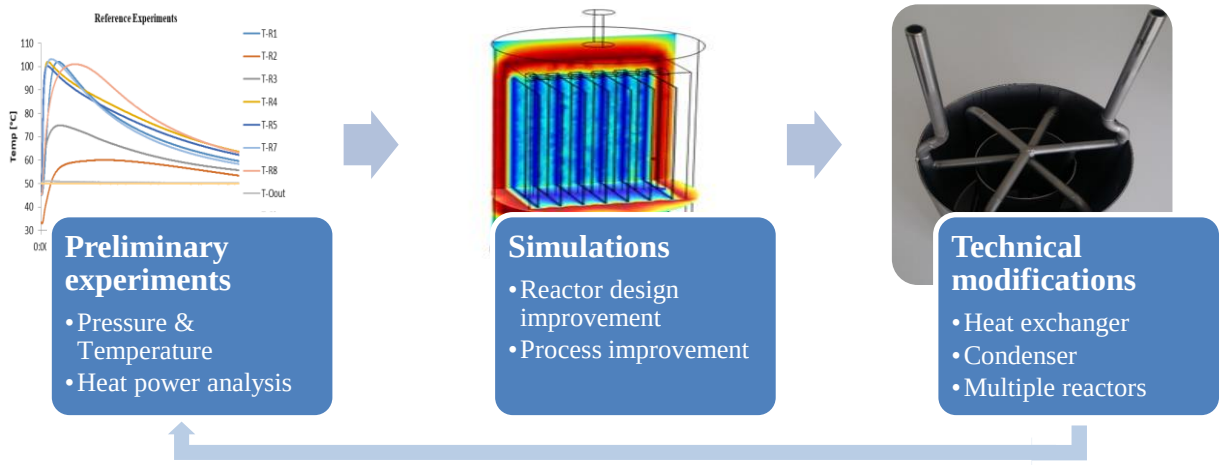

3.1. Simulations

In order to achieve the goal of this research and improve the efficiency of a heat storage system, multiple simulations were planned ahead, so that the required technical modifications could be defined.
The simulations performed during this work can be divided into two main categories, heat and mass transfer simulations and process simulations.

3.1.1. Reactor design improvement

The heat and mass transfer 3D simulations were conducted with the help of a FEM-tool (COMSOL Multiphysics). The purpose of these simulations was to identify the zones with poor heat transfer or mass transfer blockage, which were preventing the heat storage system from reaching a higher storage efficiency. With the help of the simulations' results, suitable technical modifications were planned, with the aim of realizing a better heat and mass transfer in the reactor.

3.1.2. Process improvement

As for the 0D process simulations, they were performed with a self-developed program using LabVIEW software. A numerical model of the whole heat storage system was created and validated, allowing various parameters to be investigated, such as temperatures, pressures, number of reactors and mass of adsorbent. Thus, it was possible to simulate and compare different application scenarios without the need of conducting high number of experiments. The process simulation revealed the potential of using multiple reactors-setup and assisted the technical modifications to attain this potential. A detailed explanation of the simulations used in this research is found in Chapter 4.

3.2. Technical modifications and experiments

As an important part of this investigation, technical modifications were applied on the heat storage unit, in order to test multiple operation parameters, as well as to validate the digital model, which was developed for the simulations.
Different laboratory-scale experimental units were built, allowing a range of various experiments to be run, with the possibility to adjust the parameters, test different materials and continuously record the results in order to analyze them later. Defining these modifications was based on the results and recommendations from the simulations.
The technical modifications can be divided into the following points:

3.2.1. Fans and evacuations

In order to improve the kinetics in the reactor, fans were installed in the reactor and frequent evacuations were carried out.

3.2.2. Separation between condenser and evaporator

Considering convection and water vapor flow inside the reactor, it was advisable to use an overhead condenser instead of having a combined condenser/evaporator under the reactor.

3.2.3. New heat exchanger

With the help of the heat and mass transfer simulation a new heat exchanger design was developed and implemented in the heat storage unit. The aim of this new heat exchanger is to improve the heat transfer between the zeolite packed bed and the oil cycle during both desorption and adsorption.

3.2.4. Multiple reactor unit

Following the results from process simulations, a multiple reactor unit consisting of two identical single reactor units was build, the two reactors are connected with each other in such a way, that allows the heat to be restored from both reactors either simultaneously (parallel configuration) or subsequently (serial configuration).

A detailed description of the technical modifications is found in chapter 5.

3.3. Thermal energy analysis

The performance of the adsorption heat packed bed system with different working parameters and the effect of various technical modifications is evaluated using energy analysis.

A complete reversible cycle of the closed thermochemical process is divided into three phases as desorption (charging), storing and adsorption (discharging). Both desorption and adsorption processes are assumed to be isobaric. Also, the kinetic and potential energy, vacuum pump work and fan work are neglected and the calculations are done with respect to the assumed reference temperature of 30 °C.

3.3.1. Heat shares

Before starting with the heat power analysis, the input and the output heat shares during both desorption and adsorption process must be defined.

Desorption process

The heat provided by the oil cycle during the desorption process "**total input heat**" can be divided into the following points:

- **Stored heat:** consist of
  - **Binding enthalpy:** which is being used to force the water molecules adsorbed in the zeolite pores to be desorbed.
  - **Evaporation enthalpy:** this heat is being consumed along with the binding enthalpy to evaporate the water in the zeolite packed bed. It is needed to transfer the water molecules from the adsorbed phase where the molecules are very close to each other into a gaseous state. However, this heat share could be partially recovered later in the condenser.
- **Sensible heat:**
  - Heat used to heat up the zeolite packed bed to approach the oil pre-set temperature (in this investigation 235 °C). This part is lost from the packed bed to the ambient air after the experiment is done.
  - Sensible heat because the water vapor was desorbed at super-heated temperature. This part could be partially recovered in the condenser.
- **Heat losses:** from both of the reactor and the condenser to the ambient air, this can be reduced but not totally prevented. Especially in this relatively small system and at the high temperatures the heat losses during charging (desorption) are very high.

Recovered heat: in principle a part of the total input heat could be recovered from the water cycle in the condenser. This part of heat represents the evaporation enthalpy, in addition to the sensible heat of the superheated water vapor, but not to forget that part of this heat is still lost by condensing at the condenser's vessel walls and being lost to the environment. However, in the case of this investigation the water cycle temperature in the condenser was 20°C, which makes it so difficult to find an application for such a low temperature.

Adsorption process

During the adsorption process the heat which was produced by the adsorption in the packed bed "adsorption enthalpy" can be divided into the following shares

- **Binding enthalpy:** this is being released when the water molecules are being attached to the micropores surface, and it is theoretically the same amount of energy of the one which was invested during desorption.
- **Condensation enthalpy:** this heat is released when the adsorbed water molecules start to form a quasi-liquid phase in the micropores. This is theoretically equal to the evaporation enthalpy during desorption.

Part of this adsorption enthalpy was delivered to the oil cycle as "**restored heat**", while the rest is considered as heat losses, which in its turn can be divided into:

- **Sensible heat:** in order to heat up the packed bed from the room temperature to the oil cycle temperature (in this investigation 30 °C).
- **Heat losses** from the walls of the reactor to the ambient air.

Figure 3.1 demonstrates the heat shares in both the adsorption and desorption process as well as the heat losses during adsorption (which are share of the adsorption enthalpy).

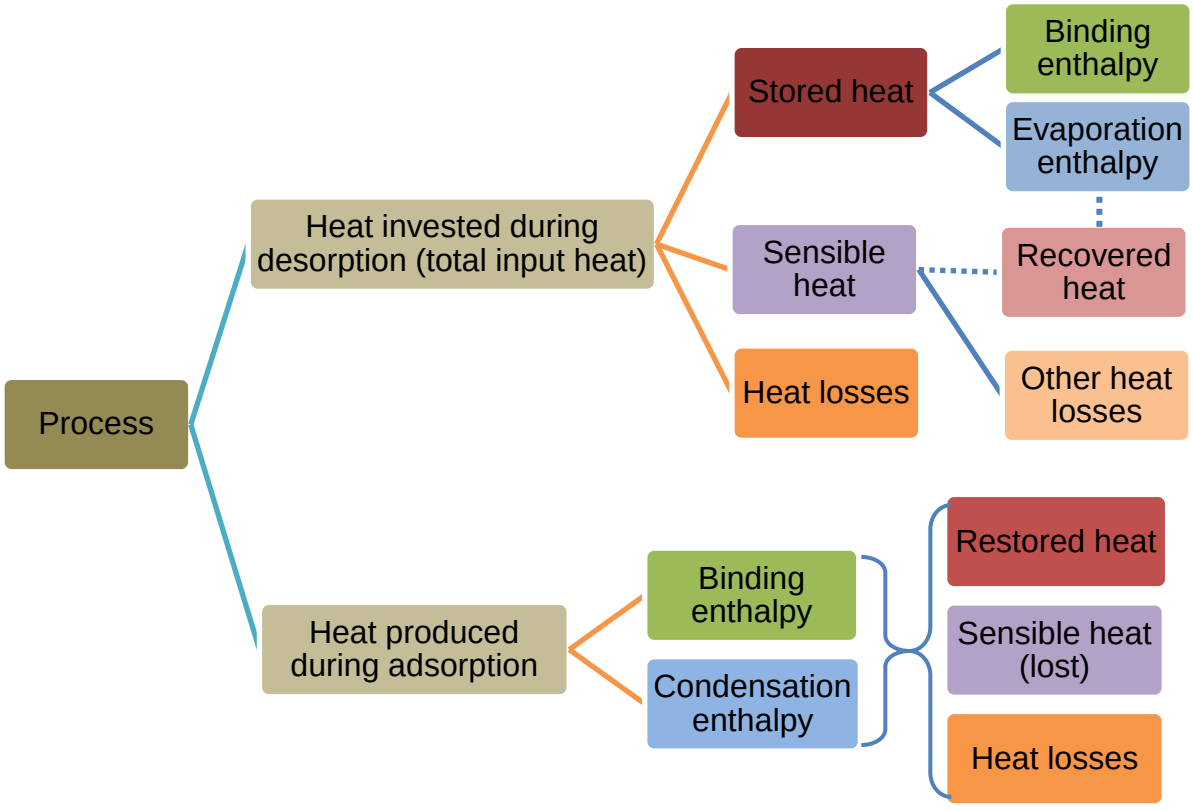

Figure 3.1 Demonstration of the heat shares during desorption and adsorption

The restored heat (condensation + binding adsorption enthalpies) should be in theory equal to the evaporation and binding desorption enthalpies (in case of the same reached temperature and loading after the complete cycle).

3.3.2. Heat power analysis

A full heat power analysis was performed during both desorption and adsorption phases, in order to calculate the overall heat storage efficiency.

- **Desorption phase**

During desorption, energy is stored in the zeolite as a result of the thermochemical dissociation between adsorbent and adsorbate. Heat from an external heat source (oil cycle of oil thermostat in this case) is supplied to the packed bed via reactor heat exchanger. A part of this heat is invested as the energy required to desorb the water from zeolite and is ultimately stored in form of chemical energy. Due to the temperature gradient between packed bed (which includes zeolite, heat exchanger and water adsorbed on zeolite) and ambient (environment and other system components), heat is lost via conduction, convection as waste heat. Some part of supplied heat is used in raising the temperature of packed bed till desorption temperature and is stored as sensible heat. The sensible heat of heat transfer fluid (HTF) and superheating of vapors is ignored. An energy balance for desorption phase is written as:

Energy invested (Q_i) = Enthalpy change during dissociation reaction + Energy lost + Sensible heat stored in the packed bed after desorption

The above balance can be expressed as:

$$\int_0^t \dot{m}\ C_{p,HTF}\left(T_{d,in} - T_{d,out}\right)dt = \Delta H_d + Q_{d,lost} + \ m\, C_{p,z}(T_d - T_0) \qquad \text{Equation 3.1}$$

where $\dot{m}$ [kg/h] is the mass flow rate of heat transfer fluid, $C_{p,HTF}$ [kJ/kg*K]is specific heat capacity of heat transfer fluid, $C_{p,z}$ [kJ/kg*K]is specific heat capacity of packed bed, $T_{d,in} - T_{d,out}$ $[K]$ is the temperature difference between inlet and outlet of the heat transfer fluid during desorption, t is the total time of desorption phase, $Q_{d,lost}$ [kJ] are the heat losses during desorption phase and the enthalpy change $\Delta H_d = \Delta H_{bind} + \Delta H_{evap}$ which is same as ΔH_{ad}.

The first term on left side in equation 3.1 is the total heat invested Q_i during desorption process including all losses (waste and sensible heat). The term $m\, C_{p,z}(T_d - T_0)$ stands for the summation of sensible heat stored in packed bed, where m is the mass of packed bed, T_d is the final temperature of the packed bed at the end of desorption process and T_0 is the reference temperature.

The energy balance and the desorption efficiency can be written as:

$$\eta_d = \frac{\Delta H_d}{\int_0^t \dot{m}\, C_{p,HTF}\,(T_{d,in} - T_{d,out})} \quad \text{Equation 3.2}$$

However, if the desorption of the system is done immediately after adsorption the system or the sensible heat stored inside the packed bed during adsorption process is kept stored and recovered during the following desorption process, the energy balance shown in equation 3.1 can be written as:

$$\int_0^t \dot{m}\, C_{p,HTF}\,(T_{d,in} - T_{d,out})\mathrm{dt} - \sum m\, C_{p,z}(T_{ad,f} - T_0) = \Delta H_d + Q_{d,lost} + \sum m\, C_{p,z}(T_d - T_0) \quad \text{Equation 3.3}$$

The term $\sum m\, C_{p,z}(T_{ad,f} - T_0)$ stands for the summation of sensible heat stored in the packed bed at the end of adsorption process, where m is the mass of packed bed, $C_{p,z}$ [kJ/kg*K] is specific heat capacity of packed bed, $T_{ad,f}$ is the final temperature of the packed bed at the end of adsorption process and T_0 is the reference temperature. In this case the left side ($\int_0^t \dot{m}\, C_{p,HTF}\,(T_{d,in} - T_{d,out})\mathrm{dt} - \sum m\, C_{p,z}(T_{ad,f} - T_0)$) of equation 3.3 is the total energy invested during desorption $Q_{i,Total}$ when the sensible heat from the previous adsorption process is recovered. Consequently, the efficiency of desorption process η_d shown in equation 3.2 can be written as $\eta_{d,SH}$ when the sensible heat from the previous adsorption process is recovered as shown in equation 3.4:

$$\eta_{d,SH} = \frac{\Delta H_d}{\int_0^t \dot{m}\, C_{p,HTF}\,(T_{d,in} - T_{d,out})dt - \sum m\, C_{p,z}(T_{ad,f} - T_0)} \quad \text{Equation 3.4}$$

- **Storage Phase**

The efficiency of the storage phase was taken as 1 assuming that no adsorption of vapor took place on zeolite and thus no heat was discharged out of the system, ignoring the sensible heat.

- **Adsorption phase**

Heat energy is produced from the charged storage system during adsorption phase. The released energy was extracted by the same oil cycle as in desorption phase via the reactor heat exchanger. A part of the released heat energy was restored as useful heat. Another part was lost as waste heat due the temperature gradient to the environment as mentioned in the desorption phase.

The part of released heat which was not restored in the given duration of time (3 hrs.) was left stored inside the packed bed as sensible heat. An energy balance for the adsorption phase can be written as:

Energy restored (Q_R) + Energy lost + Sensible heat stored at the end of adsorption = Energy released during thermochemical reaction + Sensible heat stored at the end of desorption (if adsorption is carried out immediately after desorption)

The above balance can be expressed as:

$$\int_0^t \dot{m}\, C_{p,HTF}\left(T_{ad,out} - T_{ad,in}\right) + \mathrm{Q_{lost,ad}} + \sum m\, C_{p,z}(T_{ad} - T_0) = \Delta \mathrm{H_{ad}} + \sum m\, C_{p,z}(T_d - T_0) \qquad \text{Equation 3.5}$$

where $\dot{m}$ [kg/h] is the mass flow rate of heat transfer fluid, Cp,HTF [kJ/kg*K] is specific heat capacity of heat transfer fluid, Cp,z [kJ/kg*K] is specific heat capacity of packed bed, $\left(T_{ad,out} - T_{ad,in}\right)$ [K] is the temperature difference between outlet and inlet of the heat transfer fluid during adsorption, t is the total time of adsorption phase, $Q_{lost,ad}$ [kJ] are the heat losses during adsorption phase and the enthalpy change $\Delta H_{ad} = \Delta H_{bind} + \Delta H_{cond}$ which is same as ΔH_d.

The first term on left side in equation 3.5 is the heat restored Q_R after all losses (waste- and sensible heat) from total heat produced (discharged) ΔH_{ad} during adsorption process. The term $\sum m\, C_{p,z}(T_d - T_0)$ stands for the summation of sensible heat stored in packed bed after desorption process and $\sum m\, C_{p,z}(T_{ad} - T_0)$ is the summation of sensible heat stored in packed bed at the end of adsorption process, where m is the mass of packed bed, $C_{p,z}$ is the specific heat capacity of packed bed, T_d is the final temperature of the packed bed at the end of desorption process, T_{ad} is the final temperature of the packed bed at the end of adsorption process and T_0 is the reference temperature.

However, in real applications the adsorption is not carried out immediately after desorption process. Therefore, neglecting the sensible heat stored at the end of desorption process, the energy balance and the efficiency of adsorption process can be written as:

$$\int_0^t \dot{m}\, C_{p,HTF}\left(T_{ad,out} - T_{ad,in}\right) + \mathrm{Q_{lost,ad}} + \sum m\, C_{p,z}(T_{ad} - T_0) = \Delta \mathrm{H_{ad}} \qquad \text{Equation 3.6}$$

$$\eta_{\mathrm{ad}} = \frac{\int_0^t \dot{m}\, C_{p,HTF}\left(T_{ad,out} - T_{ad,in}\right)}{\Delta \mathrm{H_{ad}}} \qquad \text{Equation 3.7}$$

- **Overall efficiency**

Neglecting the sensible heat stored, the overall efficiency of the complete cycle is written as the product of desorption and adsorption phase efficiencies:

$$\eta_o = \eta_d * \eta_{ad} \quad \text{Equation 3.8}$$

$$\eta_o = \frac{\int_0^t \dot{m}\, C_{p,HTF}\,(T_{ad,out} - T_{ad,in})}{\int_0^t \dot{m}\, C_{p,HTF}\,(T_{d,in} - T_{d,out})} \quad \text{Equation 3.9}$$

- **Energy storage density (ESD)**

The energy storage density *ESD* (Wh/kg) of the system is written as the ratio of amount of usable heat restored to the mass of zeolite used during the storage.

$$ESD = \frac{\int_0^t \dot{m}\, C_{p,HTF}\,(T_{ad,out} - T_{ad,in})dt}{M_{zeolite}} \quad \text{Equation 3.10}$$

Sensible heat recovered from heat exchanger during the process is small in comparison to total heat restored. Therefore, only mass of zeolite is considered as it the primary source of heat packed bed.

ESD (Wh/m^3) is also given in terms of packed bed volume as shown below:

$$ESD = \frac{\int_0^t \dot{m}\, C_{p,HTF}\,(T_{ad,out} - T_{ad,in})dt}{Volume\ of\ packed\ bed} \quad \text{Equation 3.11}$$

4. Simulations

Simulation is an important step during the process development, which can save both time and costs. Moreover, it provides better understanding of the system/process. However, the current numerical approach of the TES development is still inadequate [Hauer, Andreas 2020], which brings up the necessity of modeling and simulation on the whole system level as well as heat and mass transfer simulations on the reactor level.
The heat and mass transfer simulations were conducted with the help of a FEM-tool (COMSOL Multiphysics), while the process simulations were performed with a self-developed program using LabVIEW software

4.1. Reactor design improvement

For the reactor design improvement, a 3D model of the reactor was created using SolidWORKS. The 3D model consists of a reactor (with different inlets and outlets), heat exchanger and a packed bed of zeolite (as shown in Figure 4.1).

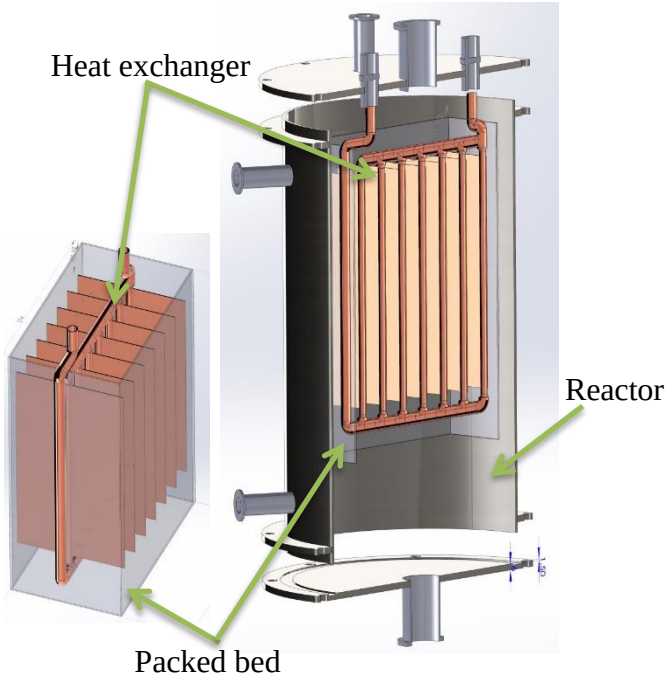

Figure 4.1 CAD model of the reactor with heat exchanger

The CAD file was imported to COMSOL Multiphysics and modified before the simulations were performed. The main goal of the modifications on the geometry was to reduce the number of sharp edges and thin surfaces and thus reducing the number of elements needed for the meshing. Another simplification was made by assuming that the zeolite packed bed is one

porous block, which has the same density, heat transfer coefficient, specific heat capacity and porosity as the packed bed made of zeolite pellets. This assumption improved the simulation speed significantly. The packed bed was then meshed using a tetrahedral mesh, taking into consideration the proper size of cells for each part of the geometry (as shown in Figure 4.2).

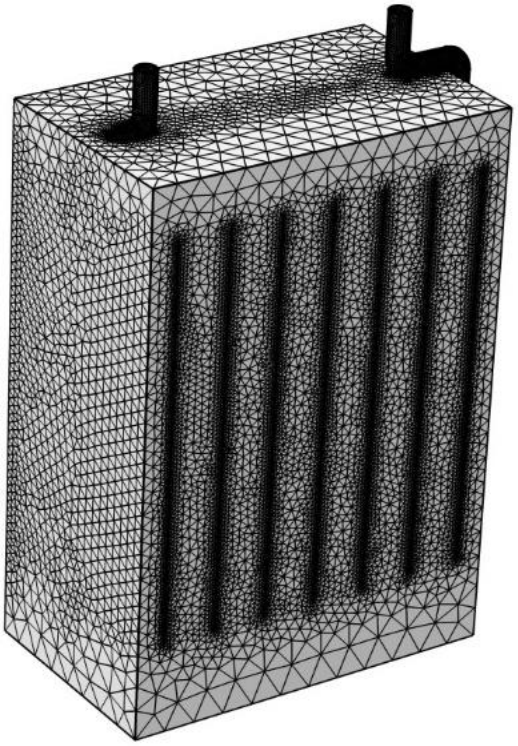

Figure 4.2 Simplified zeolite packed bed

A combined heat transfer model (conductive and convective) was used in solids (heat exchanger and packed bed) and fluids (water vapor). Reynolds-averaged Navier-Stokes (RANS) equations were used in the fluid domain to calculate the fluid flow. Whereas a K-epsilon model was used for calculating the turbulence in the reactor at the beginning when the reactor valve is opened.

Initial and boundary conditions

The geometry was divided into three regions: Heat exchanger, zeolite (packed bed) and reactor. During the desorption process, the heat exchanger was defined as a heat source, while the zeolite and the reactor's walls were defined as heat sink. On the other hand, during the adsorption the zeolite was defined as the heat source and both of the heat exchanger and reactor's walls acted as the heat sink.

Table 4-1shows the initial and boundary conditions values used during the simulation for the different regions.

Table 4-1 Initial and boundary conditions used the heat and mass transfer simulations

Geometry	Size [mm]	Initial conditions	Boundary conditions
Heat exchanger (tubes)	270x200x125	Desorption T=25°C Adsorption T=25°C	Desorption T=235°C Adsorption T=30°C
Zeolite	Pellets (sphere diameter) D= 5 Packed bed 300x214x130	Desorption T=25°C Adsorption T=25°C	Desorption T=235°C Adsorption T=120°C
Reactor	D= 275 L= 410	Desorption T=25°C P=30mbar Adsorption T=25°C P=5mbar	Desorption T=70°C Adsorption T=50°C

Materials' properties

Table 4-2 shows the materials' properties, which were used during the simulation

Table 4-2 Materials' properties used in heat and mass transfer simulations

	Density[g/l]	Thermal conductivity [W/m*K]	Specific heat capacity [J/kg*K]
Copper	8940	401	385
Zeolite	989	0.1	880
Zeolite packed bed	585	0.07	880

Both stationary and time dependent simulations were carried out for the heat and mass transfer inside the reactor by adsorption as well as desorption. By the time dependent simulation, a time step of 1 minute was chosen.

4.2. Process improvement

In order to have a wider range of results and to predict the temperature behavior for different process parameters, process simulation was carried out. By the help of LabVIEW programing language, a program was developed based on theoretical equations, which can simulate both adsorption and desorption processes. The program is able to perform transient 0Dprocess simulation with a time step of 2 seconds for unlimited process duration. Some simplifications and assumptions were applied to system model such as:

- only the mass flow of water vapor from the evaporator and into the condenser were taken into consideration without any heat transfer
- the heat transfer with the heat exchanger was assumed to be uniform on the whole exchange surface
- the water vapor was assumed to reach/leave the zeolite immediately (no adsorption/desorption kinetics were involved)

As shown in Figure 4.3, the program makes it possible to change many parameters including temperatures, pressures, time and number of reactors (with heat recovery option).

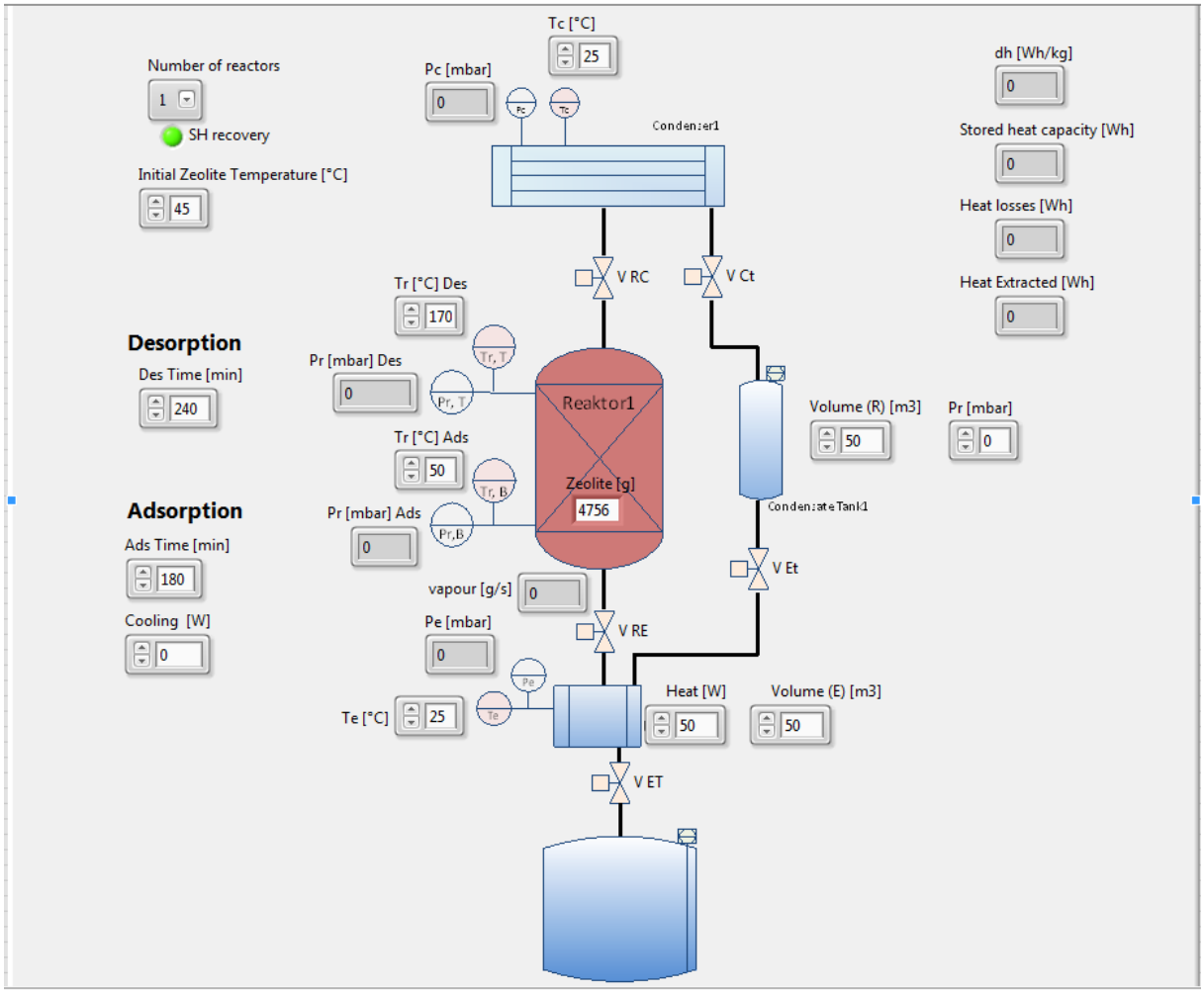

Figure 4.3: Graphical user interface (GUI) of the process-simulation program (set-up)

Figure 4.4 shows the graphical user interface (GUI) of the process-simulation program, where the results can be also saved as an excel sheet. The program calculates the temperature behavior and different heat shares, as well as the amount of adsorbed/desorbed water.

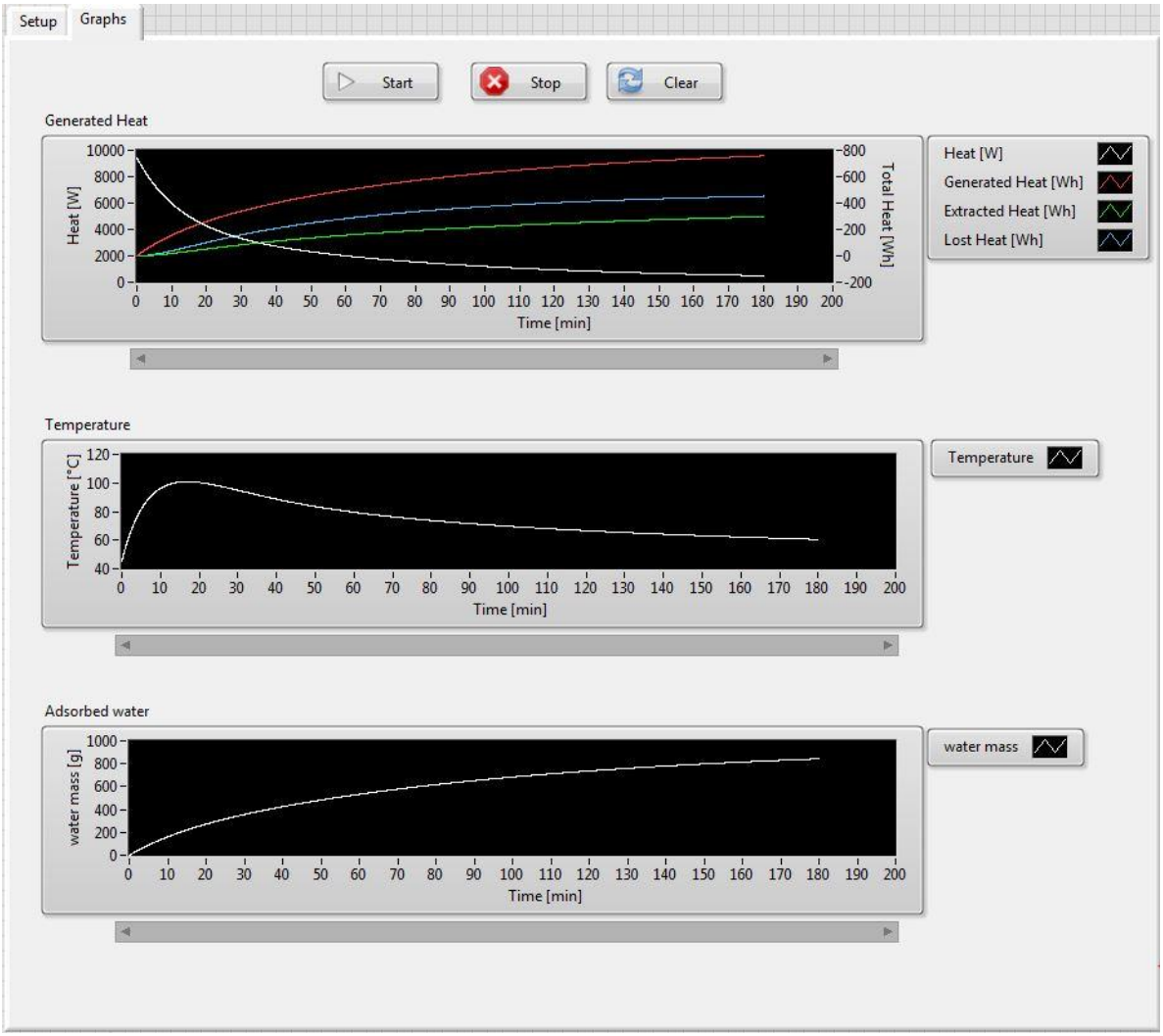

Figure 4.4: Graphical user interface (GUI) of the process-simulation program (results)

The simulation was based on the simplified Dubinin and Astakhov gauss distribution equation, which is suitable for any kind of adsorbent with a uniform pore diameter. (Wang, R. 2014)

$$X = X_0 . e^{-k\left(\frac{T}{T_s}-1\right)^n}$$ Equation 4.1

X: adsorption rate

X_0: maximum adsorption rate

k: coefficient related to the zeolite structure

n: reflects the distribution of the pore diameter of the adsorbent (2 for Zeolite)

T_s: saturation temperature

The adsorption and desorption heat of a cycle is (Wang, R. 2014):

$$H_a = \int_{x_2}^{x_1} m_a h_a dx = \int_{T_{a1}}^{T_{a2}} m_a h_a \frac{\partial x(T,T_e)}{\partial T}\, dT \qquad \text{Equation 4.2}$$

$$H_d = \int_{x_1}^{x_2} m_a h_d dx = \int_{T_{d1}}^{T_{d2}} m_a h_d \frac{\partial x(T,T_c)}{\partial T}\, dT \qquad \text{Equation 4.3}$$

Where:

H_a and H_d represent the heat of an adsorption and a desorption cycles respectively [kJ/kg]

x_1 and x_2 represent the adsorption rate at the beginning and the end of the cycle [kg_w/kg_z]

h_a and h_d are the adsorption heat and desorption heat respectively [kJ/kg] (can be taken from the characteristic curve of the Zeolite)

T_{a1} and T_{a2} are the zeolite temperatures of adsorption at the beginning and the end of the cycle

T_{d1} and T_{d2} are the zeolite temperatures of desorption at the beginning and the end of the cycle

T_e and T_c are the evaporation and condensation temperatures

m_a mass of adsorbent [kg]

For Zeolite type Y the adsorption and desorption enthalpies can be calculated from the following empirical equations based on the characteristic curve of Zeolite NaX (Mugele)

$$h_a = 33817{,}2\, {X_a}^5 - 67645{,}25\, {X_a}^4 + 38335\, {X_a}^3 - 11058\ {X_a}^2 + 4973{,}9\, X_a \qquad \text{Equation 4.4}$$

$$h_d = 33817{,}2\, {X_d}^5 - 67645{,}25\, {X_d}^4 + 38335\, {X_d}^3 - 11058\ {X_d}^2 + 4973{,}9\, X_d \qquad \text{Equation 4.5}$$

Where X_a is the water loading after adsorption [kg_w/kg_z]

X_d is the water loading after desorption [kg_w/kg_z]

Thus, the stored heat can be calculated as the following

$$\Delta h = h_a - h_d \left[\frac{J}{g}\right] \qquad \text{Equation 4.6}$$

Desorption

During desorption process the energy balance can be expressed as the following.

Energy invested (Qi) = Enthalpy change during desorption + Energy lost + Sensible heat of zeolite and adsorbed water in the packed bed

$$\int_0^t \dot{m}\ C_{p,HTF}\left(T_{d,in} - T_{d,out}\right)dt = \Delta H_d + Q_{d,lost} + \left(m_z\ C_{p,z} + m_w c_{p,w}\right).(T_d - T_0)$$

Equation 4.7

where $\dot{m}$ [kg/h] is the mass flow rate of heat transfer fluid, $C_{p,HTF}$ [kJ/kg*K]is specific heat capacity of heat transfer fluid, $C_{p,z}$ [kJ/kg*K]is specific heat capacity of zeolite, $T_{d,in} - T_{d,out}$ $[K]$is the temperature difference between inlet and outlet of the heat transfer fluid during desorption, t is the total time of desorption phase, $Q_{d,lost}$ [kJ] are the heat losses during desorption phase and the enthalpy change $\Delta H_d = \Delta H_{bind} + \Delta H_{evap}$ which is same as ΔH_{ad}.

The first term on left side in equation 4.7 is the total heat invested Qi during desorption process including all losses (waste- and sensible heat). The term $\left(m_z\ C_{p,z} + m_w C_{p,w}\right).(T_d - T_0)$ stands for the sensible heat stored in zeolite and adsorbed water, where m_z and m_w are the masses of zeolite and adsorbed water respectively, T_d is the final temperature of the packed bed at the end of desorption process and T_0 is the temperature at the beginning of the desorption.

Adsorption

Similar to the desorption, the mass balance by adsorption can be expressed as

Energy restored (QR) + Energy lost + Sensible heat stored at the end of adsorption = Energy released during thermochemical reaction

$$\int_0^t \dot{m}\ C_{p,HTF}\left(T_{ad,out} - T_{ad,in}\right)dt + Q_{lost,ad} + m_z\ C_{p,z}(T_{ad} - T_0)\ = \Delta H_{ad}$$

Equation 4.8

where $\dot{m}$ [kg/h] is the mass flow rate of heat transfer fluid, $C_{p,HTF}$ [kJ/kg.K] is specific heat capacity of heat transfer fluid, $C_{p,z}$ [kJ/kg.K] is specific heat capacity of zeolite, $\left(T_{ad,out} - T_{ad,in}\right)$ [K] is the temperature difference between outlet and inlet of the heat transfer fluid during adsorption, t is the total time of adsorption phase, $Q_{lost,ad}$ [kJ] are the heat losses during adsorption phase and the enthalpy change $\Delta H_{ad} = \Delta H_{bind} + \Delta H_{cond}$ which is same as ΔH_d.

The first term on left side in equation 4.8 is the heat restored Q_R after all losses (waste- and sensible heat) from total heat produced (discharged) ΔH_{ad} during adsorption process. The term $m_z\ C_{p,z}(T_{ad} - T_0)$ is the summation of sensible heat stored in packed bed at the end of adsorption process, where T_{ad} is the final temperature of the packed bed at the end of adsorption process and T_0 is the temperature at the beginning of the adsorption.

The heat during the adsorption/desorption is restored/invested by means of a heat exchanger. As a simplification for the process simulation, the heat transfer ratio was calculated using Fourier's law for heat conduction

$$q = -kA.\frac{\Delta T}{S} \quad [W] \qquad \text{Equation 4.9}$$

Where

k: thermal conductivity [W/m*K]

A: heat exchanger surface [m^2]

S: thickness [m]

During adsorption: $\Delta T = T_{zeo} - T_{wt}$

During desorption: $\Delta T = T_{wt} - T_{zeo}$

Where T_{zeo} is the temperature of zeolite in the fixed bed and T_{wt} is the temperature of the heat exchanger

The same formula can be used to calculate the heat losses through the conduction between the fixed bed and the surrounding water vapor in the reactor. The temperature difference in this case will be

$$\Delta T = T_{zeo} - T_R \qquad \text{Equation 4.10}$$

Where T_R is the temperature in the reactor

The equations were implemented in the program as shown in the block diagram in Figure 4.5 (which is part of the whole program). Where different possibilities were taken into consideration, from using multiple reactors to the ability to recover sensible heat from previous reactors.

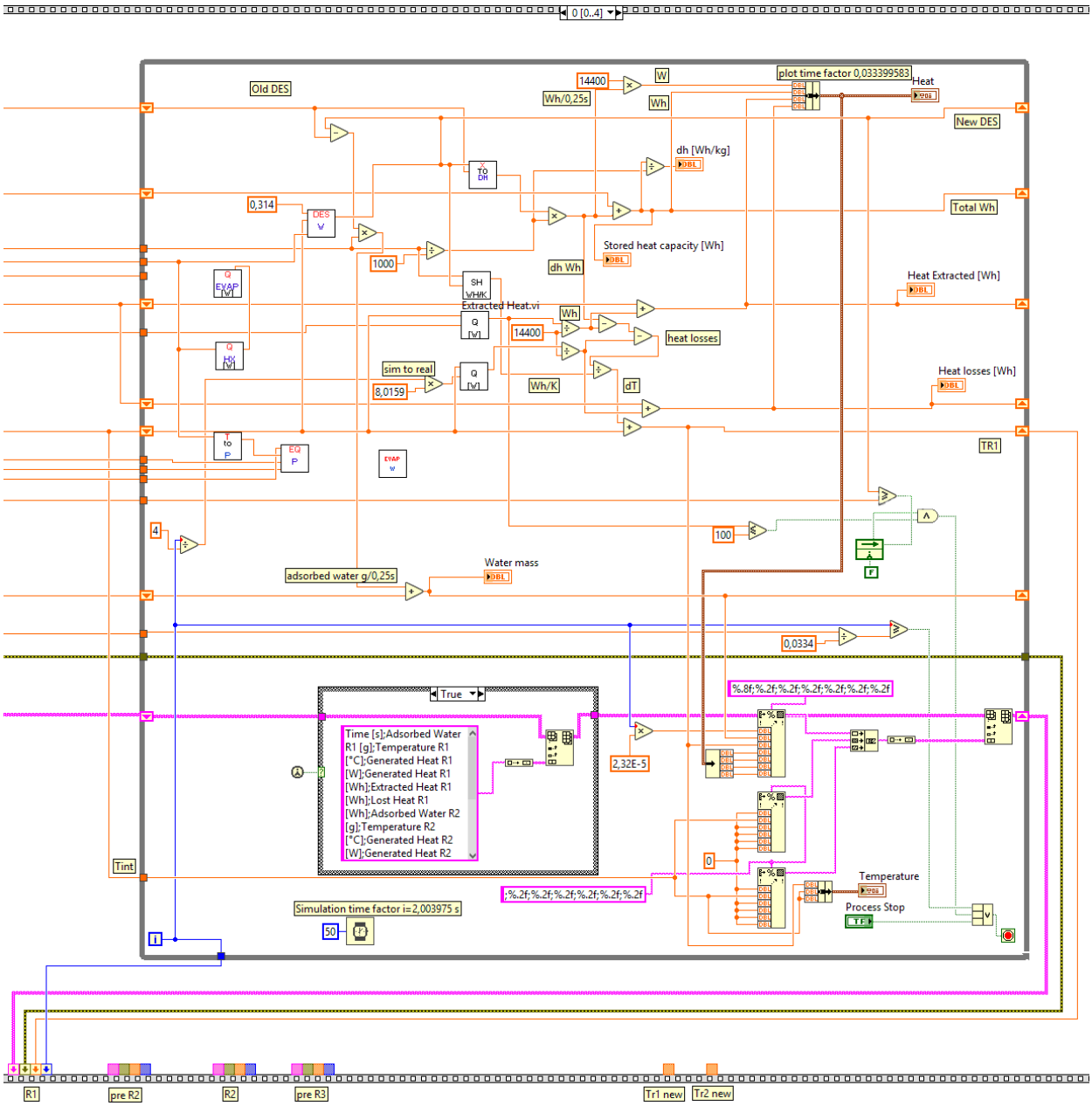

Figure 4.5 Part of the project interface of the simulation program

5. Technical Modifications

In this chapter the heat storage units and the performed technical modifications are going to be described in details.

The aim of these modifications was to improve the performance and efficiency of the heat storage system as well as testing multiple operation parameters. In addition, preliminary experiments were carried out to validate the numerical models, which were developed for both 0D-system simulations and 3D heat and mass transfer simulations.

Further modifications were later on defined and tested based on the results and recommendations from the simulations.

5.1. Single reactor unit with a combined condenser/evaporator

As a first step before starting with the technical modifications, it's important to understand the components and functions of the original pilot plant, which was used in the beginning for heat storage and was later on modified multiple times within the course of this work.

This part will describe this heat storage unit including all the auxiliary equipment. In addition, the adsorption/desorption process and the operating steps will be explained.

The unit consists mainly of a reactor, condenser/evaporator and water storage tank. Besides that, auxiliary equipment is used such as valves, sensors and pumps.

A schematic representation of the whole storage system is shown in Figure 5.1, where the following is the detailed description of each part of the system.

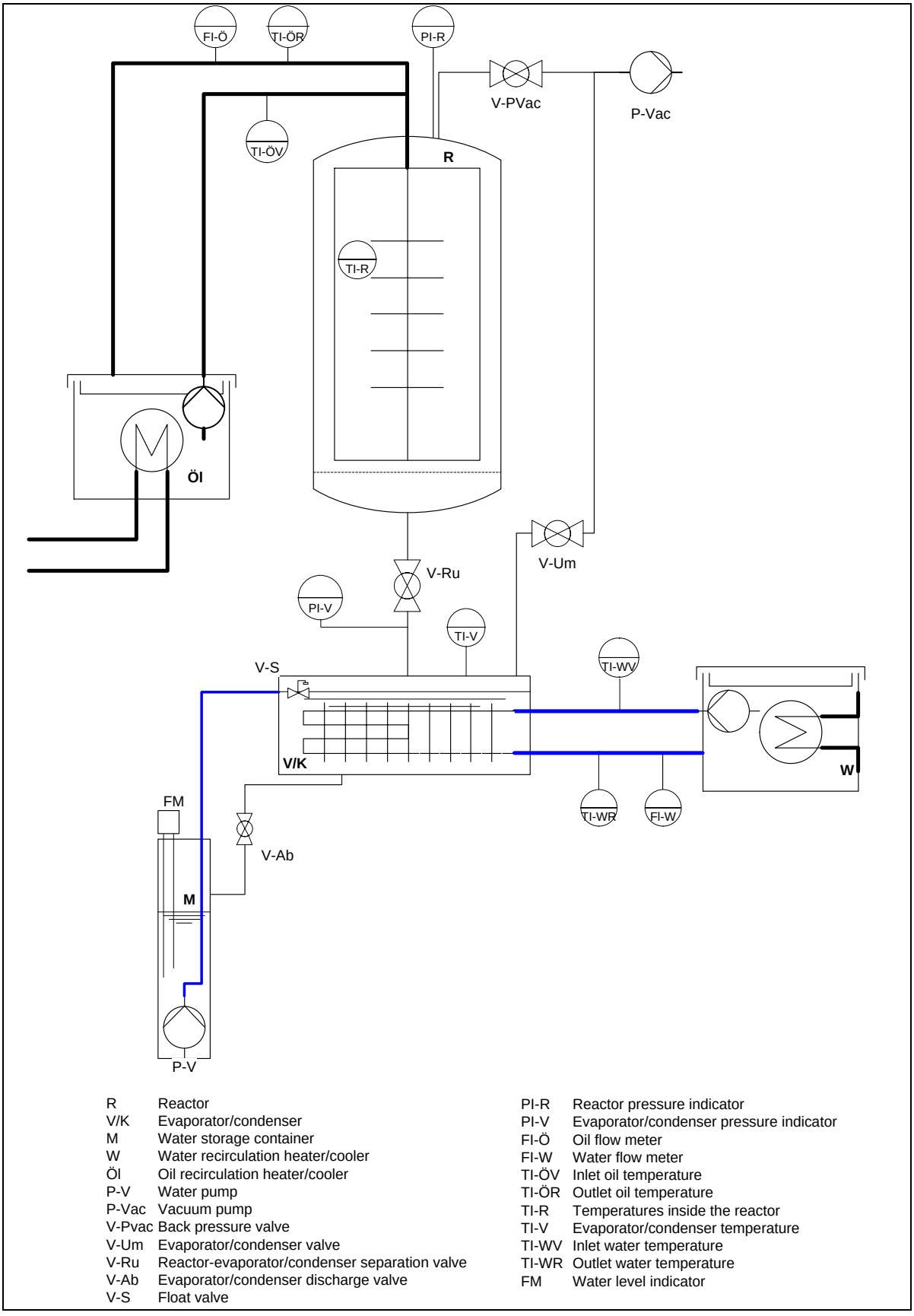

R	Reactor
V/K	Evaporator/condenser
M	Water storage container
W	Water recirculation heater/cooler
ÖI	Oil recirculation heater/cooler
P-V	Water pump
P-Vac	Vacuum pump
V-Pvac	Back pressure valve
V-Um	Evaporator/condenser valve
V-Ru	Reactor-evaporator/condenser separation valve
V-Ab	Evaporator/condenser discharge valve
V-S	Float valve

PI-R	Reactor pressure indicator
PI-V	Evaporator/condenser pressure indicator
FI-Ö	Oil flow meter
FI-W	Water flow meter
TI-ÖV	Inlet oil temperature
TI-ÖR	Outlet oil temperature
TI-R	Temperatures inside the reactor
TI-V	Evaporator/condenser temperature
TI-WV	Inlet water temperature
TI-WR	Outlet water temperature
FM	Water level indicator

Figure 5.1 Schematic representation of the sorption storage unit

- **The reactor**

The reactor (R) is where the sorption material is placed, and both of the adsorption and desorption processes are taking place. It is made from stainless steel in a cylindrical shape with a volume of about 15 l.
Inside the reactor the sorption material (in this investigation the zeolite) is located in a cage made of stainless-steel wires, in order to keep the material in contact with the heat exchanger and at the same time allowing the water vapor to pass through the pores between the material's particles.

As shown in Figure 5.2 the reactor is insulated in order to minimize the heat losses. The cover is supplied with sealed connectors for the vacuum pump, temperature sensors (TI-R) and the oil cycle which is connected to the heat exchanger inside the reactor.

Figure 5.2 The reactor

For this investigation a heat exchanger made of copper with 7 fins (Figure 5.3) was used as a reference heat exchanger to be later on compared with other heat exchanger designs.

Figure 5.3 Heat exchanger in the wired cage

The heat exchanger was completely immersed within the zeolite (Figure 5.4), different temperature sensors (thermocouples) were placed on the heat exchanger and inside the zeolite packed bed.

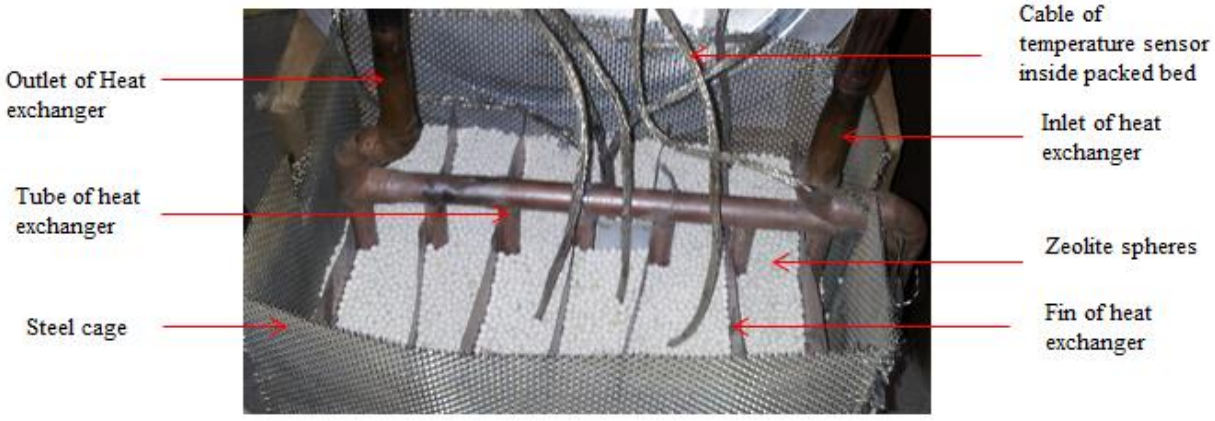

Figure 5.4 Packed bed of zeolite in between the fins of heat exchanger

- **Condenser/Evaporator (V/K)**

The condenser/evaporator is the part of the system where the heat exchanger for the water cycle is located; it is connected from the upper part to the reactor through a pneumatic valve and from the lower part to the water storage tank through another pneumatic valve. The condenser/evaporator is also provided with sealed connectors for the vacuum pump, temperature sensor and the water cycle which is connected to the heat exchanger inside.
The heat exchanger is made of aluminum and located in the lower half of the condenser/evaporator. In order to assure that the heat exchanger is totally immersed in the water during the adsorption process (which increases the contact surface leading to a better efficiency), a water level valve (V-S) was fixed inside the condenser/evaporator and connected to the water inlet coming from the water storage tank Figure 5.5.

Figure 5.5 Water level valve

The condenser/evaporator has a dual function. Firstly, it works as condenser during the desorption phase (when the heat is being stored in the reactor), in this case the condenser is connected to the heat sink forcing the water vapor coming from the reactor to condensate on the heat exchanger and thus collecting the water and lead it to the storage tank. As a second function it works as an evaporator during the adsorption phase (when the heat is being restored from the reactor). In this phase the evaporator provides the water inside with heat through the heat exchanger, and when the water temperature is higher than the evaporation temperature it starts to boil and water vapor is being produced.

- **Water storage tank (M)**

The function of the water storage tank is to store the water which is either going to be pumped to the evaporator or collected from the condenser. The pump (P-V) (see Figure 5.1) which is used for pumping the water back to the evaporator/condenser is located at the bottom of the tank.

The water storage tank is made from acrylic glass with a volume of about 7 liters. The cover of the tank is provided with two sealed connectors, one is for allowing the water tank to be connected to the condenser/evaporator through a pneumatic valve; and the other connector is to connect the water pump power cable. A water level sensor (FM) is also located on the cover, where its probe is going into the water tank through a suitable sealed hole.

- **Oil and water cycles**

Two heating/cooling cycles are needed for running the system: a water cycle and an oil one.

- **Water cycle (W)**

The main function of this cycle is to heat up the water in the evaporator during the adsorption phase, or to cool down and condense the water vapor in the condenser during the desorption process. In the real application, the ambient air temperature could be used for the purpose of evaporating the water during the adsorption process.
The cycle consists of a water thermostat, tubes and heat exchanger located inside the condenser/evaporator.
The thermostat used is manufactured by the company Julabo with the model no. FP51-SL, within the temperature working range (20-25 ^{o}C) it has a heating power of 1.3 KW and a cooling power of 2 KW. The bath fluid used in this investigation was 5 liters of water with a composition of 3 liters tap water and 2 liters de-ionized water, in order to reduce the concentration of lime in the tap water, and thus reducing the calcification in the thermostat.

- **Oil cycle (Öl)**

This cycle is responsible for introducing the heat which is required to be stored to the reactor during the desorption process, and recovering the stored heat from it during the adsorption process.
The cycle consists of an oil thermostat, isolated tubes and a copper heat exchanger. A Julabo LH50 oil thermostat has been used with a cooling capacity of about 7 KW and heating capacity of 6 KW within the range of the working temperature (30 ^{o}C for cooling, 20-235 ^{o}C for heating).

- **Sensors and valves**

For controlling the unit and monitoring the results, different valves and sensors were used.

- **Sensors**

Many types of sensors were employed in the system, with different functions, in Table 5-1 a list of the sensors, their symbols, locations and functions is shown.

Table 5-1 List of the sensors used in the sorption storage system

Symbol	Sensor type	Location	Function
TI-R (1-8)	Thermocouple	Heat exchanger in the reactor	Measure different temperatures in different locations in the sorption material
TI-WV TI-WR	Thermocouple	Water cycle	Measure the temperatures of the water in the inlet and outlet to the condenser/evaporator
TI-V	Thermocouple	Condenser/ Evaporator	Measure the temperatures of the water in the condenser/evaporator
TI-ÖV TI-ÖR	Thermocouple	Oil cycle	Measure the temperatures of the oil in the inlet and outlet to the reactor
FI-W	Flow meter	Water cycle	Measure the water flow for the water cooling/heating cycle
FI-Ö	Flow meter	Oil cycle	Measure the oil flow in the oil cycle
FM	Capacitive level sensor	Water storage tank	Measure the water level in the storage tank
PI-R	Pressure sensor	Reactor cover	Measure the pressure inside the reactor
PI-V	Pressure sensor	Condenser/ Evaporator	Measure the pressure inside the Condenser/ Evaporator

For the water flow a Proline Promag 50p flow meter (electromagnetic) was used with a measuring range of 0.01-10 m/s and a maximum measurement error of 0,5%, while for the oil flow a Proline Promass 83F (Coriolis) was used, with a measuring temperature range of -50…+350 ^{o}C and a maximum measurement error of 0,1%, which are suitable for the operating conditions. The used thermocouples were type T with an operating range of -185 to 300 °C and a tolerance of ± (0.5 +0.004×t) °C

- **Valves**

  The valves used in the system are listed in Table 5-2 below

Table 5-2 List of valves used in the sorption storage system

Symbol	Valve Type	Location	Function
V-Ru	Electro-Pneumatic 3/2 NC	Between the reactor and the condenser/evaporator	Open during operation and closed the rest of the time to keep the water content in the zeolite constant
V-PVac	Electro-Pneumatic 3/2 NC	Between the vacuum pump and the reactor	Open only during evacuating the reactor and closed the rest of the time keeping the reactor vacuum tight
V-Um	Electro-Pneumatic 3/2 NC	Between the vacuum pump and the condenser /evaporator	Open only during evacuating the condenser/evaporator and closed the rest of the time keeping the condenser /evaporator vacuum tight
V-Ab	Electro-Pneumatic 3/2 NC	Between the condenser /evaporator and water storage tank	Discharge the water from the condenser/evaporator back to the water tank
V-S	level	condenser/evaporator	Stop pumping water to the evaporator when the heat exchanger is fully submerged

5.1.1. Process description

A complete sorption cycle is divided into two phases, desorption/condensation and evaporation/adsorption. The way to achieve each of these two phases can be related directly to the applied operation parameters (pressure and temperature). Hence, by controlling the oil and water thermostats as well as the pressures inside both of the reactor and the condenser/evaporator, either a desorption process or an adsorption one can be obtained.
In the following both of the two processes are going to be explained in more details.

- **Desorption process**

The desorption process is when the heat should be stored, in this investigation the heat is introduced to the system by means of an oil thermostat, where a temperature of 235 ^{o}C is set to the thermostat (the value was chosen based on the maximum operating temperature of some sealing elements). As an initial condition the reactor is evacuated and kept under vacuum pressure (around 1 mbar absolute pressure). Then the oil thermostat starts to pump the heated oil into the reactor through the heat exchanger, which in its turn heats up the adsorbent packed bed (zeolite). When the adsorbent material reaches a certain temperature, water vapor starts to be desorbed from the adsorbent. As this process continues, the vapor formation will cause an increase of the pressure in the reactor. When the pressure in the reactor exceeds the one in the condenser, the V-Ru valve is opened allowing the water vapor to pass from the reactor to the condenser, where it gets in contact with the heat exchanger of the water cycle and cools down. As soon as the water vapor temperature gets lower than the dew point of the corresponding pressure, at this point the water vapor will start to condensate and water droplets will be formed on the walls of the condenser and the heat exchanger. After a while the water droplets will start gathering and flow from the bottom of the condenser through the discharge valve V-Ab into the water storage tank.
A discontinuous measurement was taken to the water level in the storage tank during the process using different time intervals, in order to estimate the relation between the desorbed water volume and time.

- **Adsorption process**

In order to recover the stored heat in the adsorbent material, an adsorption process must take place. As an initial condition both the reactor and the evaporator are evacuated, where the pressure in the evaporator reaches the corresponding saturation pressure to the water temperature in the storage container. The water is then pumped from the storage tank to the evaporator, where it is heated up by means of the heat exchanger and the water thermostat. Since the water temperature is getting higher than the corresponding saturation temperature, water vapor is being formed, which causes by its turn the pressure inside the evaporator to increase. As long as the V-Ru valve is closed (see Figure 5.1), the pressure inside the evaporator will keep increasing until it reaches the corresponding saturation pressure to the preset temperature in the water thermostat. At this point no further water vapor is being formed, and the pressure therefore stays constant.

The adsorption process can now be started by opening the V-Ru valve, thus the water vapor can flow from the evaporator to the reactor, where the adsorbent material starts adsorbing the water vapor and releasing heat. Due to water vapor flow from the evaporator to the reactor, pressure inside the evaporator starts to drop causing more water vapor to be formed, and the process continues as long as the adsorbent material is adsorbing the water vapor in the reactor.
In the meanwhile, the heat which is being released from the adsorbent, can be collected by means of the heat exchanger and transferred into the oil cycle and thus to the oil thermostat.
The adsorption process is considered to be finished when the water vapor adsorption stops. This can be estimated when water temperature in the evaporator reaches the preset temperature of the water thermostat and the pressure inside the evaporator reaches the corresponding saturation pressure, which means the process of forming water vapor has stopped. In this case the V-Ru valve is closed and the water is discharged from the evaporator to the storage container. The water level is then measured to calculate the adsorbed water volume.

5.1.2. Experimental procedure

Both preparation and operational procedures were performed for the sake of the experiments.

- **Preparation procedure**

Before starting with the experiments some preparation procedures were made, in order to make sure that the system will run correctly. Except of the oil degassing, these preparation procedures were repeated each time the adsorbent material was changed and before start running the next set of experiments.

Oil degassing

Whenever oil is changed or new oil is added to the oil thermostat, an oil degassing process should be performed. In the LH-50 oil thermostat the degassing process is integrated into the system, which means whenever a degassing process is needed it will be performed automatically. The aim for the degassing is to remove air bubbles, water or any other liquids trapped in the oil.

Water degassing

Dissolved gasses may exist in the water in the storage container, which could have an influence on the water adsorption process. Therefore, a water degassing process should take place prior to the operation of the system, in order to get these gasses out. This degassing should be repeated whenever the water gets in contact with the ambient air.
In this investigation the following steps were applied to degas the water:

- The condenser/evaporator is evacuated to the minimum achievable pressure.
- Temperature of the water thermostat is pre-set to 50 ^{o}C.
- While the water cycle is being heated up, an evacuation of the condenser/evaporator to the minimum achievable pressure is preformed several times, at the following input water temperatures (TI-WV) 40 ^{o}C, 45 ^{o}C and 50 ^{o}C.

- Evacuation of the condenser/evaporator when the water temperature inside it (TI-V) reaches 44 ^{o}C.
- Temperature of the water thermostat is set to 30 ^{o}C.
- Evacuation of the condenser/evaporator at the following TI-WV temperatures 45 ^{o}C, 40 ^{o}C, 35 ^{o}C, 30 ^{o}C.

Activation

When the adsorbent material (zeolite) is being changed, the new material should be activated before the experiments are carried out. The activation process is to guarantee that no water or gases are being trapped in the zeolite granules, which usually could be adsorbed by zeolite during production process, storing or when it gets in contact with the ambient air.
The activation process is carried out by setting the oil thermostat to a temperature of 235 ^{o}C and turning it on, the reactor is then evacuated as the zeolite is being heated, thus the trapped water and gasses will go out of the system. The activation was carried out for duration of 4 hours.

- **Operation procedure**

After applying the above-mentioned preparation procedures, the system (as shown in Figure 5.1) is now ready to operate. In this investigation the sorption cycle was started with an adsorption process and then followed by a desorption one. In the following, the steps of the experimental procedure are explained in detail.

Adsorption

- The control box power is switched on, and then the "Heat Saver Control" software is started. The signals from sensors are checked to make sure everything is connected. The mode in the configuration tab is set to "adsorption". To start recording the data, the data logging is then initiated.
- The V-Ab valve is opened to make sure that there is no water left inside the condenser/evaporator and all the water is in the water storage tank.
- Water level in the storage container is noted, and the V-Ab valve is closed.
- The water is pumped from the storage container to the evaporator, till the V-S valve is closed which means the heat exchanger is completely submerged in water.
- After warming up the vacuum pump for about 30 minutes before operating, the reactor is then evacuated to the minimum achievable pressure. The evaporator is evacuated as well until the evaporation pressure of the water inside is reached. The vacuum pump is then kept running for another 30 minutes to remove the water vapor trapped in the pump oil to avoid damages by corrosion.
- Both oil and water thermostats are set to the desired temperatures (for this investigation 25 ^{o}C for water thermostat and 30 ^{o}C for oil thermostat), the temperatures' values are chosen to make sure that the restored heat is not influenced by the heat transfer from the water vapor to the zeolite. The thermostats are then turned on.
- When the preset temperatures for both of the thermostats are reached and the temperature of water inside the evaporator is roughly the same of the water cycle, the V-Ru valve is then

opened allowing the water vapor to flow from the evaporator to the reactor. At this point the adsorption process is considered to be started.

- The adsorption process is carried on for the desired time, during this time the V-Ru valve is kept open.
- When the desired adsorption time is achieved (3 hours for this investigation), the adsorption process is stopped by closing the V-Ru valve, and the V-Ab valve is opened so the water left in the evaporator flows back to the storage container, the water level in the container is then noted and adsorbed water volume is calculated from the difference between the initial and final water level.

Desorption

- The control box power is switched on, and then the "Heat Saver Control" software is started, the signals from sensors are checked to make sure everything is connected, the mode in the configuration tab is set to "desorption". To start recording the data, the data logging is then initiated.
- The V-Ab valve is opened to make sure that there is no water left inside the condenser/evaporator and all the water is in the water storage tank.
- Water level in the storage container is noted, while the V-Ab valve is left open.
- After warming up the vacuum pump for about 30 minutes before operating, the reactor is then evacuated to the minimum achievable pressure. The evaporator is evacuated as well until the evaporation pressure of the water inside the water storage container is reached. The vacuum pump is then kept running for another 30 minutes to remove the water vapor trapped in the pump.
- Both oil and water thermostats are set to the desired temperatures (for this investigation 20 ^{o}C for water thermostat and 235 ^{o}C for oil thermostat), the thermostats are then turned on.
- When the preset temperatures for both of the thermostats are reached and the pressure inside the reactor is higher than the one in the condenser, the V-Ru valve is then opened allowing the water vapor to flow from the reactor to the condenser, at this point the desorption process is considered to be started.
- The desorption process is carried on for the desired time, during this time both of the V-Ru and V-Ab valves are kept open, discontinuous measurement for water level in the water storage container is taken place, using different time intervals.
- When the desired desorption time is achieved (4 hours for this investigation), the desorption process is ended by closing the V-Ru valve. The water level in the container is then noted and desorbed water volume is calculated depending on the level measurements by the different time intervals.

In order to assure the same operating conditions for all the experiments, the water content in the zeolite has to be the same before each adsorption process. Hence an extra desorption process was applied after the regular desorption whenever it was needed, so that the water content in the zeolite will go back to its initial value before the adsorption.
This extra desorption processes "desorption+" were carried out in the same way of the regular desorption, however for shorter time (ranges between 0.5 to 2 hours) depending on the water level in the water storage tank.

5.2. Single reactor unit with separated condenser and evaporator

The unit consists mainly of a reactor, condenser, evaporator, condensate tank and water storage tank. Besides that, auxiliary equipment is used such as valves, sensors and pumps.

A schematic representation of the whole storage system is shown in Figure 5.6

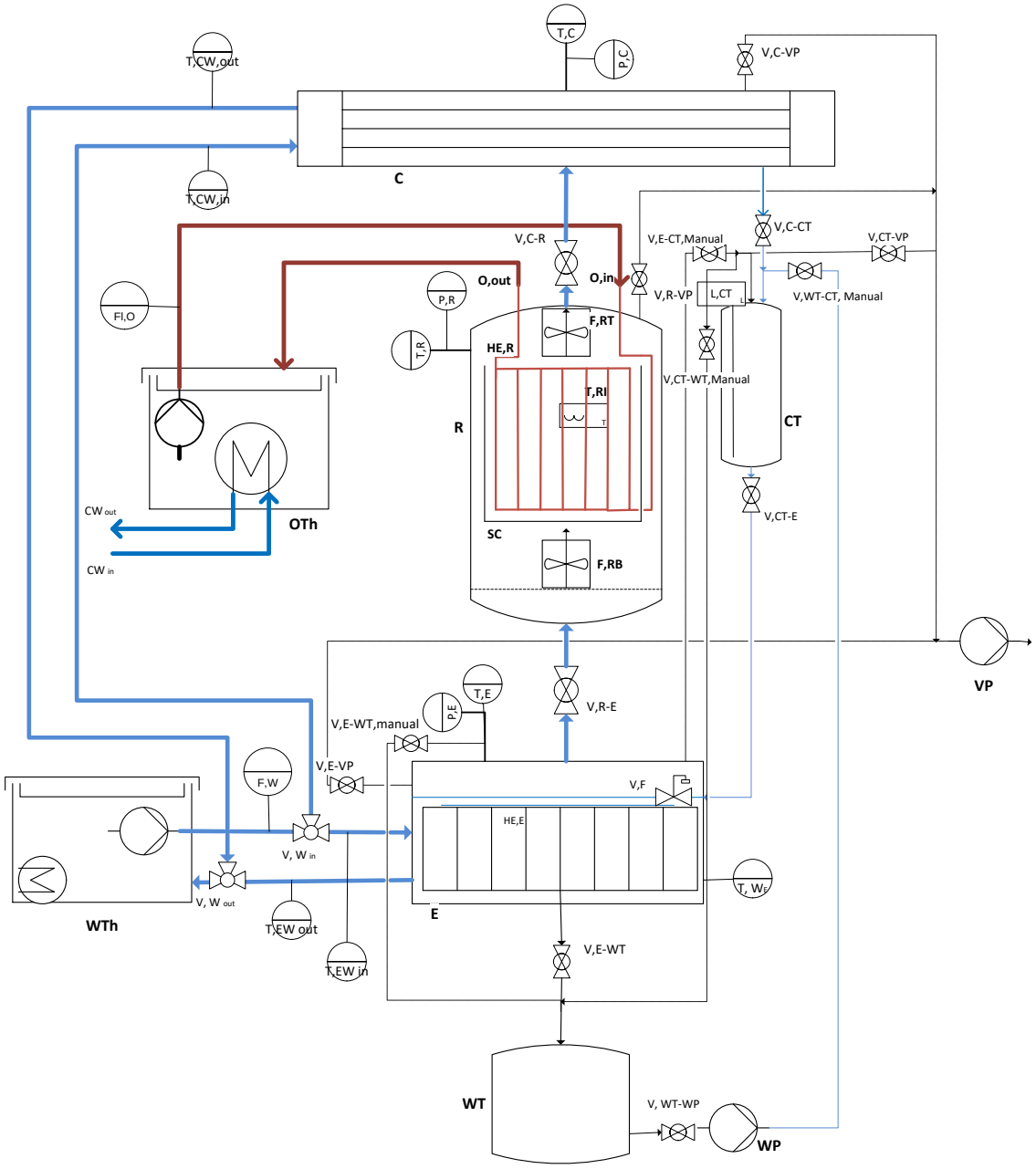

Figure 5.6: Line diagram of single reactor separated condenser/evaporator set-up

The following tables represent the different equipment, sensors and valves used in this set-up.

Table 5-3: List of equipment, sensors and valves of the single reactor separated condenser/evaporator set-up

Equipment

Symbol	*Description*
R	Reactor
E	Evaporator
C	Condenser (Overhead)
CT	Condensate tank
HE, R	Heat exchanger (Fin and tube) inside reactor
HE, E	Heat exchanger (Fin and tube) inside evaporator
VP	Vacuum pump
WP	Water pump
WT	Water tank
WTh	Water thermostat
OTh	Oil thermostat
SC	Steel cage
F,RB	Fan
F,RT	Fan

Sensors

Symbol	*Description*
F,W	Water flow meter
F,O	Oil flow meter
L,CT	Condensate tank level sensor
P,E	Evaporator pressure sensor
P,C	Condenser pressure sensor
P,R	Reactor pressure sensor
T,R	Temperature sensor for vapor inside reactor
T,C	Temperature sensor for vapor inside condenser
T,E	Temperature sensor for vapor inside evaporator
T,EW	Temperature sensor for water inside evaporator
T,Oin	Oil cycle inlet temperature sensor
T,Oout	Oil cycle outlet temperature sensor
T,B	Temperature sensors (total number 8) inside packed bed
T,EW in	Evaporator water cycle inlet temperature sensor
T,EW out	Evaporator water cycle outlet temperature sensor
T,CW in	Condenser water cycle inlet temperature sensor
T,CE out	Condenser water cycle outlet temperature sensor

Valves

Symbol	*Description*
V,E-VP	Evaporator evacuation valve
V,R-VP	Reactor evacuation valve
V,C-VP	Condenser evacuation valve
V,CT-VP	Condensate tank evacuation valve
V,C-R	Valve between condenser and reactor
V,R-E	Valve between reactor and evaporator
V,C-CT	Valve between condenser and condensate tank
V,CT-E	Valve between condensate tank and evaporator
V,E-WT	Valve between evaporator and water tank
V,WT-WP	Valve between water tank and water pump
V,CT-WT,manual	Valve between condensate tank and water tank
V,E-CT,manual	Valve between evaporator and condensate tank
V,E-WT,manual	Valve between evaporator and water tank
V,WT-CT,manual	Valve between water tank and condensate tank
V,F	Float valve

5.2.1. Technical modifications

Several technical modifications were applied during this work, in order to achieve better operation, monitoring and understanding of the various processes. Which helps developing the adsorption heat storage technology.

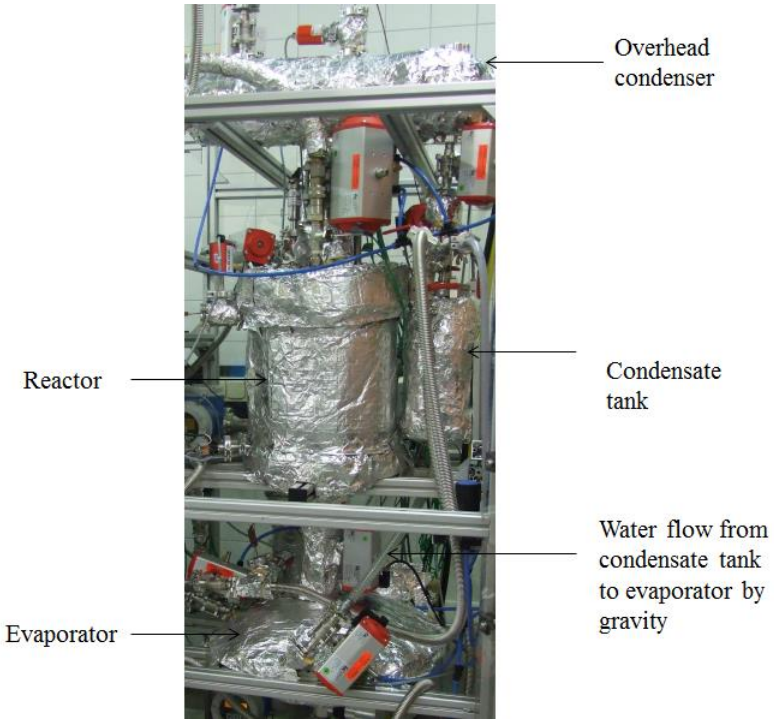

Figure 5.7: Single reactor separated condenser/evaporator set-up

The following modifications were applied

➢ **Installation of new equipment**

- **Overhead condenser (C)**

  The water vapors desorbed from the zeolite move upwards the reactor due to natural convection. In previous combined condenser/evaporator test set-up the vapors were condensed in the evaporator/condenser connected below the reactor. Therefore, an overhead condenser is installed horizontally at the top of the reactor which uses the natural convection of the vapors to draw them out of the reactor.
  The overhead condenser is a 1-2 pass stainless steel tube *'Shell and Tube'* type heat exchanger.

- **Condensate tank (CT)**

  The condensate tank is connected at the bottom end of the condenser through a valve. The purpose of this tank is to draw out and hold the water vapors condensed during desorption. In addition, the rate of desorption can be measured by measuring the rate of level increase inside the condensate tank. The level inside the tank is measured by a capacitive float type level sensor.
  During adsorption, a constant water level inside the evaporator is maintained which is controlled by a float valve *V,F*. The evaporation of water lowers the level and thus more water flows down from condensate tank to the evaporator by gravity. This helps in calculating the rate of evaporation by measuring the rate of level decrease inside the condensate tank. Assuming that all the water evaporated is adsorbed immediately on zeolite, rate of evaporation is equal to the rate of adsorption.

- **Fans (F,RB and F,RT)**

  Two fans one at the bottom *F,RB* and another one at the top *F,RT* of reactor are installed. The fan at the bottom is used during adsorption in order to force the vapors through the packed bed of zeolite. Whereas, the other at the top operates during desorption to induce the forced convection of vapors from reactor to condenser.

Figure 5.8: Fan used inside the reactor

➢ **Installation of new sensors**

- **Temperature sensors**

  Multiple temperature sensors were installed inside the reactor, evaporator and condenser to measure the vapor temperature during various processes. In addition, sensors inside the ingoing and outgoing streams of the cooling water cycle of condenser were installed to calculate the heat of condensation.

- **Pressure sensor**

  New pressure sensor was installed at the condenser to measure the behavior of pressure during desorption.

5.2.2. Adsorption procedure

The procedure of adsorption is as follows:

1. The power supply is turned on to all the electrical equipment and then the 'Lab-View' program is started to operate the process.
2. All sensors installed at the set-up are verified by checking the signals received by the program.
3. The data logging in the configuration tab is turned on, which starts the logging of data from all the sensors during the operation.
4. Both thermostats are turned on and set to the required temperatures of oil and water cycles.
5. The reactor is first evacuated till the minimum achievable pressure and then the evaporator till the corresponding saturation pressure at the prevailing temperature.
6. When the water temperature inside the evaporator is equivalent to the set temperature of water cycle, the valve *V,CT-E* is opened.
7. When the temperature inside the packed bed is equivalent to the set temperature of oil cycle, the fan *F,RB* is turned on and the valve *V,E-R* is opened to start the adsorption process.
8. After running this process for desired duration (3hours during this thesis work), the fan *F,RB* is turned off and the valve *V,R-E* is closed which ends the adsorption process.
9. The program is stopped and both heating and oil cycles are turned off.
10. The difference between the final and initial value of the water level inside the condensate tank, detected by the level sensor is the amount of water adsorbed during the entire process.

Note: The evacuation of the reactor is done three times at an interval of 30 min, 45 min, and 60 min starting from the time at the start of adsorption process. The reactor is evacuated each time for 10 second and during the evacuations the valve between evaporator and reactor is kept closed in order to avoid the entrainment of water vapors from evaporator to the vacuum pump.

5.2.3. Desorption procedure

The procedure of desorption is as follows:

1. The power supply is turned on to all the electrical equipment and the 'Lab-View' program is started to operate the process.
2. All sensors installed at the set-up are verified by checking the signals received by the program.
3. The data logging in the configuration tab is turned on, which starts the logging of data from all the sensors during the operation.
4. The reactor is first evacuated till the minimum achievable pressure and then the condenser along with the condensate tank till the corresponding saturation pressure at the prevailing temperature.
5. Both thermostats are turned on and set to the required temperatures of oil and water cycles.
6. When the pressure inside the reactor is higher than the saturation pressure of water, the fan *F,RT,* is turned on and then valve *V,R-C* and *V,C-CT* are opened.
7. After running this process for desired duration (4hours during this thesis work), the fan *F,RT* is turned off and the valves *V,R-C* and *V, C-CT* are closed which ends the desorption process.
8. The program is stopped and both heating and oil cycles are turned off.
9. The difference between the final and initial value of the water level inside the condensate tank, detected by the level sensor is the amount of water desorbed during the entire process.

5.3. New heat exchanger design

Based on the simulations' results (see 6.1.1.3), a new design of heat exchanger was selected. This design allows the oil coming from the inlet to flow inside the heat exchanger in both downwards and upwards directions, before it gets collected at the outlet. For technical reasons regarding the manufacturing (welding process), the heat exchanger was made of stainless steel instead of copper as the old heat exchanger was.

The following pictures show the new design and how it was placed in the reactor.

Figure 5.9: New heat exchanger design used in the multiple reactor set-up

The new heat exchanger design was installed inside both reactors of multiple reactor unit, and was tested in both single and multiple reactor configurations.

5.4. Multiple reactor unit with separated condenser and evaporator

The multiple reactor unit consists in principle of two identical single reactor units (with separated condenser/evaporator) connected with each other in such a way, which allows the heat to be restored from both reactors either simultaneously (parallel configuration) or subsequently (serial configuration). These configurations will be explained later in details. Figure 5.10 represents a line diagram of the multiple reactor unit, and Figure 5.11 shows the laboratory set-up.

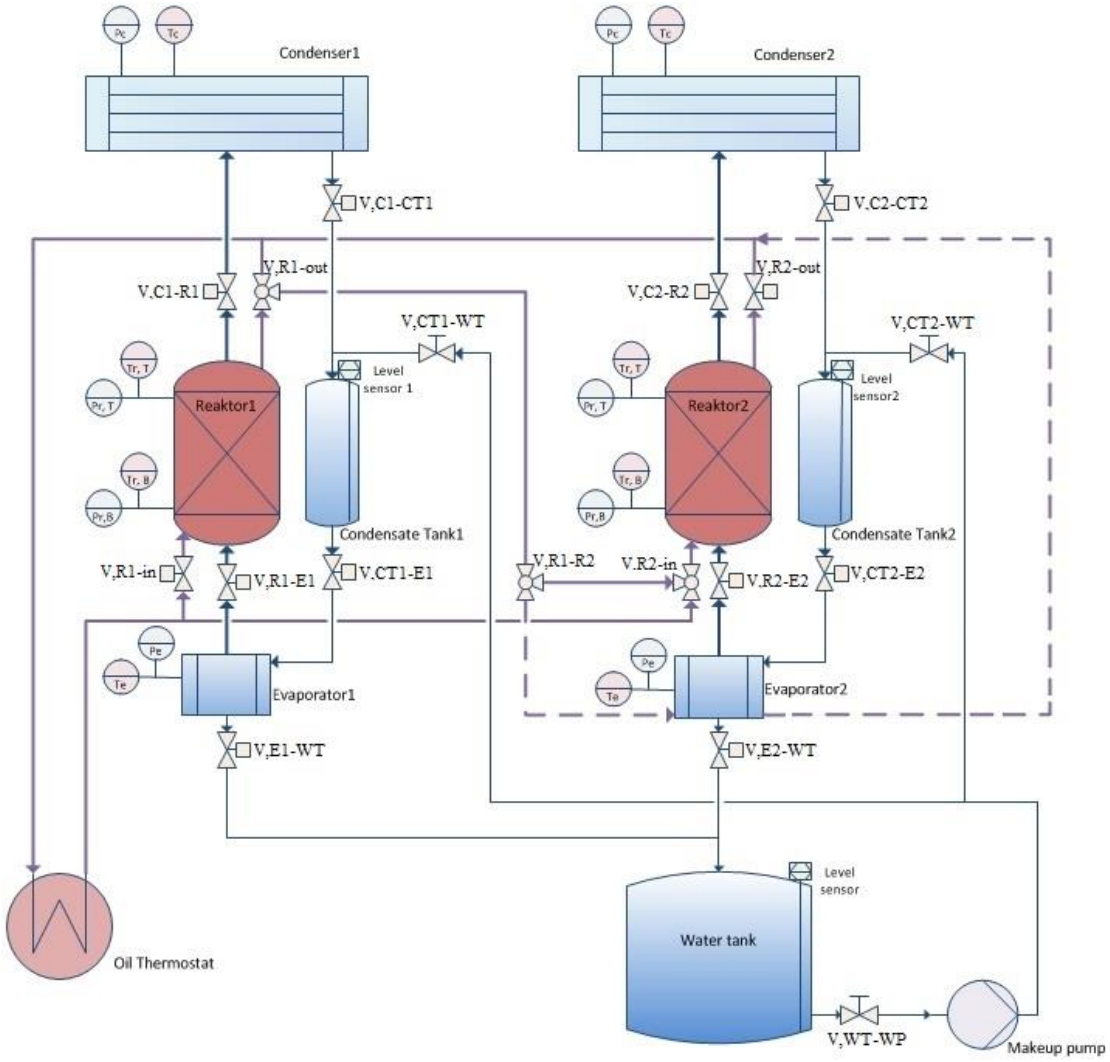

Figure 5.10: Line diagram of multiple reactor separated condenser/evaporator set-up

Table 5-4 lists the valves used in this set-up.

Table 5-4: List of valves of the multiple reactor separated condenser/evaporator set-up

Valves	
Symbol	*Description*
V,R1-in	Valve between oil thermostat and reactor1
V,R2-in	3-way valve between (oil thermostat/reactor1) and reactor2
V,R1-out	3-way valve between reactor1 and (V,R1-R2/back flow to oil thermostat)
V,R2-out	Valve between reactor2 and back flow to oil thermostat
V,R1-R2	3-way valve between reactor1 and (reactor2/evaporator2)
V,C1-R1	Valve between condenser1 and reactor1
V,C2-R2	Valve between condenser2 and reactor2
V,R1-E1	Valve between reactor1 and evaporator1
V,R2-E2	Valve between reactor2 and evaporator2
V,C1-CT1	Valve between condenser1 and condensate tank1
V,C2-CT2	Valve between condenser2 and condensate tank2
V,CT1-E1	Valve between condensate tank1 and evaporator1
V,CT2-E2	Valve between condensate tank2 and evaporator2
V,E1-WT	Valve between evaporator1 and water tank
V,E2-WT	Valve between evaporator2 and water tank
V,CT1-WT,manual	Valve between condensate tank1 and water tank
V,CT2-WT,manual	Valve between condensate tank2 and water tank
V,WT-WP	Valve between water tank and water pump

The sensors used in this multiple reactor setup are identical to the ones from the single reactor unit shown in Table 5-3, with the difference that two sets of sensors were required, one for each storage unit.

Figure 5.11: experimental set-up of multiple reactor separated condenser/evaporator unit

5.4.1. Parallel configuration

This configuration is used when a high heat recovery rate is required or a high amount of heat is available to be stored. In this case the oil cycles for the two reactors are connected in parallel configuration, which means that the inlets of the two oil cycles are connected with each other and so are the outlets.

Adsorption procedure

During adsorption water vapors are allowed to enter both reactors simultaneously, the heat produced from the adsorption process in both reactors is collected directly with the oil cycle.

The procedure steps of adsorption can be described as follows:

1. The power supply is turned on to all the electrical equipment and then the ‘Lab-View’ program is started to operate the process.
2. All sensors installed at the set-up are verified by checking the signals received by the program.

3. The data logging in the configuration tab is turned on, which starts the logging of data from all the sensors during the operation.
4. Both thermostats are turned on and set to the required temperatures of oil and water cycles.
5. Both reactors are first evacuated till the minimum achievable pressure and then the evaporators till the corresponding saturation pressure at the prevailing temperature.
6. When the water temperature inside the evaporators is equivalent to the set temperature of water cycle, the valves *V,CT1-E1* and *V,CT2-E2* are opened.
7. When the temperature inside both packed beds is equivalent to the set temperature of oil cycle, the valves *V,R1-E1* and *V,R2-E2* are opened to start the adsorption process.
8. After running this process for desired duration (3hours during this thesis work), the valves *V,R1-E1* and *V,R2-E2* are closed which ends the adsorption process.
9. The program is stopped and both heating and oil cycles are turned off.
10. The difference between the final and initial values of the water levels inside both condensate tanks, detected by the level sensors is the amount of water adsorbed during the entire process.

Desorption procedure

During desorption both reactors are heated at the same time. Which allows high amounts of heat to be stored within a relatively short time.

The procedure of desorption is as follows:

1. The power supply is turned on to all the electrical equipment and the ‘Lab-View’ program is started to operate the process.
2. All sensors installed at the set-up are verified by checking the signals received by the program.
3. The data logging in the configuration tab is turned on, which starts the logging of data from all the sensors during the operation.
4. Both reactors are first evacuated till the minimum achievable pressure and then both condensers along with the condensate tanks till the corresponding saturation pressure at the prevailing temperature.
5. Both thermostats are turned on and set to the required temperatures of oil and water cycles.
6. When the pressure inside each reactor is higher than the saturation pressure of water, the corresponding valves *V,C1-R1* and *V,C1-CT1* for the first reactor or *V,C2-R2* and *V,C2-CT2* for the second reactor are opened.
7. After running this process for desired duration (4hours during this thesis work), the valves *V,C1-R1*, *V, C1-CT1*, *V,C2-R2* and *V,C2-CT2* are closed which ends the desorption process.
8. The program is stopped and both heating and oil cycles are turned off.

9. The difference between the final and initial values of the water levels inside both condensate tanks, detected by the level sensors is the amount of water desorbed during the entire process.

5.4.2. Serial configuration

This configuration is used when the amount of recovered heat is more important than the recovery rate (adsorption), or when the amount of heat available to be stored is relatively low. In this case the oil cycles for the two reactors are connected in serial configuration, which means that the oil cycle outlet of the first reactor can be connected with the oil cycle inlet of the second reactor.

Adsorption procedure

In this configuration the adsorption process in the first reactor is similar to the case of single reactor, however the sensible heat left in reactor 1 can be utilized in two ways, either by preheating reactor 2 or by heating the water in evaporator 2.

The procedure of adsorption is as follows:

1. The power supply is turned on to all the electrical equipment and then the ‘Lab-View’ program is started to operate the process.
2. All sensors installed at the set-up are verified by checking the signals received by the program.
3. The data logging in the configuration tab is turned on, which starts the logging of data from all the sensors during the operation.
4. Both thermostats are turned on and set to the required temperatures of oil and water cycles.
5. Both reactors are first evacuated till the minimum achievable pressure and then the evaporators till the corresponding saturation pressure at the prevailing temperature.
6. When the water temperature inside the evaporator 1 is equivalent to the set temperature of water cycle, the valves *V,CT1-E1* is opened.
7. When the temperature inside the packed bed in reactor 1 is equivalent to the set temperature of oil cycle, the valves *V,R1-E1* is opened to start the adsorption process.
8. After running this process for desired duration (3 hours during this thesis work), the valve *V,R1-E1* is closed which ends the adsorption process in the first reactor.
9. The valve V,R1-out is positioned in a way to allow the oil cycle to transfer the sensible heat left in reactor 1 to either reactor 2 or evaporator 2 depending on the chosen strategy.
10. Both V,R1-R2 and V,R2-in valves are positioned in a way to lead the oil from the oil cycle either to reactor 2 or to evaporator 2.
11. When the water temperature inside the evaporator 2 is equivalent to the set temperature of water cycle, the valves *V,CT2-E2* is opened.

12. When the temperature inside the packed bed in reactor 2 is equivalent to the set temperature of oil cycle, the valves *V,R2-E2* is opened to start the adsorption process.
13. After running this process for desired duration (3hours during this thesis work), the valve *V,R2-E2* is closed which ends the adsorption process in the first reactor.
14. The program is stopped and both heating and oil cycles are turned off.
15. The difference between the final and initial values of the water levels inside both condensate tanks, detected by the level sensors is the amount of water adsorbed during the entire process.

Note: during the second adsorption process (in reactor 2), if the temperature in reactor 1 drops down to the water temperature in evaporator 2 or the temperature in reactor 2 (depending on the chosen strategy), this indicates that the left sensible heat in reactor 1 is maximally utilized. In this case the valves V,R1-out, V,R1-R2 and V,R2-in are positioned in a way, so that reactor 2 (or evaporator 2) will be heated up directly from the oil thermostat.

Desorption procedure

In this configuration the desorption process in the first reactor is similar to the case of single reactor, however the sensible heat left in the first reactor after desorption could be used to preheat the second reactor.

The procedure of desorption is as follows:

1. The power supply is turned on to all the electrical equipment and the 'Lab-View' program is started to operate the process.
2. All sensors installed at the set-up are verified by checking the signals received by the program.
3. The data logging in the configuration tab is turned on, which starts the logging of data from all the sensors during the operation.
4. Both reactors are first evacuated till the minimum achievable pressure and then both condensers along with the condensate tanks till the corresponding saturation pressure at the prevailing temperature.
5. Both thermostats are turned on and set to the required temperatures of oil and water cycles, but only the first reactor is heated to the set temperature.
6. When the pressure inside reactor 1 is higher than the saturation pressure of water, the corresponding valves *V,C1-R1* and *V,C1-CT1* for the first reactor are opened.
7. After running this process for desired duration (4 hours during this thesis work), the valves *V,C1-R1* and *V, C1-CT1* are closed which ends the first part of the desorption process.
8. The valve V,R1-out is positioned in a way to allow the oil cycle to transfer the sensible heat left in reactor 1 to reactor 2.
9. Both V,R1-R2 and V,R2-in valves are positioned in a way to lead the oil from the oil cycle to reactor 2.
10. When the pressure inside reactor 2 is higher than the saturation pressure of water, the corresponding valves *V,C2-R2* and *V,C2-CT2* for the first reactor are opened.

11. After running this process for desired duration (4hours during this thesis work), the valves *V,C2-R2* and *V, C2-CT2* are closed which ends the second part of the desorption process.
12. The program is stopped and both heating and oil cycles are turned off.
13. The difference between the final and initial values of the water levels inside both condensate tanks, detected by the level sensors is the amount of water desorbed during the entire process.

Note: during the second desorption process (in reactor 2), if the temperature in reactor 1 drops down to the temperature in reactor 2, this indicates that the left sensible heat in reactor 1 is maximally utilized. In this case the valves V,R1-out, V,R1-R2 and V,R2-in are positioned in a way, so that reactor 2 will be heated up directly from the oil thermostat.

5.5. System control

Developing algorithms for an automatic control of the adsorption TES system comes on a high importance in order to achieve an optimal overall performance of the system.
Thus, controlling algorithms corresponding to both parallel and serial configurations were developed and implemented to a software for the heat storage unit (using LabVIEW), offering the capability of controlling the different elements of the heat storage unit and the flexibility to modify its structure in order to get the best performance (as shown in Figure 5.12).

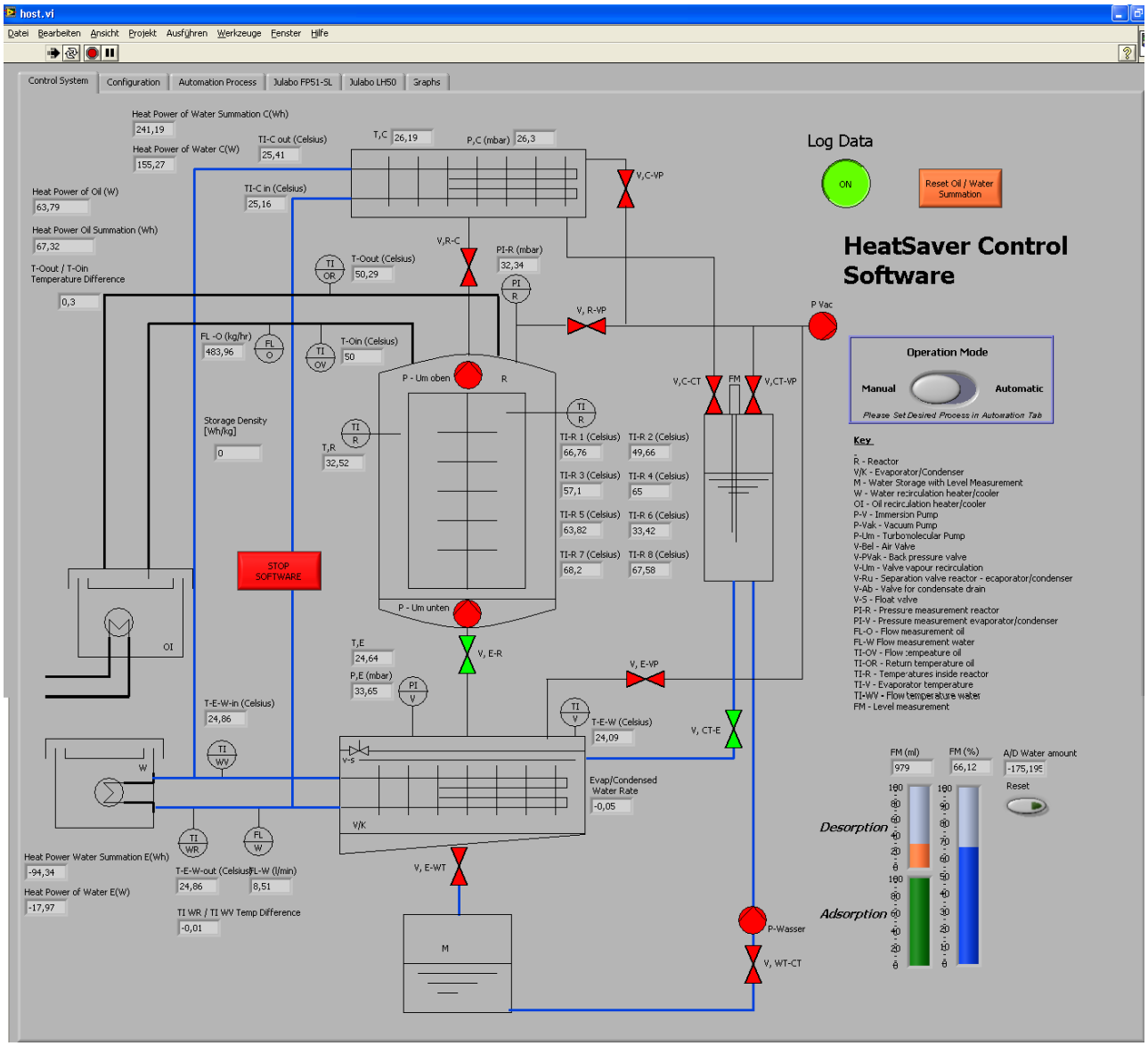

Figure 5.12 User interface of the TES controlling software (set-up)

Additionally, the software offers instant and continuous calculation of the different heat shares, including the stored and wasted heat amounts (Figure 5.13). With the real-time functionality, the system is able to directly detect to any parameter changes and react accordingly, in a way to assure the optimal overall efficiency of the system.

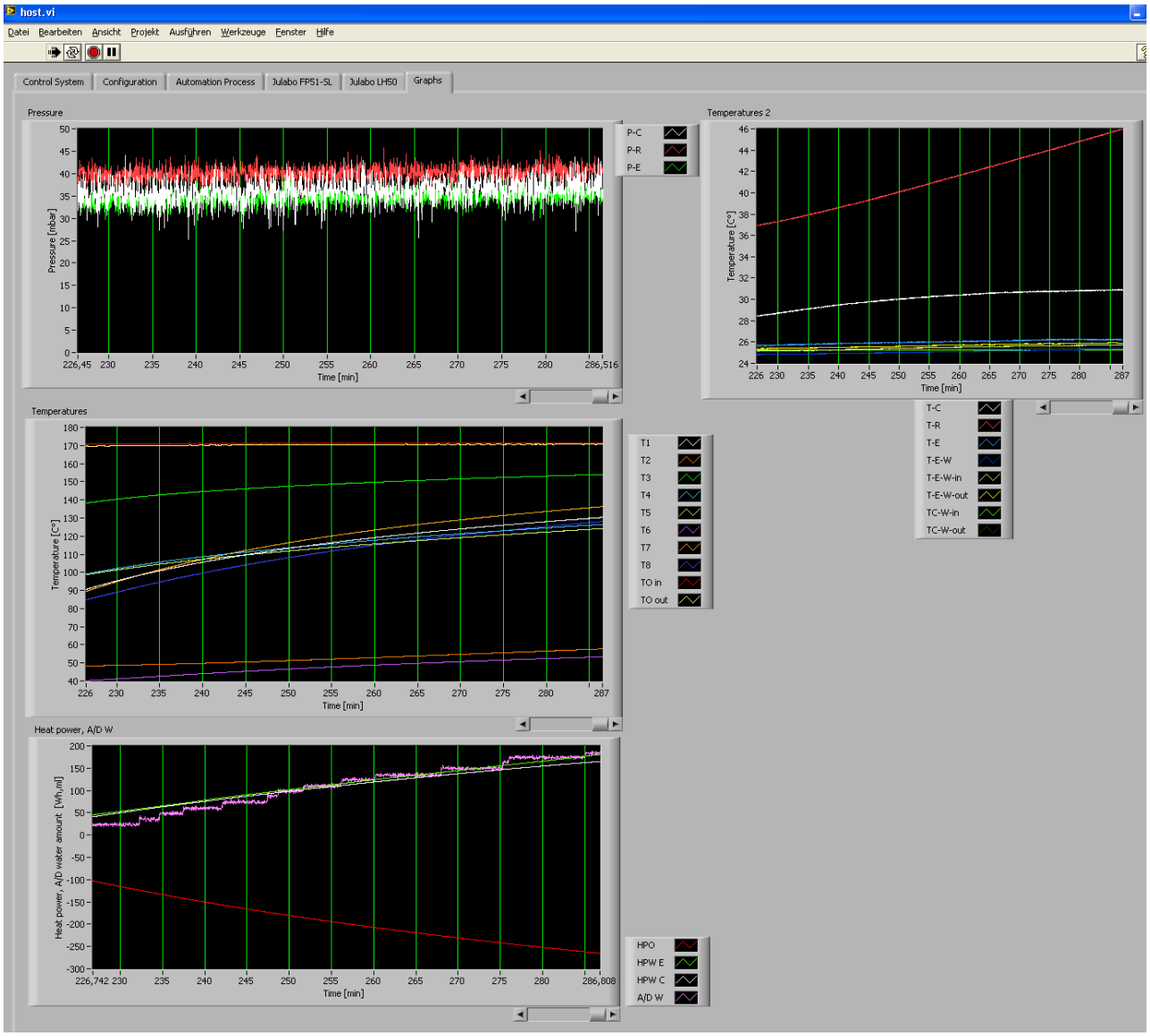

Figure 5.13 User interface of the TES controlling software (results)

Furthermore, the automated process increases the operational safety of the system, by continuous monitoring of all the critical criteria and by taking appropriate measures and sending alarm signals in case of emergency.

6. Results and Discussion

In this chapter the results from both, the sorption thermal storage unit and the simulations are being presented and discussed. The first part will focus on the simulations, while the second part is dedicated for the technical modification and the conducted experiments.

6.1. Simulation

Within this work, two different types of simulations were carried out. On one hand a heat and mass transfer simulation was performed to achieve an optimal heat distribution in the packed bed, and on the other hand a process simulation was done in order to test different control strategies with different parameters for the heat storage system.

6.1.1. Reactor design improvement

With the help of FEM simulation program (COMSOL), simulations for heat and mass transfer were carried out, in order to visualize the temperature distribution inside the reactor, and to observe how it's influenced by the flow during both adsorption and desorption.

As the main focus is the heat transfer in the reactor, both adsorption and desorption processes were simplified. Therefore, the adsorption/desorption process on the micro level was replaced with an interface using the preliminary experimental values.

6.1.1.1. Adsorption

During adsorption, the zeolite packed bed was defined as heat source with 120°C (value was taken from preliminary experiments) in order to simulate the adsorption effect by its peak. The heat exchanger was defined as heat sink with 30°C (corresponding to the inlet temperature of the oil cycle). Mass flow of water vapor at 25°C was introduced form the inlet at the bottom of the reactor. Figure 6.1 shows the steady state temperature distribution during an adsorption process

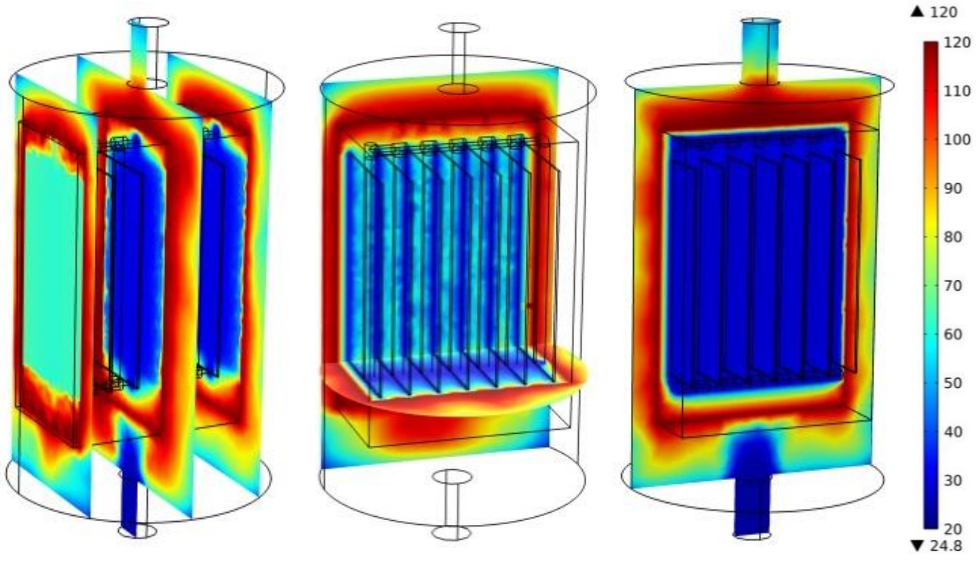

Figure 6.1 Temperature distribution inside the reactor during adsorption process

The results have shown that the water vapor in the reactor gets heated from the packed bed. Due to natural convection, the heated vapor flows to the top, and with continues heating, it gets pushed downwards along the reactor sides.

It's also noticeable that the cooling effect of the current design of the heat exchanger is limited within the inner part of the fixed bed and its influence doesn't exceed to the outer side of the packed bed. Hence, an enhanced design of the heat exchanger is needed, in order to achieve lower temperatures of zeolite and water vapor surrounding the packed bed and thus improving the adsorption process.

6.1.1.2. Desorption

During desorption, the reactor's walls were defined as heat sink with 25°C (ambient temperature). The heat exchanger tubes were defined as heat source with 235°C (corresponding to the temperature of the oil cycle).

Stationary simulation

Figure 6.2 represents the result of a stationary simulation for temperature distribution during a desorption process

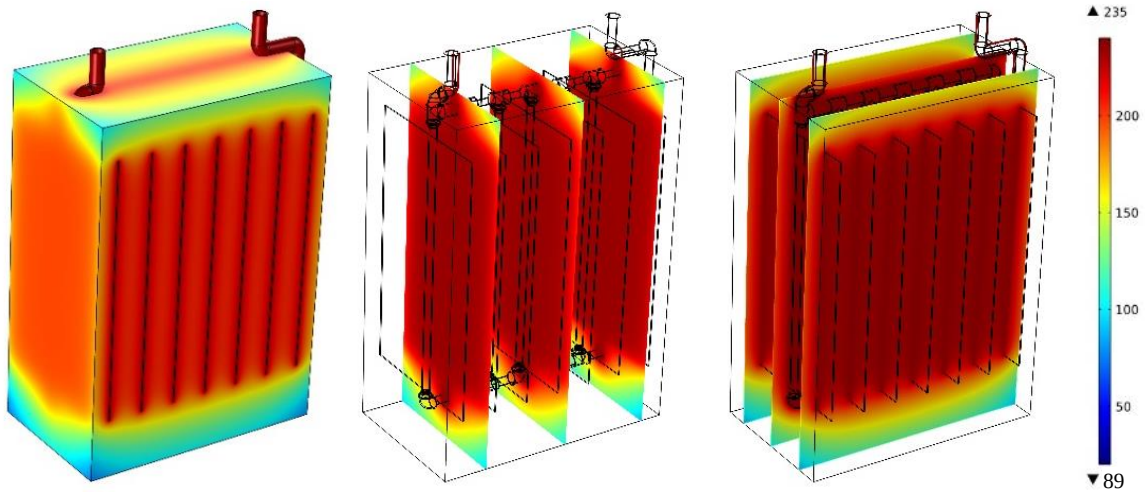

Figure 6.2 Temperature distribution inside the packed bed during desorption process

The simulation's result has shown that the temperature in the packed bed is not equally distributed. A minimum temperature of 89°C still can be noticed at the lower corners of the packed bed, even after reaching the stationary state (which is about 32% of the temperature at the inlet). This means that the zeolite at the bottom of the packed bed will still have a higher level of water load after the end of the desorption process, due to the relatively low temperature. Therefore, a better design of the heat exchanger is required to improve the heat storage capacity. It's also worth mentioning, that there is a temperature gradient alongside the fins, however the gradient is small compared to the relatively large temperature-scale used to present the results.

Transient (time-dependent) simulation

For a better understanding of the temperature distribution during desorption process, a time dependent simulation was performed. Figure 6.3 shows the simulation result with a 10-minutes time interval.

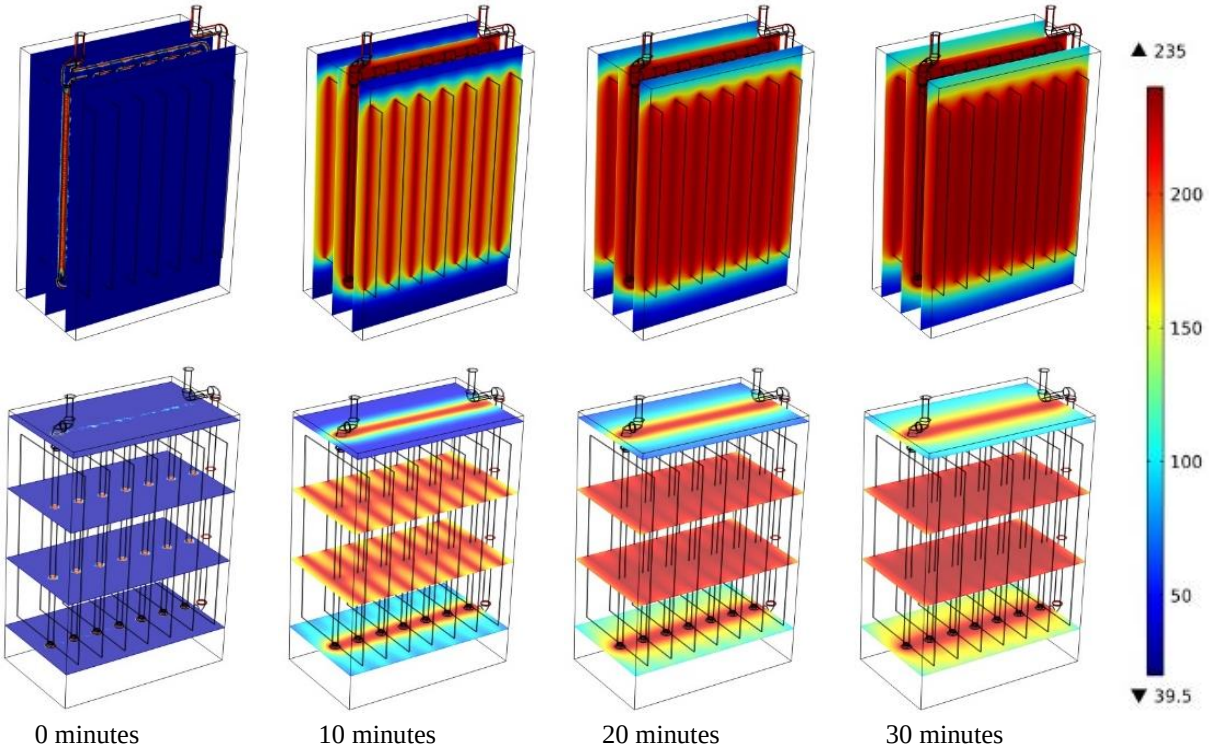

Figure 6.3 Temperature distribution change inside the packed bed during the first 30 minutes of desorption

The simulation's results have shown that within the first 20 minutes, high temperature of zeolite between the fins of the heat exchanger is reached. However, even after 30 minutes of desorption the temperature at the bottom of the packed bed is still around 39.5°C. This can be related to the low thermal conductivity of zeolite, which reflects the need for a heat exchanger that can deliver heat to the entire packed bed.

6.1.1.3. Heat exchanger design

The results from the heat transfer simulation expressed the importance of having an optimal heat exchanger design in order to improve both of the adsorption and desorption processes, which in its turn increases the heat storage efficiency.

Therefore, different designs of heat exchanger were analyzed and simulated to reach the optimal design for the corresponding heat storage unit.

All the simulations for the different designs were stationary, with the heat exchanger as heat source at 120°C and the reactor walls as heat sink at 25°C.

Plates and tubes heat exchanger

The first studied design was for a plates and tubes heat exchanger. The design consists of 5 parallel plates each one has tubes inside, allowing the oil to flow evenly through the plate. All the plates are connected from the top with main inlet and outlet tubes.

Figure 6.4 represents the result of a stationary simulation for temperature distribution with the plates and tubes heat exchanger

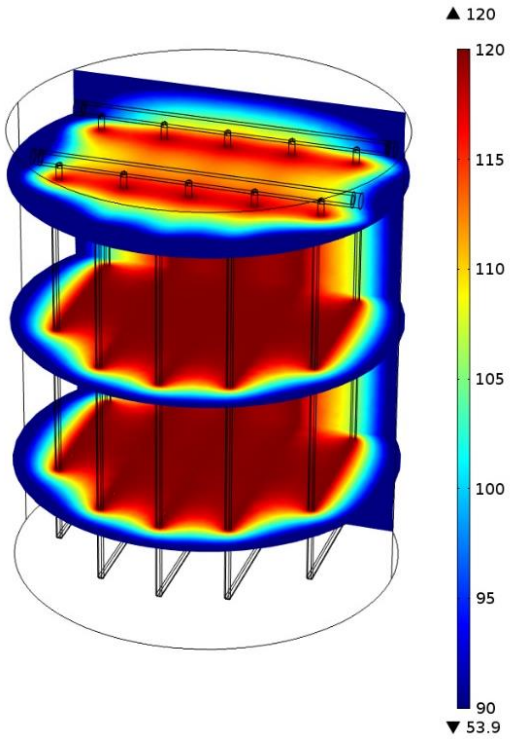

Figure 6.4 Temperature distribution inside the reactor with the plates and tubes heat exchanger

As the results show, a minimum temperature of 53.9°C was reached in the reactor, which is about 45% of the temperature at the inlet (maximum temperature).

Tubes heat exchanger

The next studied design consists of tubes-only heat exchanger. The goal was to achieve an evenly distributed temperature along the vertical direction, by having upwards and downwards oil streams in the heat exchanger.

Figure 6.5 shows the result of a stationary simulation for temperature distribution with the tubes heat exchanger

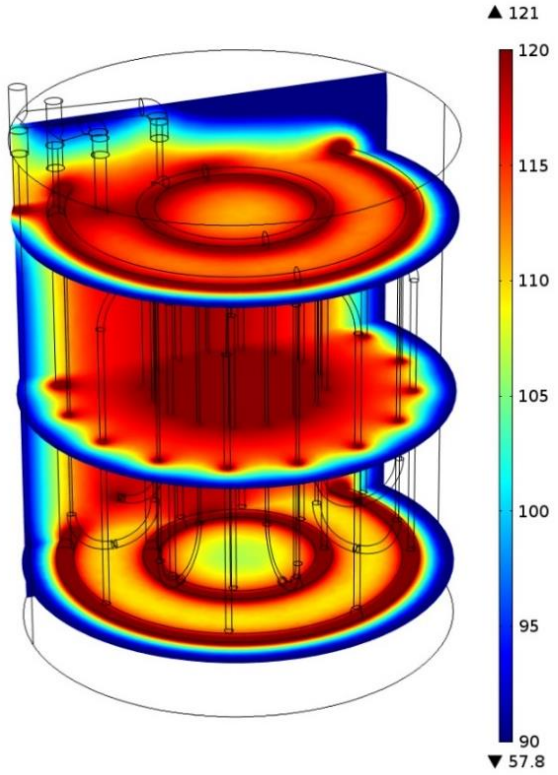

Figure 6.5 Temperature distribution inside the reactor with the tubes heat exchanger

As the results show, a minimum temperature of ca.57.8°C was reached in the reactor, which is about 48% of the temperature at the inlet (maximum temperature).

Cylinders and tubes heat exchanger

Further heat exchanger designs were studied, where a combination of tubes and cylindrical metal sheets was used. The designs can fall into two categories: one-direction flow and double-direction flow designs. All the designs consist of two cylindrical metal sheets connected with each other

One direction flow

By the one-direction flow design, the tubes were built in such a way that the oil flows from the inlet, gets distributed in many finer tubes, where it flows downwards. Finally, it gets collected at the bottom of the heat exchanger and flows towards the outlet.

Two different designs with one-direction flow were tested, one design with three main inlet tubes (as shown in Figure 6.6) and another design with 5 main inlet tubes.

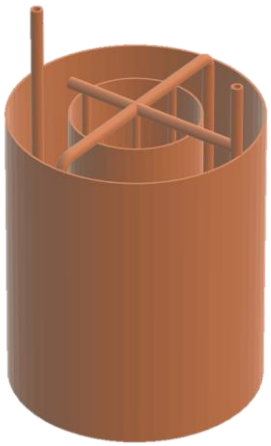

Figure 6.6 Design of cylinders and tubes heat exchanger (one-direction flow) with 3 main inlet tubes

Figure 6.7 represents the results of a stationary simulations for temperature distribution with the cylinders and tubes heat exchanger for both 3-tubes inlet and 5-tubes inlet designs

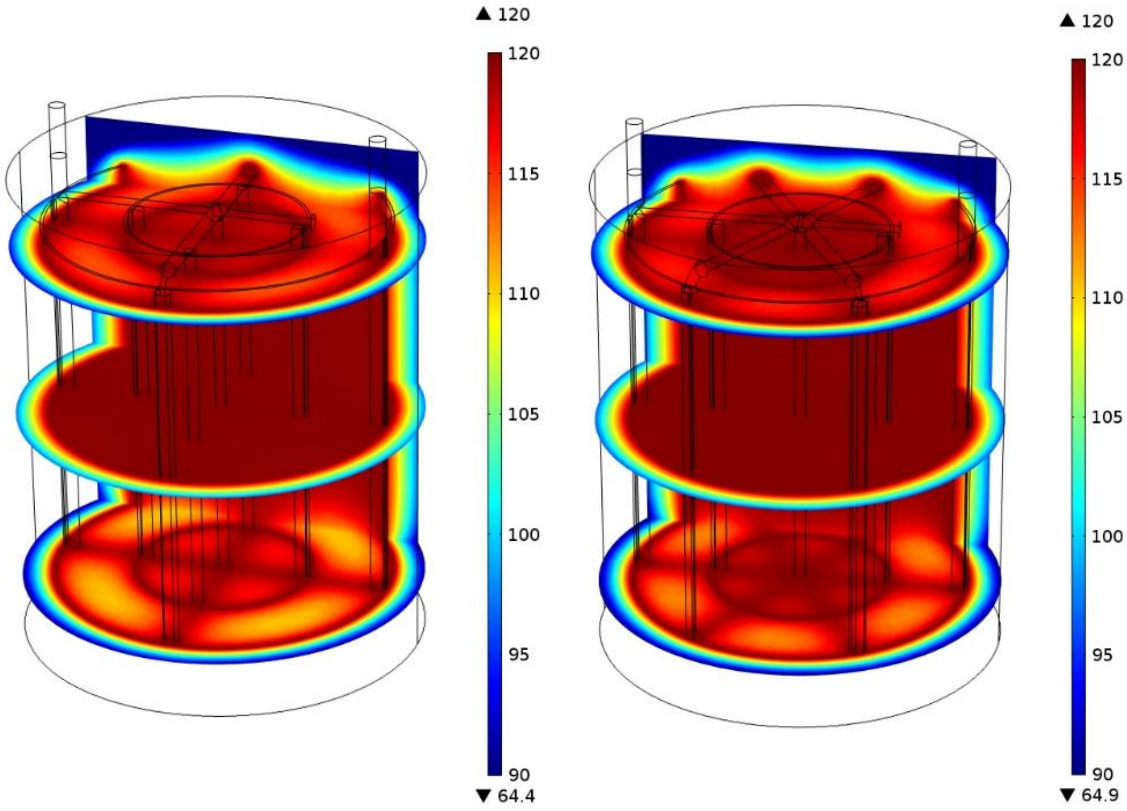

Figure 6.7 Temperature distribution inside the reactor with the cylinders and tubes heat exchanger (one-direction flow) for 3-tubes inlet (left) and 5-tubes inlet (right)

The results have shown, that a similar minimum temperature was reached in the reactor for both 3-tubes and 5-tubes inlet with 64.4°C and 64.9°C respectively, which is about 54% of the temperature at the inlet (maximum temperature).

This reveals that increasing the number of main inlet tubes doesn't significantly improve the reached minimum temperature in the reactor. However, the temperature distribution in the reactor was better with the 5-tubes inlet design, as can be noticed from the results.

Double direction flow

By the double-direction flow design, the tubes were built in such a way that the oil flows from the inlet, gets distributed in many finer tubes. The oil flows in three tubes downwards and in another three tubes it flows upwards. Finally, it gets collected at the bottom and the top of the heat exchanger and flows towards the outlet.

Figure 6.8 represents the results of a stationary simulations for temperature distribution with the cylinders and tubes heat exchanger (double-direction flow).

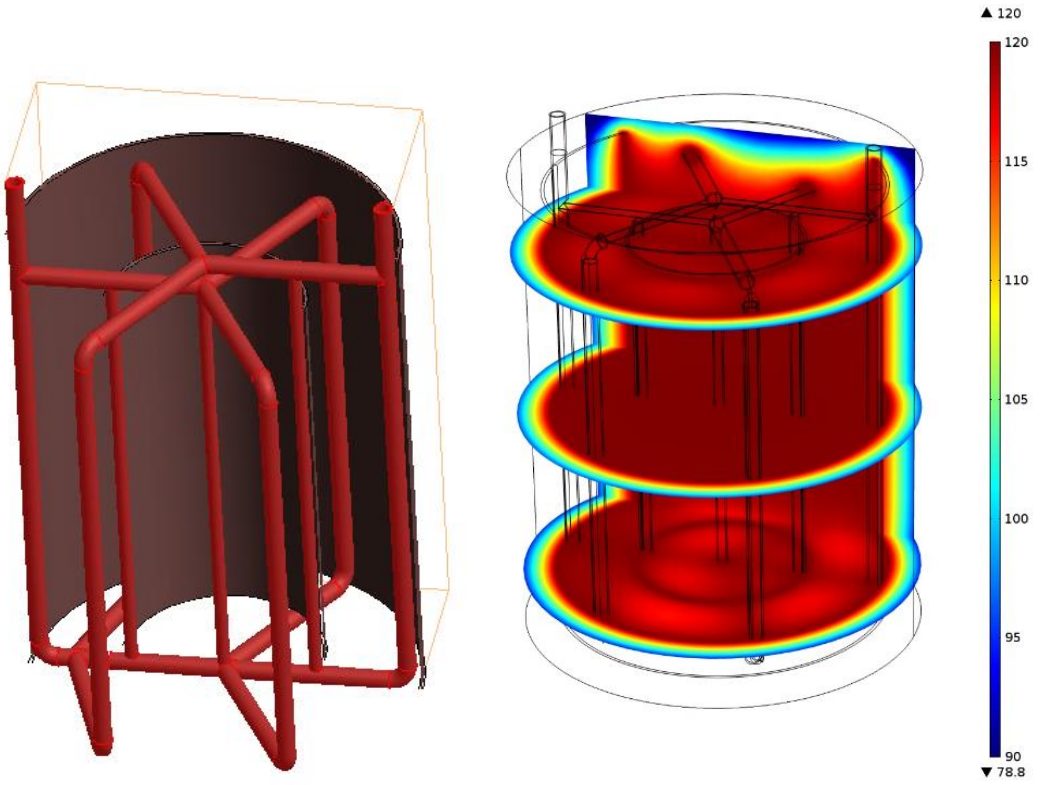

Figure 6.8 Temperature distribution (right) and geometry (left) inside the reactor with the cylinders and tubes heat exchanger (double-direction flow)

As the results show, a minimum temperature of 78.8°C was reached in the reactor, which is about 65.8% of the temperature at the inlet (maximum temperature). This design has given the best performance regarding the temperature distribution, where the minimum temperature was about two thirds of the maximum temperature. Therefore, this design was chosen for the heat storage unit, in order to perform further experimental testing. The following table summarizes the results from all tested designs.

Table 6-1 Lowest temperature in packed bed with different designs of heat exchanger

Design	Plates and tubes	Tubes	Cylinders and tubes		
			One direction flow		Double direction flow
			3 tubes	5 tubes	
T_{min} [°C]	53.9	57.8	64.4	64.9	78.8

6.1.2. Process improvement

Process simulations were performed using LabVIEW for both desorption and adsorption processes. For each process, the temperature behavior with single- and multiple-reactor setup were simulated. Furthermore, the different heat shares were calculated. The simulations' results were then compared to preliminary experimental values.

6.1.2.1. Desorption

With the help of desorption process simulation, the average temperature behavior inside the reactor was calculated. The result of the simulation was compared to measurements done with different temperature sensors in different locations. Figure 6.9 shows the measured temperature behavior during the preliminary experiments compared to the simulation.

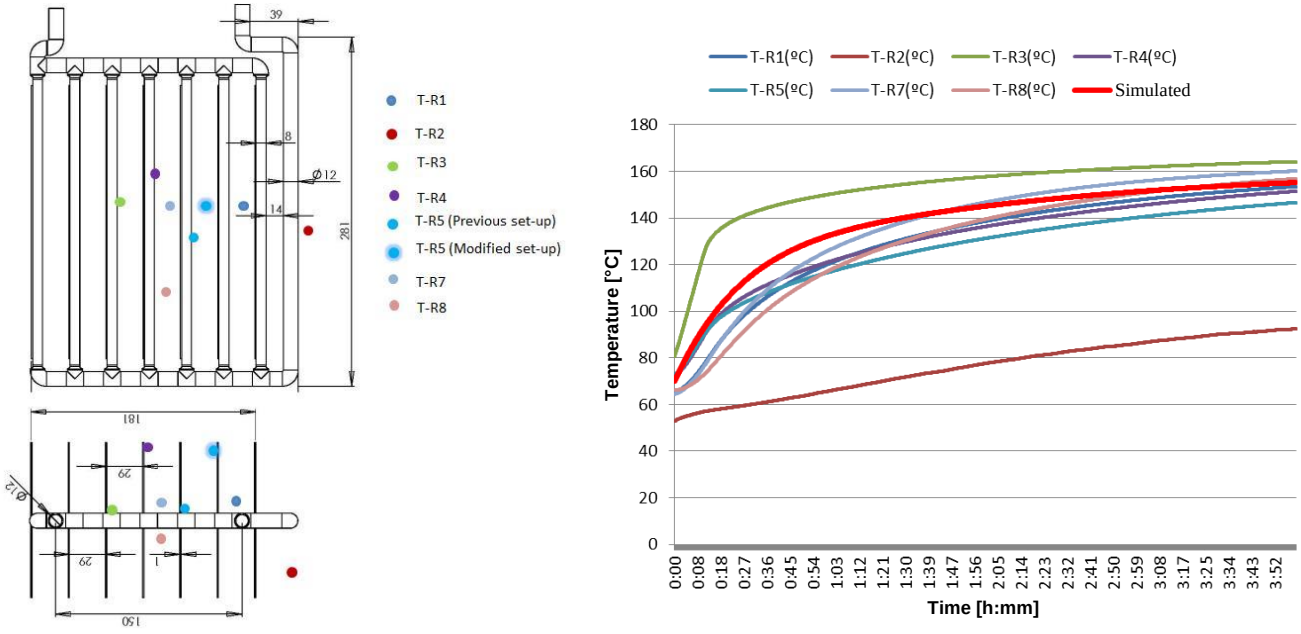

Figure 6.9 Simulated temperature behavior (red) inside the reactor during desorption compared to measured temperatures at different locations

The result has shown, that the simulated temperature behavior (average value) has a similar behavior as the measured temperatures. This can confirm that the calculated values are valid.

The simulation was carried out further, in order to simulate the potential recoverable energy, when multiple reactors are used.

Figure 6.10 represents the simulated temperature during desorption inside three reactors connected with serial configuration, where the sensible heat after the end of each desorption

process is being recovered to preheat the next reactor. The duration of the simulated heat recovery was 40 minutes.

The initial temperature was given as 70°C assuming that the desorption process took place directly after the end of the adsorption process, which is only the case during the laboratory experiments and doesn't reflect the real-life application of the heat storage system.

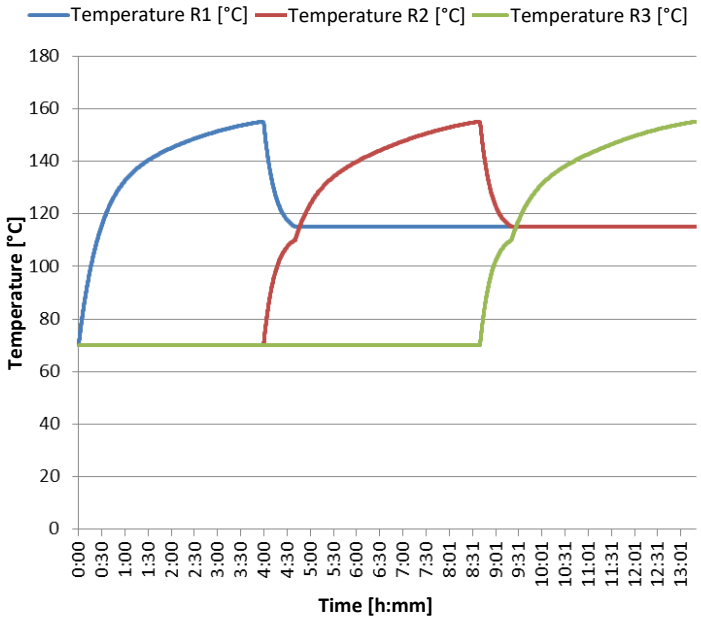

Figure 6.10 Simulated temperature behavior during desorption inside three reactors connected with serial configuration (with sensible heat recovery)

Figure 6.11 shows the amount of heat invested in each reactor during desorption.

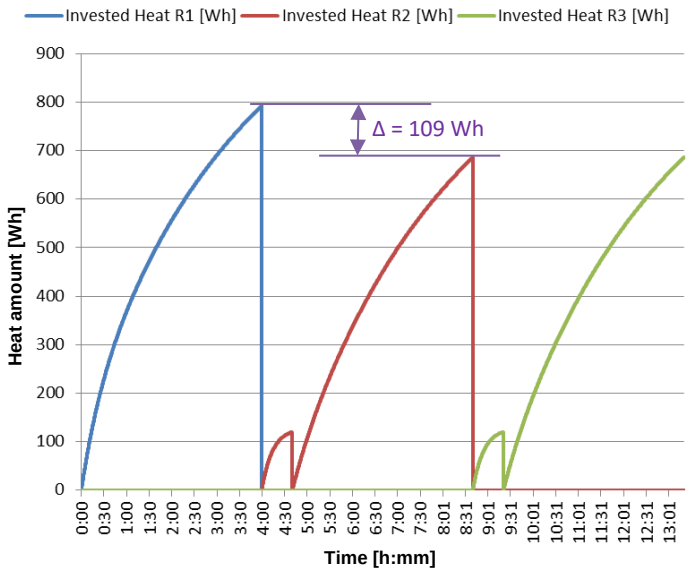

Figure 6.11 Heat amount invested in each reactor during desorption (with sensible heat recovery)

From the result, it is noticeable that about 13.75% of the invested energy can be reduced, by using the sensible heat from one reactor to preheat the next one.

The different energy shares of the total invested heat during desorption were also simulated as shown in Figure 6.12.

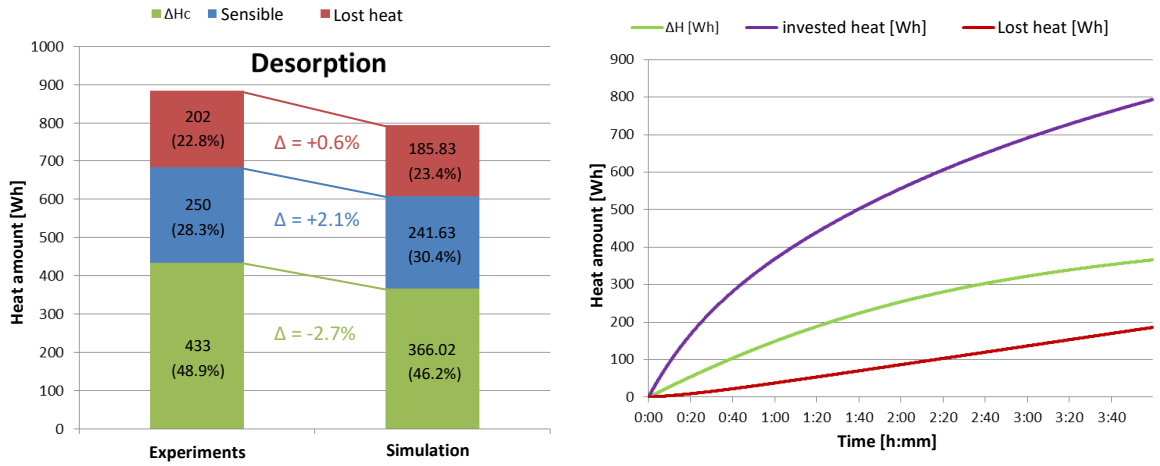

Figure 6.12 Heat shares of the total invested heat during desorption

By comparing the results of heat shares from simulation and experiments, it's noticeable that the total invested heat by simulation was about 10% less than the calculated value from the results. This could be related to many reasons, such as the simplifications and assumptions which were included in the simulation.

However, the heat shares from both simulation and experimental values have shown similar distribution values. The share of the stored heat was 2.7% lower by the simulation compared to the experiments, whereas the shares of sensible and lost heat were higher by 2.1% and 0.6% respectively.

6.1.2.2. Adsorption

With the help of adsorption process simulation, the average temperature behavior inside the reactor was calculated. The comparison between the experimental and simulated values is shown in Figure 6.13. Where it's clear that simulated temperature behavior is similar to the real one.

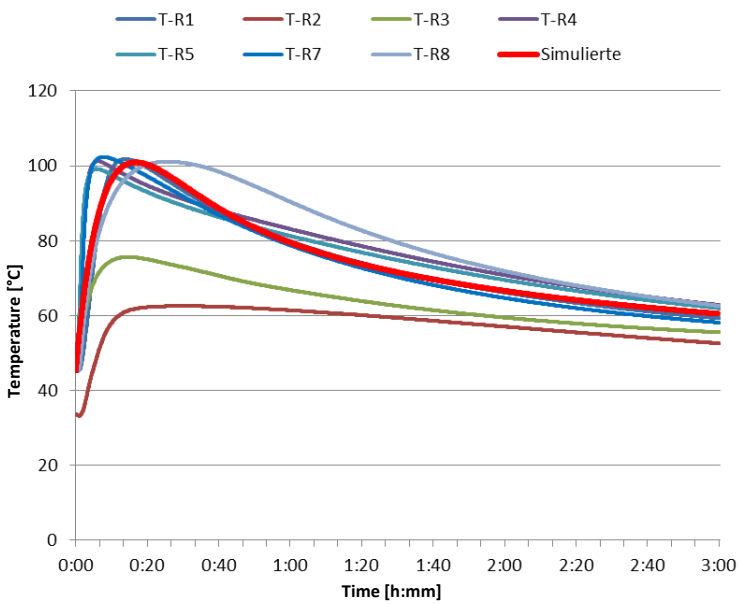

Figure 6.13 Simulated temperature behavior (red) inside the reactor during adsorption compared to measured temperatures at different locations

For a better visualization, the simulated temperature behavior was compared to average temperatures from 3 experimental repetitions of adsorption process, the results are shown in Figure 6.14

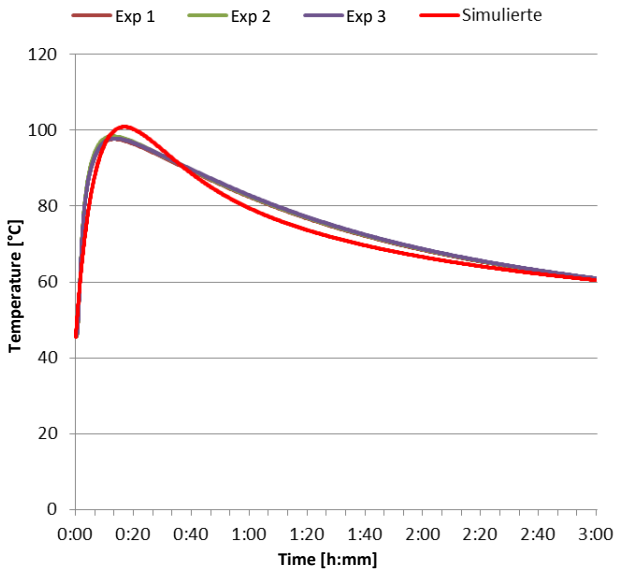

Figure 6.14 Simulated temperature behavior (red) inside the reactor during adsorption compared to average temperatures from different experiments

The result has shown, that the simulated temperature behavior has a similar behavior as the average of the measured temperatures. This can confirm that the calculated values are valid.

The simulation was carried out further, in order to simulate the potential recoverable energy, when multiple reactors are used.

Figure 6.15 represents the simulated temperature during adsorption inside three reactors connected with serial configuration, where the sensible heat after the end of each adsorption process is being recovered to preheat the next reactor.

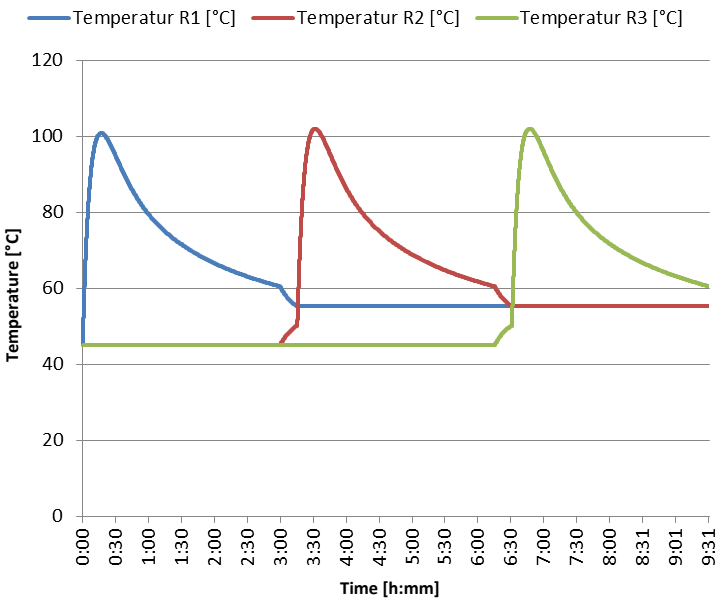

Figure 6.15 Simulated temperature behavior during adsorption inside three reactors connected with serial configuration (with sensible heat recovery)

Figure 6.16 shows the amount of heat recovered from each reactor during adsorption.

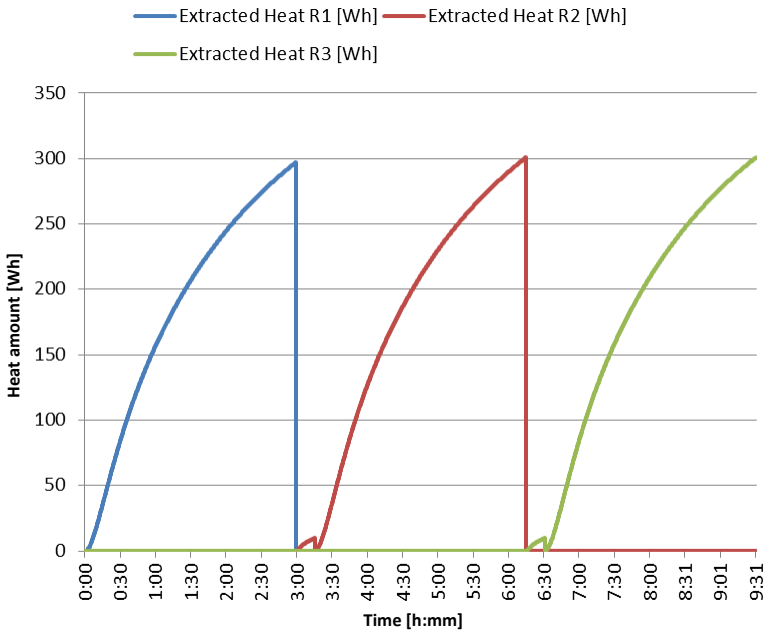

Figure 6.16 Heat amount recovered from each reactor during adsorption (with sensible heat recovery)

From the result, it is noticeable that contribution of the recovered sensible heat to the total recovered heat is not significant (about 1%) and thus using the sensible heat to preheat the next reactor during adsorption will not improve the heat storage efficiency. Such a result was expected, because the temperature difference between the start and the end of an adsorption process is relatively low (15 °C).

However, the sensible heat left in the reactor after adsorption can still be used to heat the evaporator of the next reactor.

6.2. Technical modifications

The effect of various technical modifications is described in this part, the modifications consist mainly from the implementation of fans, separation of evaporator/condenser (with extra insulation), heat exchanger optimization and using multiple reactors.

6.2.1. Fans and evacuations

The reactor and condenser of the modified set-up are evacuated during adsorption and desorption respectively, in order to remove any traces of trapped gases. Furthermore, fans inside the reactor are used both during adsorption as well as desorption process. The effect of fans and evacuations is evaluated by performing experiments with different combinations as:

- With fans (F)
- With fans and evacuations (F+E)

The performance of system is compared for different combinations of components with that during reference experiments (R) as shown in Table 6-2 . The additional electrical power consumption was not taken into consideration, although it should be considered if this process is to be used in the future. All experiments are conducted using parameter set-A with modified set-up. The amount of dry zeolite used during the experiments is 4.756 kg

Table 6-2: Comparison of different operation sets in the modified set-up

Experiment set	Q_R	Q_i	ΔH_{ad}	η_{ad}	η_d	η_o	ESD	Water uptake
	[Wh]	[Wh]	[Wh]	[%]	[%]	[%]	[Wh/kg]	kg water/kg zeolite
R	210	885	433	48.5	48.9	23.7	44.1±0.4	0.095
F	198	896	433	45.8	48.3	22.1	41.7±0.3	0.095
F+E	205	904	433	47.4	47.9	22.7	43.1±0.9	0.095

From Table 6-2, it is clear that the system shows the best performance in terms of overall efficiency η_o *and* energy storage density *ESD* during reference experiments. However, the difference in performance for three different experiment sets is within 6%. The calculations shown in Table 6-2 are done by assuming the same water uptake by zeolite as well as the same minimum and maximum load for all experiment sets. Therefore, the small difference in performance may be due to the small variation in load conditons.

Figure 6.17 shows the bar graphs of above data along with the difference between the three repetitions for each set shown by error bars (based on maximum and minimum values between the repetitions).

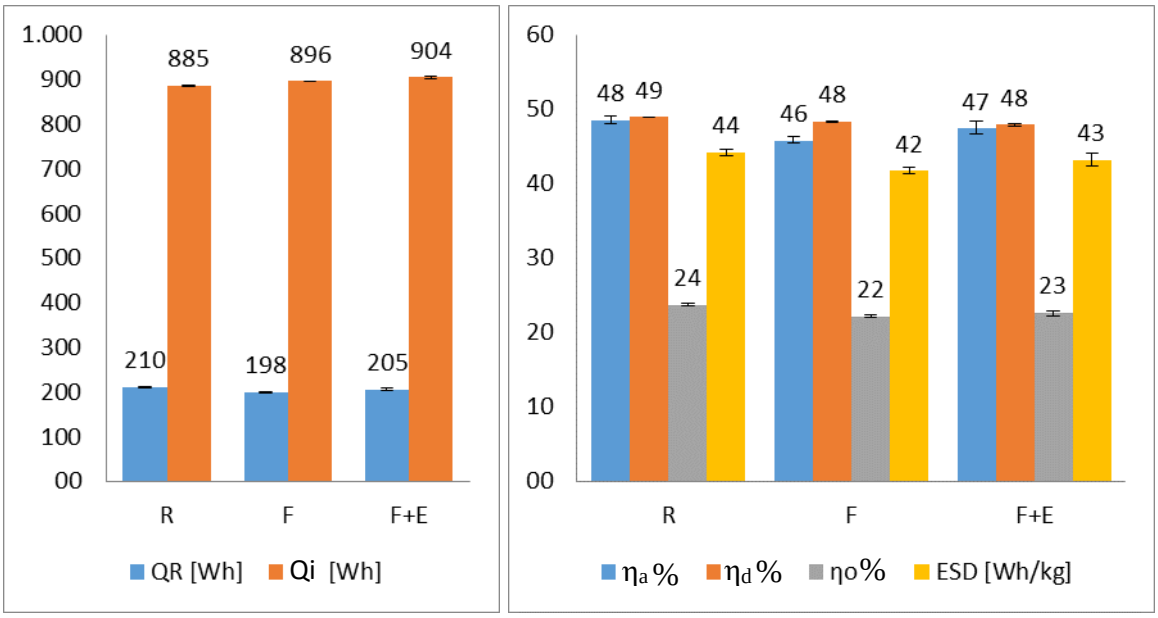

Figure 6.17: Comparison between different operation-sets used with modified set-up

Adsorption

- **Rate of adsorption**

The amount of water adsorbed during the adsorption process is the function of pressure ratio p/p^0. The amount of vapor adsorbed increases as the pressure approaches the partial pressure of the vapor and reaches the maximum value at a pressure ratio of 1. During the experiments the pressure ratio is nearly 1.

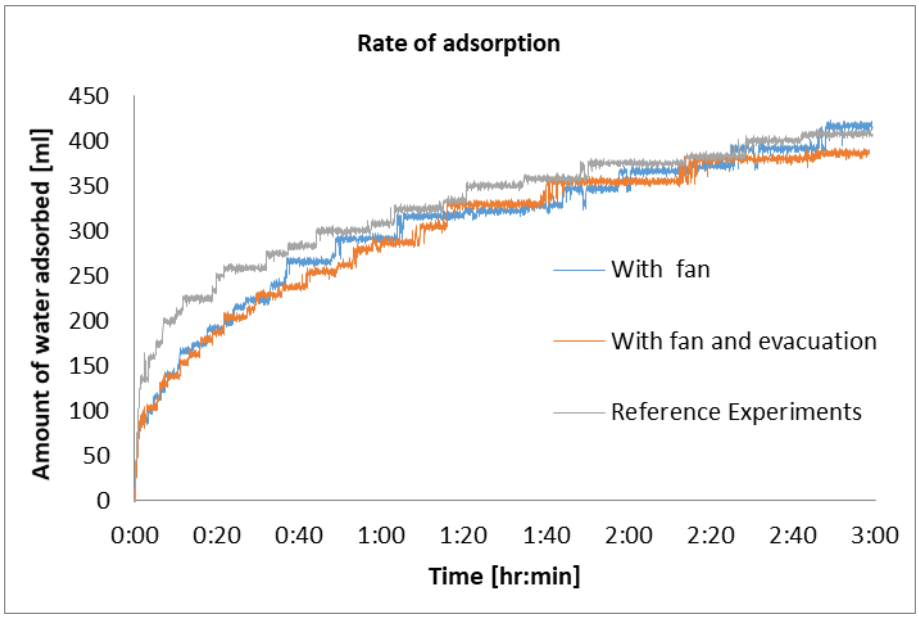

Figure 6.18: Rate of adsorption for different experiment sets

The typical behavior of adsorption rate is shown in Figure 6.18. The rate of adsorption is very high at the start of the process and around 25% of the total volume is adsorbed immediately within a minute. The water load of zeolite is very low at the start of adsorption process. Therefore, the affinity of zeolite for water vapor is very high which results in high amount of water adsorbed at the beginning. The rate decreases afterward and is very low after one hour of operation. 75% of adsorption is over during first hour of operation.

The adsorbed amount of water profiles for different experiment sets is similar except for that of reference experiments. This may be due to the small variation in the initial water load conditions of zeolite before starting the adsorption, which caused the higher rate of adsorption during reference experiments at the beginning as compared to that during experiments with fans and with fans and evacuations.

- **Temperature profiles inside packed bed**

The main aim of installing fan inside the reactor is to force the vapors inside the packed bed during adsorption. The effect of fan is analyzed by comparing the temperature profiles inside the packed bed during operation with and without fan. The temperature profiles at different locations inside the packed bed are shown by the temperature thermocouples (T-R1 to T-R8) with T-R1, T-R4, T-R5, T-R7,T-R8 placed inside the packed and T-R4,T-R5 placed in contact with the two different fins of heat exchanger at different heights inside the packed bed. T-O_{out}, T-O_{in} are the outgoing and incoming temperature of heat transfer fluid inside the heat exchanger. For exact location of different sensors.

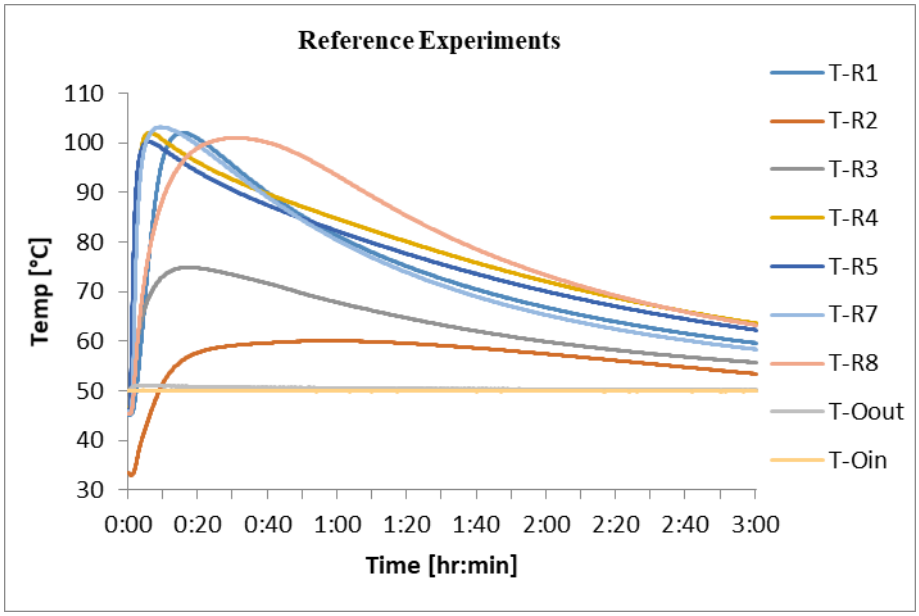

Figure 6.19: Temperature profile inside packed bed during adsorption without ventilator

The temperature peaks within first 10 minutes of operation are evident from Figure 6.19. As we know that, the adsorption potential and thus the adsorption enthalpy decreases with increase in amount of vapor adsorbed and vice versa. Therefore, at the start of adsorption process when the material is in the state of minimum load, high amount of water vapor is adsorbed and therefore high amount of adsorption heat is released. As the process continues, less amount of vapor is adsorbed and thus less mount of adsorption heat is released. Also, the released heat is removed continuously by the heat exchanger. Therefore, the temperature reaches a maximum value depending upon the load of material and then decreases due to continuous extraction of heat on one side and decrease in amount of released heat energy on other side.

Similar temperatures and temperature variation are observed except for T-R2 and T-R3 which are showing relatively lower temperatures during the entire process. This is due to the fact that T-R2 is placed at the steel cage which holds zeolite. Therefore, the temperature at this point is lower due to the conduction between zeolite and steel cage. Whereas thermocouple T-R3 is placed at the tube of heat exchanger containing heat transfer fluid inside the packed bed. Due the immediate vicinity of HTF at this point, the rate of heat transfer through copper tube is high. Therefore, temperature does not show peak similar to that obtained at other points inside the packed bed, where heat transfer rate is comparatively low due to low thermal conductivity of packed bed of zeolite (0.08 W/m.K) as compared to thermal conductivity of copper (350 W/m.K).

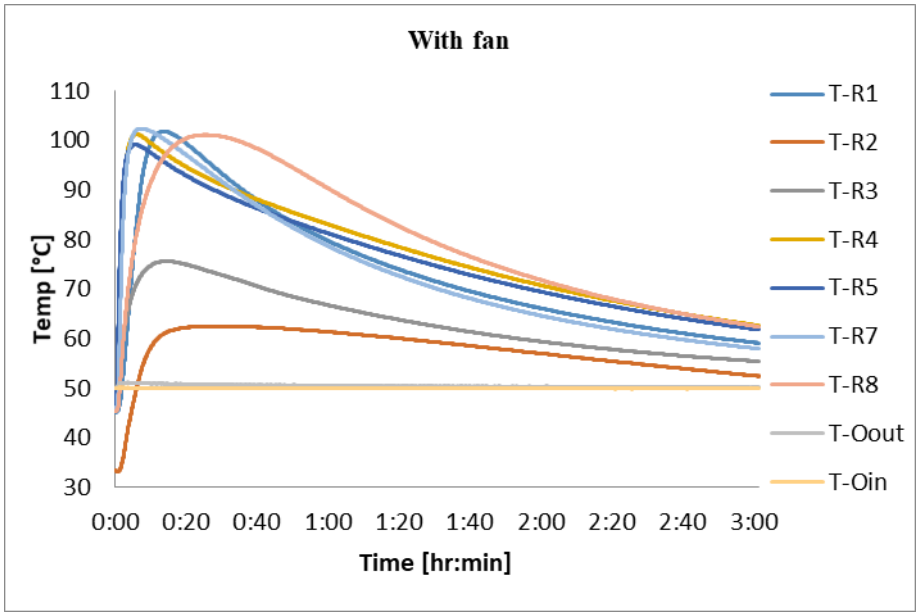

Figure 6.20: Temperature profile inside packed bed during adsorption with ventilator

Figure 6.19 and Figure 6.20 show similar temperature profiles during operation with and without fan. This indicated that the amount of released heat is also similar, and thus, the effect of fan in pushing the vapors through the packed bed of zeolite is negligible.

The temperature profiles at different locations inside packed bed during the use of fan and evacuation is as shown in Figure 6.21.
During the evacuations, the reactor is isolated from evaporator and then evacuated for 10 sec. This is done in order to remove any traces of trapped gases in the pores of zeolite. However,

some water vapor also gets evacuated during this process. A sudden jump in the temperature peaks is observed after evacuating the reactor.

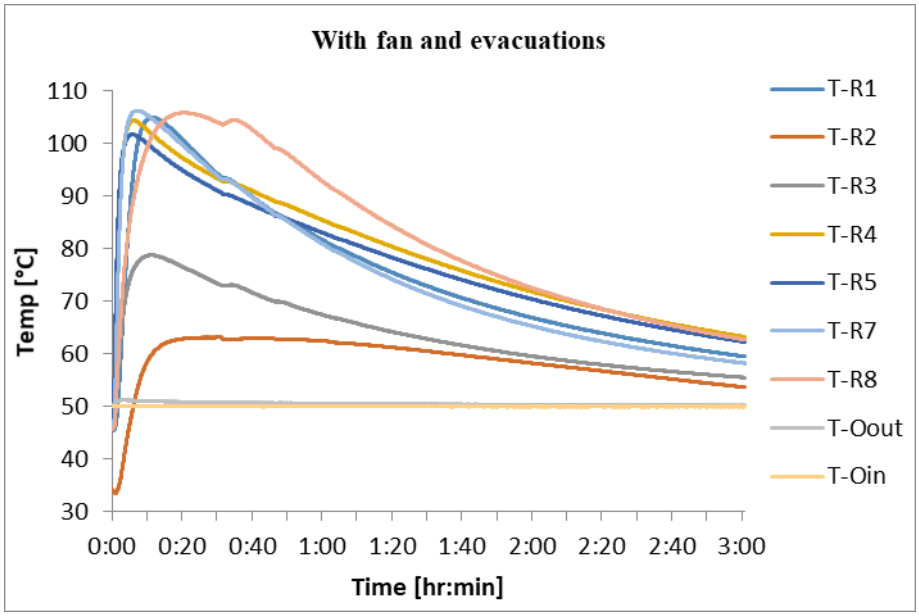

Figure 6.21: Temperature profiles inside packed bed during adsorption with overhead condenser, fan and evacuations of reactor

This peak is due to the decrease in pressure, which results in a decrease in the adsorption equilibrium loading and therefore an increase in adsorption, in addition the evacuation causes small traces of trapped gases in the pores of zeolite to be removed, this allows more water to be adsorbed on zeolite.
The sudden increase in amount of water adsorbed after evacuations leads to comparatively higher amount of energy release which results in the temperature jumps as shown in Figure 6.21. However, intensity of temperature jump decreases with subsequent evacuations and no effect is observed after one hour of operation. This is due to the reason that the zeolite is nearly saturated after this duration of time.

The Figure 6.22 shows the temperature profiles for different experiment sets at two different locations inside the packed bed. The sensor T-R4 is located at the end of fin (inside packed bed) of the heat exchanger. On the other hand, sensor T-R7 is placed between the zeolite particles inside the packed bed. The temperature profiles for three different experiment sets show similar variation at a particular location.
In addition, the temperature at two different locations indicates that the vapors are able to penetrate though the packed bed. However, the small difference in profiles is due to the pressure drop inside the packed bed due to adsorption of vapors on one hand and resistance to vapor flow by packed particles of zeolite on other hand. The difference in the temperature at two different positions increases after approx. 40 minutes.

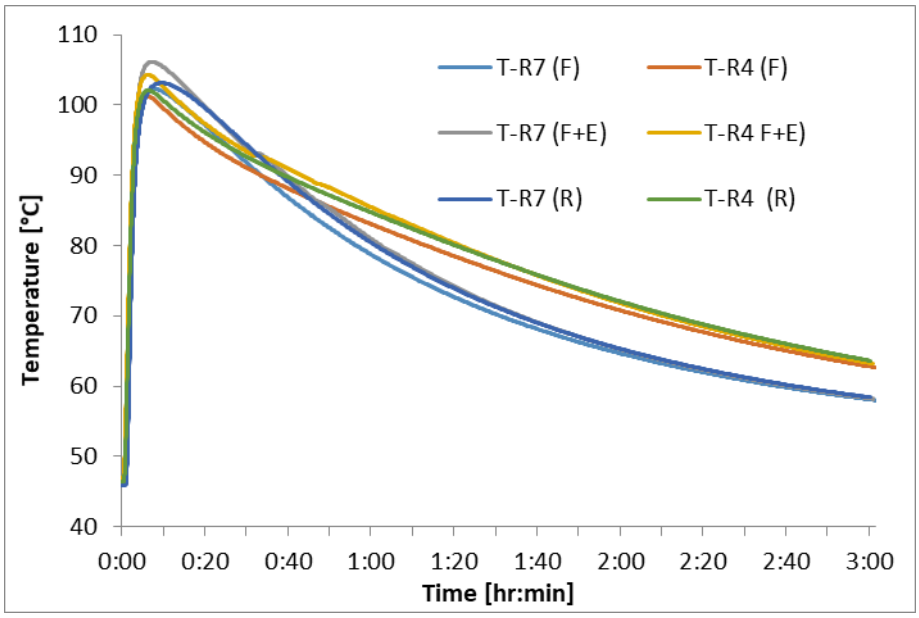

Figure 6.22: Comparison between temperature profiles for different experiment sets

The temperature shown by T-R4 is higher as compared to that shown by T-R7 after first 40 minutes for the entire duration of adsorption process. This may be due to the two reasons. Firstly, the vapor penetration decreases as water load of zeolite increases. In other words, the resistance to mass transfer increases with the increasing load of zeolite. Therefore, less amount of water is adsorbed on zeolite particles present inside the packed bed as compared to those present at the boundary of packed bed. Secondly, the heat transfer from location of T-R7 is higher which is closer to the tube containing heat transfer fluid as compared to that from T-R4. Due to higher heat transfer, temperature shown by T-R7 is lower. This indicates that the fins are not effective in extracting heat from particles away from heat transfer fluid.

6.2.2. Separation between condenser and evaporator

The major modification from the previous test set-up is the installation of a new overhead condenser at the top of reactor along with a condensate tank. As shown in Table 6-3, the effect of this modification is analyzed by comparing the performance of the two set-ups (combined and separated condenser/evaporator). The amount of dry zeolite used during previous and modified set-up is 4.031 kg and 4.756 kg respectively.

Table 6-3 Comparison between previous and modified set-up

Set-up	Q_R	Q_i	ΔH_{ad}	η_{ad}	η_d	η_o	ESD	Water uptake
	[Wh]	[Wh]	[Wh]	[%]	[%]	[%]	[Wh/kg]	kg water/kg zeolite
Previous	471	1413	544	86.6	38.5	33.3	117	0.139
Modified	499	1376	699	71.4	50.8	36.3	105	0.152

The overhead condenser along with condensate tank operates during the desorption process in order to condense the water vapor desorbed from zeolite. The condensed vapors are drawn out of overhead condenser by the condensate tank. Despite of the higher amount of zeolite used, the total heat energy invested *Qi* during desorption in modified set-up is lower. Consequently, the efficiency of desorption η_d and overall efficiency η_o in modified set-up is higher by approx. 32% and 9% respectively than in previous set-up. Therefore, it is evident from the above data that the installation of overhead condenser has affected the convection during desorption of water vapor thus reducing the amount of heat required to desorb the zeolite.

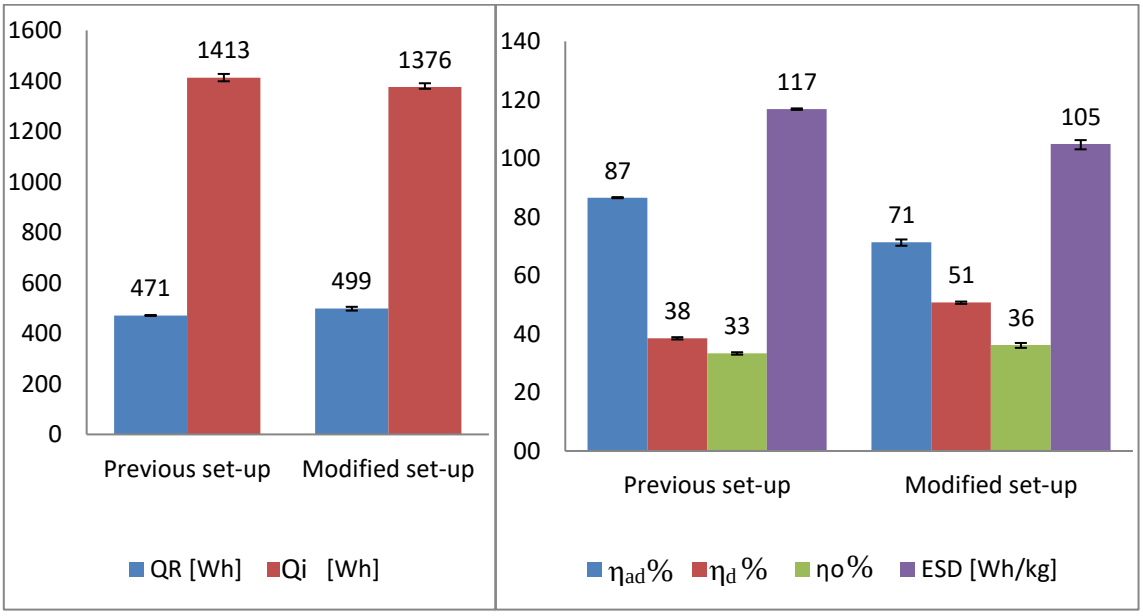

Figure 6.23 Left: heat energy restored and consumed (invested); Right: Efficiency and energy storage density of previous and modified set-up.

However, it is also noticeable that the adsorption efficiency η_{ad} and *ESD* are lower by 18% and 8% respectively in the modified set-up. This is because more amount of zeolite is used in modified set-up and thus the water uptake by zeolite and consequently the change of the adsorption enthalpy ΔH_{ad} for the total tested zeolite amount is higher as shown in Table 6-3. In order to recover more amount of heat energy, the adsorption process should be carried out for longer duration of time in modified set-up as compared to that in previous set-up. Though the process runs for same duration of time (3 hours) in both set-ups. Therefore, the fraction of energy restored is lower. Hence, adsorption efficiency η_{ad} and *ESD* are lower in modified set-up.

Different heat shares during desorption:

The sensible heat stored in the packed bed depends upon its heat capacity and the temperature rise from reference temperature (30°C) to the temperature at the end of desorption process (220 °C). The heat lost $Q_{d,lost}$ during the desorption process is calculated by using Eq. 3.6. The

calculated amount of heat required to desorb the zeolite ΔH_d, sensible heat of the packed bed $Q_{d,SH}$ and the heat lost during the desorption process $Q_{d,lost}$ are shown in Table 6-4.

Table 6-4 Different heat shares during desorption

Set-up	Q_i	Mass of zeolite	ΔH_d	$Q_{d,SH}$	$Q_{d,\ lost}$
	[Wh]	[kg]	[Wh]	[Wh]	[Wh]
Previous	1413	4.031	544	288	581
Modified	1376	4.756	699	336	341

The amount of sensible heat stored in modified set-up is higher because of the higher mass of zeolite. But, the amount of heat lost as waste heat is lower in modified set-up and thus the total amount of invested heat during desorption is also lower. Figure 6.24 shows the percentage of different heat shares in the total heat invested during desorption in respective set-ups.

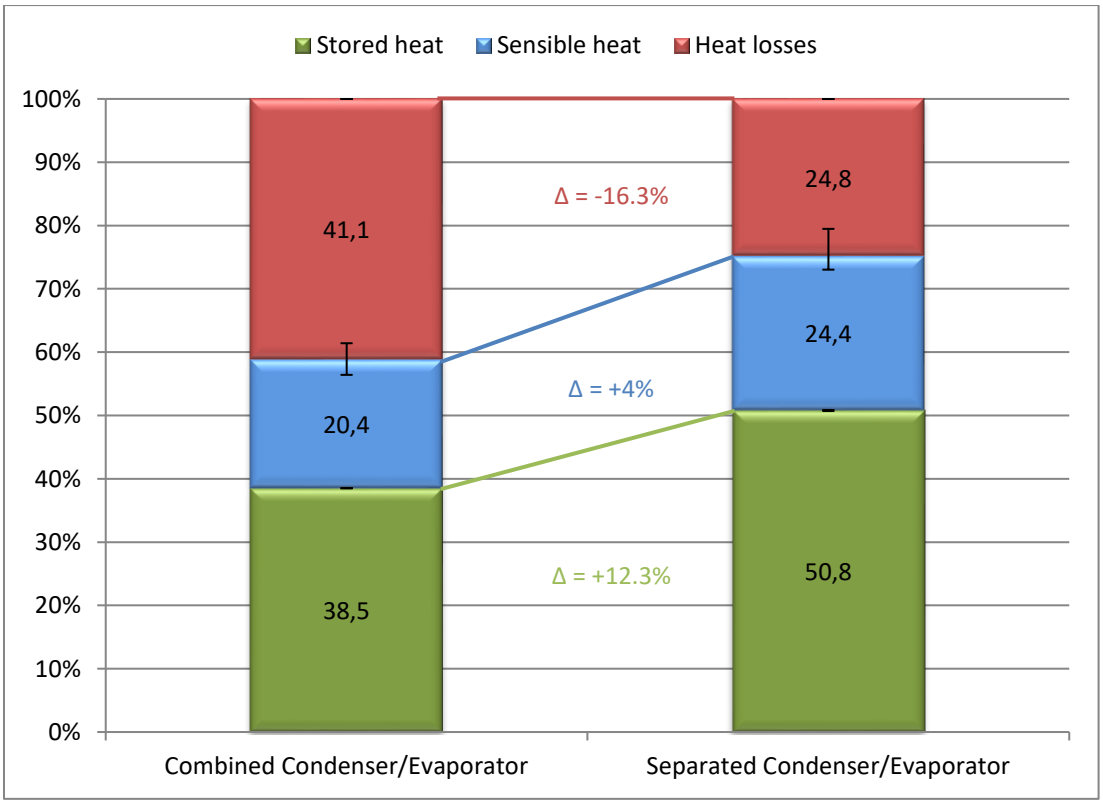

Figure 6.24 Left: % share of different heats during desorption in combined condenser/evaporator set-up; Right:% share of different heats during desorption in separated condenser/evaporator set-up

The percentage share of sensible heat $Q_{d,SH}$ in the total heat consumed is only ca. 4% more in modified set-up. This is due to the already explained fact that higher amount of zeolite is used in modified set-up. Whereas, the share of heat lost $Q_{d,\ lost}$ has decreased from ca. 41.1% in previous set-up to ca. 24.8% in the modified set-up. Furthermore, ca. 50.8% of the total invested energy during desorption with the modified set-up is stored as compared to ca. 38.5% with the previous set-up (this corresponds to an increase of ca. 32% of the stored heat share). The lower amount of heat energy invested in modified set-up could be the result of lower heat losses due to the overhead condenser which utilizes the convection of the vapors desorbed from the zeolite.

It's also important to mention that the sensible heat share with both of the set-ups represent about 50% of the stored heat, which shows the necessity to improve the sensible heat recovery after desorption.

6.2.3. Evaporator insulation

During adsorption, heat energy is released which raises the temperature of packed bed up to 120°C. The heat is extracted continuously by the heat transfer fluid via heat exchanger. However, the bed temperature is higher than 50°C during the entire course of adsorption process as shown in Figure 6.19. A part of the heat energy released is dissipated to the other equipment of the system via conduction and convection. In order to reduce the heat transfer between system and the surroundings, the entire modified set-up is insulated using glass wool. However, in previous set-up the evaporator is not insulated but exposed to the ambient atmosphere. The effect of thermal insulation of evaporator is analyzed from the adsorption process during previous and modified set-up.

Figure 6.25 shows the typical temperature profiles of heating cycle and water inside evaporator. $T_{,W}$ is the temperature of water inside evaporator, $T_{,in}$ and $T_{,out}$ are the incoming and outgoing temperature of heating cycle.

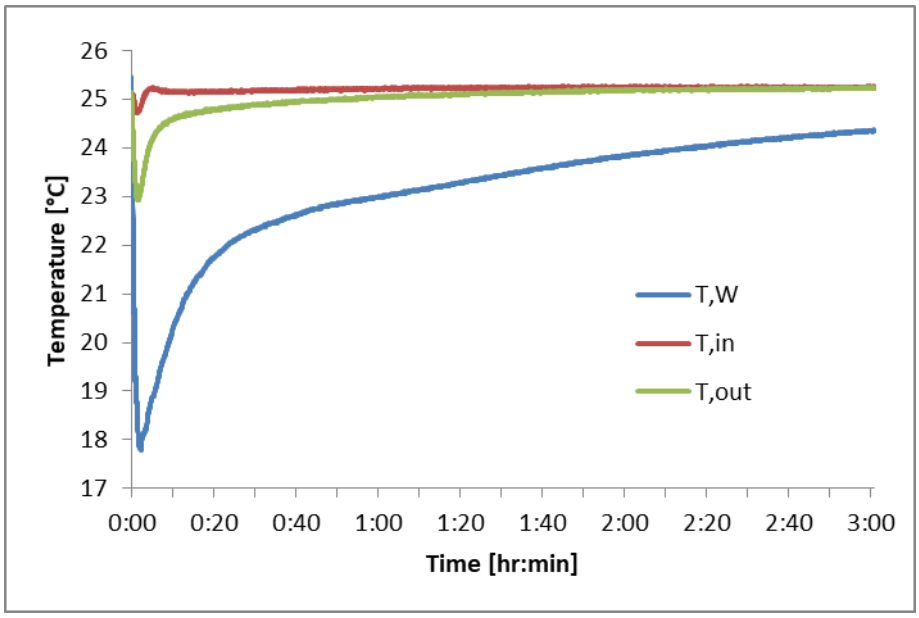

Figure 6.25 Typical temperature profiles of heating cycle and water inside evaporator during adsorption

Before starting the adsorption process, the temperature of water inside evaporator is raised till 25°C by heating cycle. As the adsorption process is started, the temperature inside the evaporator drops to approx. 18°C. This is due to the very fast evaporation of water at the beginning. The energy required to evaporate water comes from the bulk of water present inside the evaporator and from the metal parts like evaporator shell, heat exchanger inside evaporator. Therefore, a sharp decrease in temperature occurs at the beginning. Afterwards, it increases

slowly mainly due to the heat supplied by heating cycle, heat dissipated from the reactor and partially by the heat from ambient if the evaporator is not thermally insulated.

Now in previous set-up, the evaporator is not insulated which results in the heat transfer between evaporator and ambient. When the temperature of water inside evaporator is lower than the ambient temperature (25°C), heat transfer takes place from ambient to evaporator. Heat is also dissipated from reactor to evaporator via conduction and convection through metal and water vapor. A part of the heat dissipated from reactor is lost to ambient and other part is absorbed by water inside evaporator. The heat losses from heating water cycle are compensated by the heat transfer from ambient and reactor to evaporator. Therefore, the heat supplied and required are in similar range.

Table 6-5 Heat dissipated from the reactor to evaporator

Set-up	**Water adsorbed**	**Heat supplied by heating cycle**	**Heat required**	**Difference**
	[ml]	[Wh]	[Wh]	[Wh]
Previous	566	412	398	14
Modified	700	350	493	-143

On the other hand, heat delivered by the heating cycle is lower than actual amount of heat required to evaporate the total amount of water adsorbed in modified set-up. This may be due to the reason that heat transfer is minimized between ambient and evaporator by insulating the evaporator. Therefore, the heat dissipated from the reactor is not lost to ambient rather absorbed by water inside evaporator. This in turn decreases the amount of heat to be supplied by the heating water cycle. Thus, the total heat supplied by heating cycle is lower than the actual amount of heat required in modified set-up as shown in Table 6-5. Assuming the negligible heat transfer between evaporator and ambient, the difference between heat supplied and required is the amount of heat dissipated from reactor to evaporator.

Cooling power

During the adsorption process and due to the intense adsorption, water is being forced to evaporate, which leads to a temperature drop in the evaporator. This cooling effect can be utilized in different applications as a cooling source.

By examining the temperature behavior and cooling power during an adsorption process as presented in Figure 6.25 and Figure 6.26. It’s noticeable that due to the intense adsorption at the beginning of the process, a low temperature peak is observed accompanied by a high cooling power peak. However, as shown in Figure 6.26 the cooling power drops after some time.

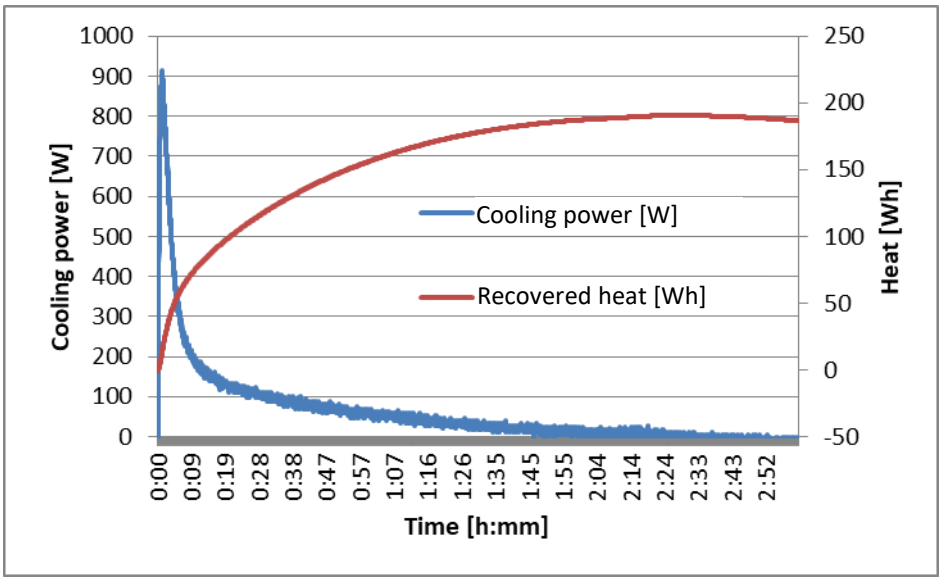

Figure 6.26 cooling power in evaporator during adsorption

By cooling at 25°C a cooling storage density of about 30-35 Wh/kg$_z$ was achieved. It's important to mention that the cooling power is strongly dependent on the amount of zeolite/water used in the adsorption process.

6.2.4. New heat exchanger

After selecting a new design of heat exchanger based on the results of heat transfer simulations. This design was then experimentally tested using the multiple reactor unit, in order to validate the simulated data.

The aim of the experiments was to measure the maximum heating/cooling power of the new heat exchanger design during desorption/adsorption. The results have shown that the maximum power was achieved while heating up the zeolite packed bed during desorption.

Figure 6.27 shows a comparison between the maximum heating power of the new and old heat exchanger designs.

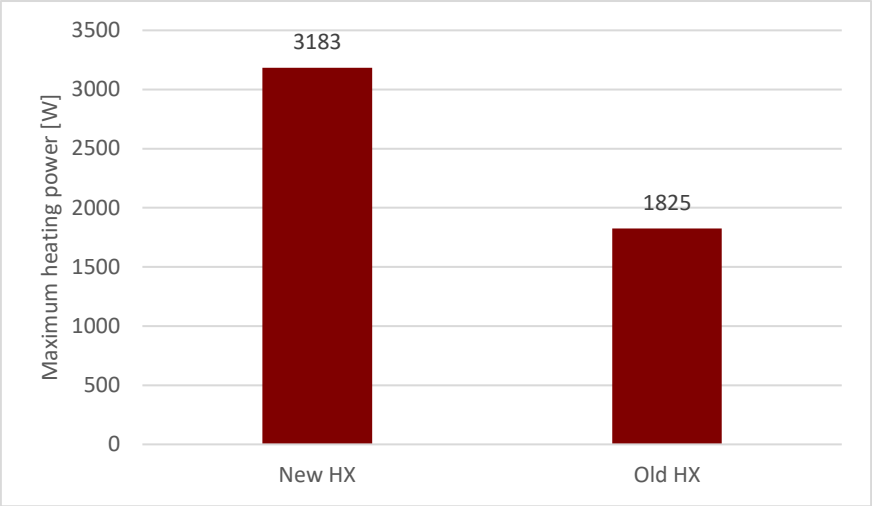

Figure 6.27 Comparison between the maximum heating power of the new (left) and old (right) heat exchangers

By comparing the results, it's noticeable that the heating power of the new design is higher of about 74% than the old design. This increment on the performance can contribute to the improvement of the heat storage efficiency of the system, by reducing the desorption time and thus decreasing the heat losses.

6.2.5. Multiple-reactor unit

The conducted experiments with the multiple reactor unit aimed to observe the temperature behavior in both reactors during sensible heat recovery. As the simulations show, the heat recover is only noteworthy when it's performed during the desorption process.

The results shown in Figure 6.28 represent the temperature behavior in different locations inside the second reactor during heat recovery from the first reactor. The heat recovery was performed after the desorption process in the first reactor has ended. The temperature at the end of desorption in the first reactor was 170, as for the second reactor the initial temperature was the room temperature (20° C)

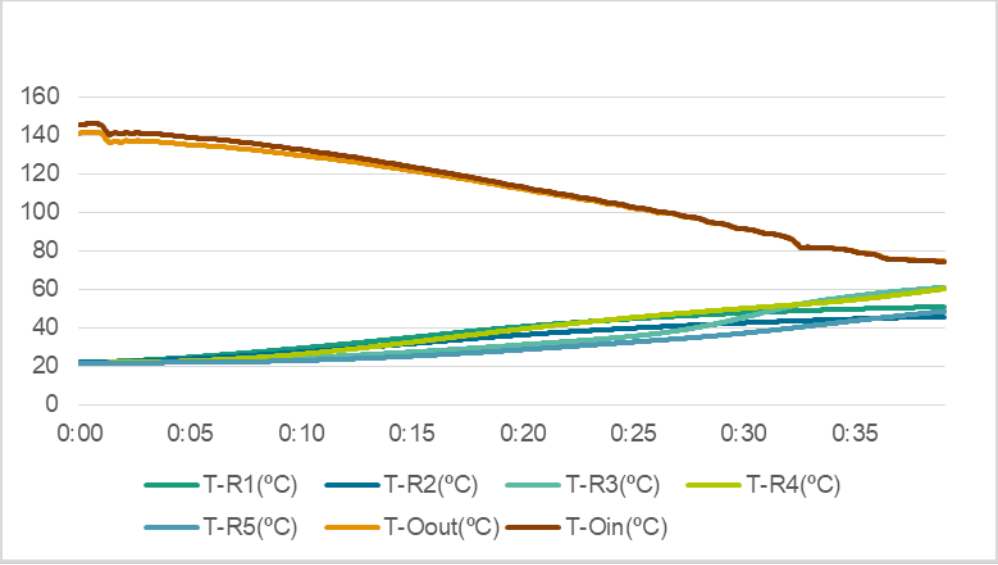

Figure 6.28 Temperature behavior inside the second reactor during heat recovery from the first reactor

As the results show, the oil starts with a temperature around 145° C, however this temperature starts to sink with time as the source temperature (reactor 1) starts also to drop due to the sensible heat recovery. The heat recovery was stopped after about 40 minutes, because the temperature difference between both reactors was less than 20°C, which has led to lower heat recovery rate.

Heat recovery

The heat amount which was recovered from the sensible heat left in the first reactor after desorption was calculated. The resulted curve is presented in Figure 6.29.

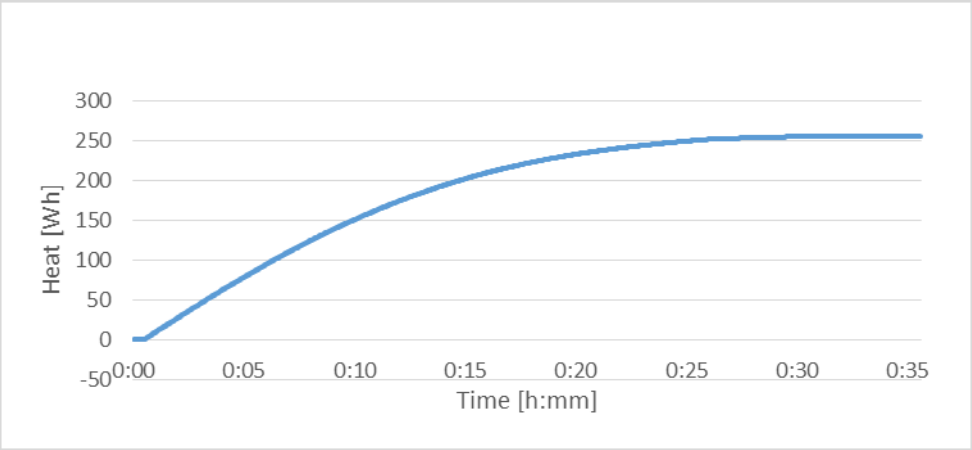

Figure 6.29 Amount of sensible heat recovered from the first reactor after desorption

From observing the results, it's noticeable that the total amount of heat recovered is ca. 255[Wh], which is about 9% of the total heat invested during desorption. This recovered amount represents also ca. 36% of the sensible heat left in the reactor after desorption.

A slightly higher recovery rate can be achieved by prolonging the heat recovery time; however, this depends directly on the type of application the heat storage unit is used for, and how long is it allowed to wait before starting the desorption of the next reactor.

7. Summary and Outlook

7.1. Summary

This work investigated mainly the different setups and arrangements of the heat storage system, specifically regarding energy utilization and time efficiency. The following points were concluded.

- **Process simulation**

  Heat storage system model was built for process simulation, the model was validated with experiments. Both simulation and experimental results are comparable and have the same behavior. The results have revealed, that process simulation is very helpful to improve the system overall efficiency. Thanks to the short simulation time compared to the real experimental time, numerous tests with different parameters were performed and thus a lot of time was saved.

  Another important application of process simulation was to simulate tests which are difficult to be experimentally tested, either due to operational limits of the used components (e.g. high temperature or pressure) or because of the higher costs of including extra components (e.g. high number of reactors).

- **Fans and evacuations**

  Due to the low pressure inside the reactor, improving the kinetics through fans or frequent evacuations has shown no significant effect on the total efficiency of the heat storage system.

- **Separation between condenser and evaporator**

  From heat and mass transfer simulations it was noticeable, that the heated water vapor gathers in the upper part of the reactor during desorption, which is due to the natural convection. Therefore, a separation between condenser and evaporator was recommended in order to improve the kinetics during desorption. The experimental results have confirmed the simulation by showing 32% increase of the stored-heat share as well as a reduction up to 40% of heat losses.

  The desorption efficiency η_d and overall efficiency η_o of the system were improved with ca. 32% and 9% respectively.

- **Heat exchanger design**

  Simulation has proven to be a powerful tool by predicting the heat transfer inside the reactor. The results have shown that the old design of heat exchanger was hindering the heat storage system from reaching its full potential.

  Hence, different designs of heat exchanger were simulated with the help of FEM software (COMSOL Multiphysics), and the best design in terms of temperature distribution was chosen for the technical modifications. The selected design has a new concept compared to the heat exchangers used in the literature. This concept allows the oil to flow in both vertical directions, which has significantly increased the lowest temperature in the reactor from 53.9 °C to 78.8 °C. The simulation's results of the new design were later on validated through experimental tests, which shown an improvement on the heating power with about 74%.

- **Multiple-reactor unit**

  While the current research in the literature is focused on a single reactor storage unite. The process simulations in this work suggested the use of multiple reactors in the heat storage system, presenting the possibility of implementing different operational strategies depending on the required application. A parallel configuration can be used to acquire high power for short time, while a sequential configuration can be used to obtain the highest heat storage efficiency. According to the simulations, the total heat storage efficiency can be improved up to 13.75%, the experiments' results with 40 minutes recovery time have shown an improvement of 9% on the heat storage efficiency.

- **Sensible heat recovery**

  As a result of having multiple-reactor unit, the sensible heat left in one reactor at the end of desorption can be recovered and used to preheat the next reactor. Hence, when running on the sequential configuration, the total heat invested during desorption was reduced by 9% (109 Wh), which represents ca. 36% of the sensible heat left in the reactor after desorption.

7.2. Outlook

During the investigation of this work, some problems or unwanted conditions have been faced, which could be avoided in the future work. In addition, extra improvements and experiments can be carried out to optimize the system further. Therefore, the following tips are recommended.

- **Improve thermal conductivity**

  The low thermal conductivity of zeolite has been a hold back point for the system improvement, thus using different methods to increase this thermal conductivity is favored. This can be achieved by introducing other materials to the packed bed which has higher thermal conductivity (such as copper).

- **Longer adsorption time**

  The suggested adsorption time in this investigation was 3 hours, however the results showed that further adsorption process was still possible and could give a significant increase to the total restored heat. This will increase the heat storage efficiency of the system.

- **Control the adsorption rate**

  Depending on the application, it is sometimes necessary to control the amount of heat discharged from the system, this can be done by controlling the mass flow in the oil cycle. However, the rest of the restored heat which is not needed will be lost. Thus, for a better utilization of the system, the control of the restored heat rate should be performed by controlling the water uptake during adsorption. Therefore, the system should continuously measure the required amount of heat and change the open/close frequency of the valve between the reactor and the evaporator, which in its turn control the amount of water vapor going into the reactor. The drawback of this method is that the peak at the beginning of adsorption will be lost if an application with a discontinuous adsorption is needed.

- **Improve the kinetics**

  Especially during the desorption process, where it takes long time for the desorbed water vapor in order to be transported into the condenser, besides to the amount of vapor which stays in the reactor after the process is over. As for the adsorption process this may enhance the adsorption of the zeolite by making it easier for the water vapor to pass though the

packed bed. This kinetics can be improved by using a fan (which is suitable for vacuum) between the reactor and condenser/evaporator, which will provide both faster movement for the water vapor on one hand, and on the other hand a continuous pressure difference between the reactor and the condenser/evaporator.

- **Improve reactor's design**

  So far, all the investigations were focusing on the idea of having a fixed bed of zeolite. A common challenge with this design is to reach a good heat transfer without significantly increasing the mass and volume of the heat exchanger, which leads to a lower heat storage density. In addition, due to the large amount of zeolite packed inside the reactor, it is difficult for the water vapor to reach the inner part of the reactor without extra built-in air channels.

  A different approach to the reactor's design could bring significant improvements to the system. An example of a new reactor's design is shown in Figure 7.1, where the reaction chamber and zeolite storage tank are separated from each other.

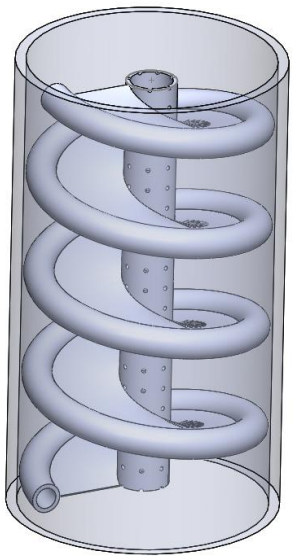

Figure 7.1 A draft design of a moving bed reactor

In this design the zeolite pellets flow from the storage tank downwards throw the reactor to another storage tank. The reactor has an air channel in the middle, from which water vapor is introduced (during adsorption), or to which the water vapor is being collected

(during desorption). The pellets flow on a plate connected from the outer part to a tube, where the oil from the oil-cycle flows. This design gives the possibility to fully adsorb/desorb the zeolite pellets, by dealing with small amounts of zeolite pellets instead of having them all at once.

Another advantage to this method is the full control over the amount of zeolite being desorbed/adsorbed depending on the heat provided/heat demand of the different applications.

In order to improve the heat storage density of such a design, it's advisable to use multiple-tank system as shown in Figure 7.2.

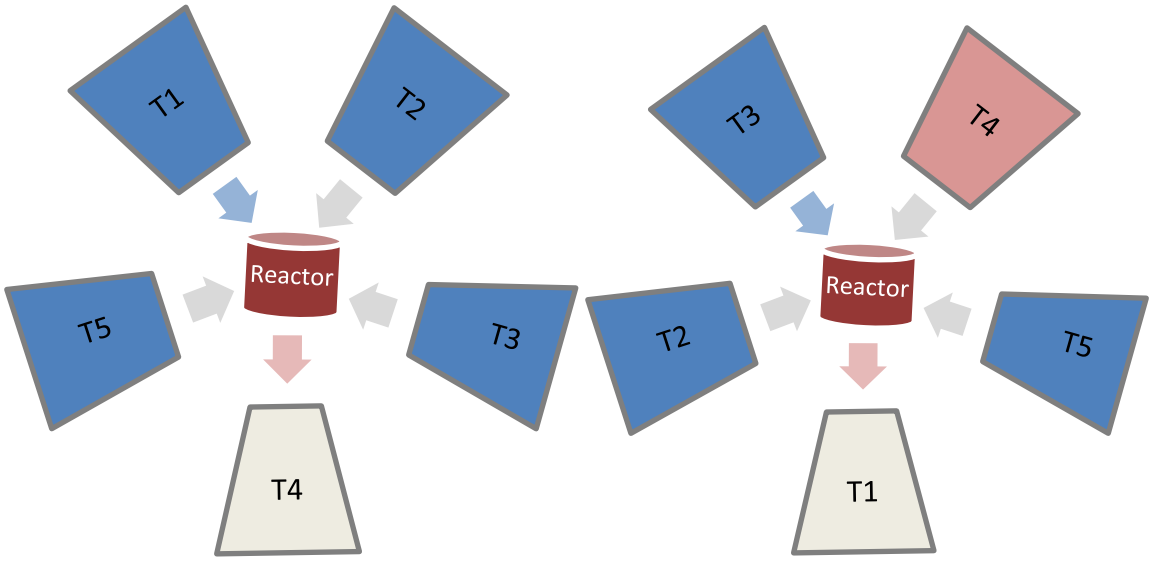

Figure 7.2 Configuration of multiple-tank system with moving bed reactor

- **Sensible heat recovery during adsorption**

  As the simulations' results have shown, the amount of sensible heat left in reactor after the end of adsorption is not significant in order to use it for preheating the next reactor. However, when performing an adsorption process without having an extra low-heat source for the evaporator, this remaining sensible heat in the reactor can be used in order to evaporate the water in the evaporator of the next reactor.

8. References

Abedin, Ali H. ; Rosen, Marc A.: "A critical review of Thermochemical Energy storage Systems". *In: The Open Renewable Energy (2011)*.

http://benthamopen.com/torej/articles/V004/42TOREJ.pdf

IPCC: More efficient conversion of fossil fuels.

http://www.gcrio.org/ipcc/techrepI/energysupply.html. – Technical report-1

Andrej Gibelhausa, Franz Lanzeratha, Jan Seilera, Andreas Möllerb, André Bardow „Model-based parameter estimation of heat and mass transfer coefficients using small-scale experiments", *RWTH Aachen University, Institute of Technical Thermodynamics, May 2019* SorpLib: Dynamic simulation of adsorption energy systems - RWTH AACHEN UNIVERSITY Chair of Technical Thermodynamics - English (rwth-aachen.de)

Aristov, Yuriy I.: "Challenging offers of material science for adsorption heat transformation: A review". *In: Applied Thermal Engineering 50 (2013), Nr. 2, 1610 - 1618.* http://dx.doi.org/http://dx.doi.org/10.1016/j.applthermaleng.2011.09.003. – DOI

http://dx.doi.org/10.1016/j.applthermaleng.2011.09.003. – ISSN 1359–4311. – Combined Special Issues: {ECP} 2011 and {IMPRES} 2010

Atakan, Aylin ; Fueldner, Gerrit ; Munz, Gunther ; Henninger, Stefan ; Tatlier, Melkon: "Adsorption kinetics and isotherms of zeolite coatings directly crystallized on fibrous plates for heat pump applications". *In: Applied Thermal Engineering 58 (2013)*, 273 - 280. http://dx.doi.org/http://dx.doi.org/10.1016/j.applthermaleng.2013.04.037. – DOI

http://dx.doi.org/10.1016/j.applthermaleng.2013.04.037. – ISSN 1359–4311 Bibliography 89

Atul Sharma , V.V. Tyagi, C.R. Chen, D. Buddhi, "Review On Thermal Energy Storage With Phase Change Materials And Applications", *Elsevier Ltd* 2007, www.elsevier.com/locate/rser

Bauer, J.; Herrmann, R.; Mittelbach, W.; Schwieger, W."Zeolite/aluminum composite adsorbents for application in adsorption refrigeration". Int. J. Energy Res. 2009, 33, 1233–1249.

Biehler, Simon: "Heat storage system for industrial application". *Department of Physical Process Technology, Fraunhofer Institute for Interfacial Engineeing and Biotechnology.*

https://energy-changes.com/de/node/892

Cao Sunliang, "State of the Art Thermal Energy Storage Solutions for High Performance Buildings", *Department of Physics, University of Jyväskylä*, 2010.

https://www.researchgate.net/publication/277851503_State_of_the_art_thermal_energy_storage_solutions_for_high_performance_buildings

Chih-Hang Hsieh, "Vapor Pressure Lowering in Porous Media", *Department of Petroleum Engineering, Stanford University. 1980.*

https://pangea.stanford.edu/ERE/pdf/SGPreports/SGP-TR-038.pdf

Danny Schuring, "Diffusion in Zeolites: Towards a Microscopic Understanding", [Phd Thesis 1 (Research TU/e / Graduation TU/e), Chemical Engineering and Chemistry] *Eindhoven University of Technology, Netherlands*. 2002. https://doi.org/10.6100/IR558779

Demir, H.; Mobedi, M.; Ülkü, S. "A review on adsorption heat pump: Problems and solutions". Renew. Sustain. Energy Rev. 2008, 12, 2381–2403.

Douglas Levan, M., G. Carta, et al. "Adsorption and Ion Exchange", *Perry's Chemical Engineers' Handbook (8th Edition), 2008*. D. W. Green and R. H. Perry, McGraw-Hill.

Dr. K. J. Bell, Dr. A. C. Mueller, "Wolverine Engineering Data Book II", *Wolverine Tube, Inc. Research and Development Team.* 2001.

Dubinin, M.M.: "Fundamentals of the theory of adsorption in micropores of carbon adsorbents: characteristics of their adsorption properties and microporous structures". *In: Pure and Applied Chemistry 61 (1989), Nr. 11, S. 1841–1843*

Gantenbein, Paul: "Sorption storage unit with zeolite (Silica gel)/ water / International Energy Agency". *Institut fuer Solartechnik SPF, HSR Hochschule fuer technik, Oberseestraße 0, CH-8640 Rappeswill, January 2008*. – Report B4 of Subask B, Laboratory tests of Chemical Reactions and Prototype Sorption Storage units

Gross, B. Dawoud E.H. Amer D.: "Experimental investigation of an adsorptive thermal energy storage". *In: International Journal of Energy Research (2007)*, Nr. 31, S. 135–147

Hauer, Andreas: „Beurteilung fester Adsorbentien in offenen Sorptionssystemen für energetische Anwendungen", *Von der Fakultät Prozesswissenschaften der Technischen Universität Berlin, Ph.D. Thesis, July 2002*

Hauer, Andreas: IRENA-ETSAP Tech Breif E17 Thermal Energy Storage / ZAE Bayern. Version: 21013.
http://www.irena.org/DocumentDownloads/Publications/IRENA-ETSAP%20Tech%20Brief%20E17%20Thermal%20Energy%20Storage.pdf
21013. – Forschungsbericht

Hauer, Andreas; Van Helden, Wim: „Material And Component Development For Thermal Energy Storage“, *the 89th ECES ExCo meeting May 2020. International Energy Agency, Executive Committee of the Energy Storage technology collaboration programme (ES TCP).*

Huston, Nick D. ; Yang, Ralph T.: “Theoretical Basis for the Dubinin- Radushkevitch (D-R) Adsorption Isotherm Equation”. *In: Kluwer Academic publishers (1996)*, July, Nr. 3, S. 189–195

IEA-ETSAP and IRENA ©, “Thermal Energy Storage”, *Technology Policy Brief E17 – January 2012* - www.etsap.org - http://www.irena.org

Incropera, Frank P. ; Dewitt, David P. ; Bergman, Theodore L. ; Lavine, Adrienne S.: “Principles of Heat and Mass Transfer”. Edition 7. 2011. ISBN: 978-1-119-38291-1

IRENA (2020), “Innovation Outlook: Thermal Energy Storage”, *International Renewable Energy Agency, Abu Dhabi*. ISBN 978-92-9260-279-6

Irvine, T. F. and P. E. Liley. “Steam and Gas Tables with Computer Equations”, *Academic Pr. 1984*. ISBN 978-0-12-374080-9

J. Carrasco Portaspana, “High Temperature Thermal Energy Storage Systems Based On Latent And Thermo-Chemical Heat Storage”, *Faculty of Mechanical and Industrial Engineering, Technische Universität Wien* 2011.

https://www.researchgate.net/publication/277040552_High_temperature_thermal_energy_storage_systems_based_on_latent_and_thermo-chemical_heat_storage

J.P.Edwards: “Design and Rating of Shell and Tube Heat Exchangers”. (2008), August, Nr. 29, 11-12. www.pidesign.co.uk

Jaehnig, Dagmar: “Solid Sorption System Storage (MODESTORE)” / *International Energy Agency. AEE, INTEC, Austria, January 2008*. – Report B4 of Subask B, Laboratory tests of Chemical Reactions and Prototype Sorption Storage units

Jong, Ween N.: "Study of heat transfer and the effect of process parameters on the efficiency of closed sorption thermal storage unit", *University of Stuttgart, 2011*

L.McCabe, Warren ; Smith, Julian C. ; Harriot, Peter: "Heat transfer to Fluids with Phase Change". *In: Unit Operation of Chemical Engineering. Sixth. McGraw Hill, 1981*, Capital 13, S. 377–390

Langhof, Timo: "Elaboration of fundamentals for the conception of a modular thermo chemical heat storage system", *University of Stuttgart, 2009*

Langmuir, I.: "The Adsorption of Gases on Plane Surfaces of Glass, Mica and Platinum." *In: Journal of the American Chemical Society 40 (1918)*, S. 1361–1402

Li, Gang ; Qian, Suxin ; Lee, Hoseong ; Hwang, Yunho ; Radermacher, Reinhard: "Experimental investigation of energy and exergy performance of short term adsorption heat storage for residential application." *In: Energy 65 (2014)*, Nr. 0, 675 -691. http://dx.doi.org/http://dx.doi.org/10.1016/j.energy.2013.12.017. – DOI

http://dx.doi.org/10.1016/j.energy.2013.12.017. – ISSN 0360–5442

Li, T., et al., "Performance analysis of an integrated energy storage and energy upgrade thermochemical solid–gas sorption system for seasonal storage of solar thermal energy". *Energy, 2013. 50(0): p. 454-467.*

Li, Tingxian ; Wang, Ruzhu ; Kiplagat, Jeremiah K. ; Kang, YongTae: "Performance analysis of an integrated energy storage and energy upgrade thermochemical solid-gas sorption system for seasonal storage of solar thermal energy." *In: Energy 50 (2013)*, Nr. 0, 454 Bibliography 90- 467. http://dx.doi.org/http://dx.doi.org/10.1016/j.energy.2012.11.043. – DOI http://dx.doi.org/10.1016/j.energy.2012.11.043. – ISSN 0360–5442

ME 4331, "Boiling Heat Transfer Fundamentals", *College of Science & Engineering, University of Minnesota.* 2010. from:

http://www.me.umn.edu/courses/me4331/boilingFundamentals.shtml

M. F. M. Post, "Diffusion in zeolite molecular sieves, in: Introduction to zeolite science and practice", H. van Bekkum, E. M. Flanigen, and J. C. Jansen, eds., vol. 58 of "Studies in surface science and catalysis", pp. 391–443, Elsevier, Amsterdam (1991).

Michelangelo Di Palo, Vincenzo Sabatelli, Fulvio Buzzi and Roberto Gabbrielli, "Experimental and Numerical Assessment Of A Novel All-In-One Adsorption Thermal Storage With Zeolite For Thermal Solar Applications", *Dipartimento di Ingegneria Civile e Industriale dell'Università di Pisa, 56126 Pisa, Italy.*
Applied Sciences 2020, 10, 8517; doi:10.3390/app10238517. Published: 28 November 2020

Mugele, Jan: „Optimierung von Speichermaterialien für den Einsatz in geschlossenen thermochethermo Wärmespeicheren für gebäudetechnische Anwendungen", *Von der Fakulät Prozesswissenschaften der Technischen Universität Berlin*, Ph.D. Thesis, Mai 2005 Bibliography 88

Network, Joint I.: "Energy Storage: Phase Change Materials for Thermal Energy Storage." http://www.climatetechwiki.org/technology/jiqweb-pcm-0

O. Ercan Ataer, (2006), "Storage Of Thermal Energy", in *Energy Storage Systems*, [Ed. Yalcin Abdullah Gogus], in *Encyclopedia of Life Support Systems (EOLSS)*, Developed under the Auspices of the UNESCO, Eolss Publishers, Oxford ,UK, [http://www.eolss.net]

Polanyi, Michael: "The Potential Theory of Adsorption". *Volume 141 (1963)*, September, p.1010-1013. http://www.sciencemag.org/content/141/3585/1010.full.pdf

Pool Boling Regime. Version: 2010. http://www.thermalfluidscentral.org/e-books/book-viewer.php?b=42&s=11&q=pool++boiling+regimes. In: Transport Pheneomena in Multiphase Systems. Thermal Fluids Central, 2010, Kapitel 10, p. 767

R. Lang, T. Westerfeld, A. Gerlich And K.F. Knoche, "Enhancement of the Heat and Mass Transfer in Compact Zeolite Layers ", *Lehrstuhl für Technische Thermodynamik, RWTH, Aachen.* 1995.

Richard G. Holdich, "Fundamentals of Particle Technology", *Department of Chemical Engineering, Loughborough University, UK, 2002.*

Ruthven, Douglas M.: "Priciples of Adsorption and Adsoprtion Processes". *JOHN WILEY & SONS, 1984,* http://aevnmont.free.fr/SACH-BOOKS/Adsorption/Ruthven-Adsorption.pdf

S.A.Vijay Padmaraju, M.Viginesh, N.Nallusamy "Comparitive Study Of Sensible And Latent Heat Storage Systems Integratedwith Solarwater Heating Unit ", *International Conference on Renewable Energy and Power quality-2008*, March 12-14, 2008,Santander, Spain.

Salvatore Vasta, Vincenza Brancato, Davide La Rosa, Valeria Palomba, Giovanni Restuccia, Alessio Sapienza and Andrea Frazzica "Adsorption Heat Storage: State-of-the-Art and Future Perspectives", *Nanomaterials 2018, 8, 522; doi:10.3390/nano8070522.*

Schawe, D. "Theoretical and Experimental Investigations of an Adsorption Heat Pump with Heat Transfer between two Adsorbers". *Institut für Kernenergetik und Energiesysteme*. Stuttgart, University of Stuttgart, 2010.

Schmidt, Ferdinand P.: "Optimizing Adsorbents for Heat Storage Applications: Estimation of Thermodynamic Limits and Monte Carlo Simulations of Water Adsorption in Nanopores", *Fakultät für Mathematik und Physik der Albert-Ludwigs-Universität Freiburg im Breisgau, Inaugural-Dissertation, Juli 2004*

Singh, Mandeep : „Investigation of technical modifications and process parameters in a closed thermo-chemical adsorption heat storage system". *Department 1-Process Engineering and Energy Technology University of Applied Sciences, Bremerhaven 2014*

Sircar, Shivaji ; Myers, Alan L.: "Gas seperation by zeolites". Version: 2003. http://aussiezeolite.com.au.p8.hostingprod.com/yahoo_site_admin/assets/docs/ DK2772_ch22.166185814.pdf. In: *Handbook of Zeolite Science and Technology. Marcel Dekker, Inc., 2003*, Kapitel 22, p.8

Stephen Brunauer, Edward T. P.H. Emmett E. P.H. Emmett: "Adsorption of Gases in Multimolecular Layers". *In: Journal of the American Chemical Society (1938)*, February, S.309–319

Storch, G., G. Reichenauer, et al. "Hydrothermal stability of pelletized zeolite 13X for energy storage applications", *Adsorption, 2008.* https://doi.org/10.1007/s10450-007-9092-7

Treybal, Robert E.: "Adsorption and Ion Exchange. In: Mass Transfer Operations". *Third Edition. McGRAW-HILL, Kapitel 11, S. 566*

Vieillard and Mathieu "Prediction Of Enthalpies Of Hydration Of Zeolites", *American Mineralogist, Volume 94, pages 565–577, 2009*

Wang, R., Wang, L. and Wu, J. (2014) "Design and Performance of the Adsorption Refrigeration System, in Adsorption Refrigeration Technology: Theory and Application", *John Wiley & Sons, Singapore Pte. Ltd, Singapore. doi: 10.1002/9781118197448.ch8*

Yu, N.;Wang, R.Z.;Wang, L.W. "Sorption thermal storage for solar energy". *Prog. Energy Combust*. Sci. 2013, 39,489–514
https://doi.org/10.1016/j.pecs.2013.05.004

Zanter, K.-D., „Entwicklung und Synthese von trägergestützten Kristallisationen und Evaluation von Katalysator-Gewebepackungen mit krustenartigen Carrierfilmen", *in Fakultät für Mathematik und Naturwissenschaften. 2005, Carl von Ossietzky Universität Oldenburg.*

http://oops.uni-oldenburg.de/109/1/zanent05.pdf

9. Appendix

Water Vapor Pressure

The saturation vapor pressure of water for the temperature between 273.15 K and 647.3 K can be computed with the following equation: [Irvine and Liley, 1984]

$$\ln(p_s) = \sum_{i=0}^{9}\left(A_i \cdot T_s^i\right) + \frac{A_{10}}{T_s - A_{11}}$$

and the following coefficients:

A_0 = 1.04592 x 10	A_4 = -1.01520 x 10^{-9}	A_8 = 7.79287 x 10^{-22}
A_1 = -4.04897 x 10^{-3}	A_5 = 8.65310 x 10^{-13}	A_9 = 1.91482 x 10^{-25}
A_2 = -4,17520 x 10^{-5}	A_6 = 9.03668 x 10^{-16}	A_{10} =-3.96806 x 10^{3}
A_3 = 3.68510 x 10^{-7}	A_7 = -1.99690 x 10^{-18}	A_{11} = 3.95735 x 10

T_s [°C]	p_s [mbar]	T_s [°C]	p_s [mbar]
0	6,11	31	45,01
1	6,57	32	47,63
2	7,06	33	50,39
3	7,58	34	53,29
4	8,13	35	56,33
5	8,72	36	59,52
6	9,35	37	62,86
7	10,02	38	66,37
8	10,73	39	70,04
9	11,49	40	73,89
10	12,29	41	77,92
11	13,14	42	82,14
12	14,04	43	86,55
13	14,99	44	91,16
14	16,00	45	95,99
15	17,07	46	101,03
16	18,20	47	106,30
17	19,40	48	111,80
18	20,67	49	117,55
19	22,00	50	123,55
20	23,41	51	129,81
21	24,90	52	136,34
22	26,48	53	143,14
23	28,14	54	150,24
24	29,89	55	157,64
25	31,73	56	165,34
26	33,67	57	173,36
27	35,71	58	181,72
28	37,86	59	190,41
29	40,13	60	199,46
30	42,51		

Equillibrium data for zeolite NaX-water

W	A		W	A		W	A
[cm3/g]	[J/g]		[cm3/g]	[J/g]		[cm3/g]	[J/g]
0.33211458	83		0.24210991	640		0.09996064	1200
0.33188239	85		0.24085713	645		0.0990405	1205
0.33130597	90		0.23959774	650		0.09813189	1210
0.33073498	95		0.2383319	655		0.09723489	1215
0.33016897	100		0.23705972	660		0.09634956	1220
0.32960748	105		0.23578137	665		0.09547597	1225
0.32905006	110		0.23449699	670		0.09461418	1230
0.32849629	115		0.23320672	675		0.09376425	1235
0.32794574	120		0.23191071	680		0.09292623	1240
0.32739798	125		0.23060912	685		0.09210018	1245
0.32685261	130		0.2293021	690		0.09128613	1250
0.32630922	135		0.2279898	695		0.09048414	1255
0.32576742	140		0.22667239	700		0.08969423	1260
0.32522682	145		0.22535002	705		0.08891645	1265
0.32468704	150		0.22402286	710		0.08815082	1270
0.32414772	155		0.22269106	715		0.08739737	1275
0.32360848	160		0.2213548	720		0.08665612	1280
0.32306897	165		0.22001424	725		0.08592709	1285
0.32252885	170		0.21866956	730		0.08521029	1290
0.32198777	175		0.21732091	735		0.08450573	1295
0.32144541	180		0.21596847	740		0.08381341	1300
0.32090142	185		0.21461242	745		0.08313333	1305
0.32035551	190		0.21325293	750		0.08246549	1310
0.31980735	195		0.21189017	755		0.08180988	1315
0.31925664	200		0.21052433	760		0.08116648	1320
0.31870309	205		0.20915558	765		0.08053527	1325
0.31814641	210		0.20778411	770		0.07991623	1330
0.31758631	215		0.20641008	775		0.07930934	1335
0.31702252	220		0.20503369	780		0.07871454	1340
0.31645478	225		0.20365512	785		0.07813182	1345
0.31588282	230		0.20227455	790		0.07756112	1350
0.3153064	235		0.20089217	795		0.07700239	1355
0.31472525	240		0.19950816	800		0.07645559	1360
0.31413915	245		0.19812271	805		0.07592064	1365
0.31354785	250		0.19673601	810		0.0753975	1370
0.31295114	255		0.19534824	815		0.07488608	1375
0.31234879	260		0.1939596	820		0.07438631	1380
0.3117406	265		0.19257028	825		0.07389812	1385

0.31112635	270		0.19118046	830		0.07342141	1390
0.31050584	275		0.18979033	835		0.0729561	1395
0.30987888	280		0.18840009	840		0.07250208	1400
0.30924529	285		0.18700993	845		0.07205926	1405
0.30860488	290		0.18562004	850		0.07162753	1410
0.30795747	295		0.18423061	855		0.07120677	1415
0.30730291	300		0.18284184	860		0.07079686	1420
0.30664103	305		0.18145391	865		0.07039769	1425
0.30597166	310		0.18006702	870		0.07000911	1430
0.30529467	315		0.17868137	875		0.06963099	1435
0.30460991	320		0.17729714	880		0.06926319	1440
0.30391724	325		0.17591453	885		0.06890555	1445
0.30321653	330		0.17453373	890		0.06855793	1450
0.30250765	335		0.17315493	895		0.06822016	1455
0.30179048	340		0.17177833	900		0.06789207	1460
0.30106491	345		0.17040412	905		0.06757349	1465
0.30033084	350		0.16903249	910		0.06726424	1470
0.29958815	355		0.16766363	915		0.06696413	1475
0.29883675	360		0.16629773	920		0.06667297	1480
0.29807654	365		0.16493499	925		0.06639056	1485
0.29730745	370		0.16357559	930		0.0661167	1490
0.29652939	375		0.16221973	935		0.06585117	1495
0.29574228	380		0.16086759	940		0.06559375	1500
0.29494606	385		0.15951936	945		0.06534422	1505
0.29414066	390		0.15817523	950		0.06510234	1510
0.29332602	395		0.15683538	955		0.06486788	1515
0.29250208	400		0.15550001	960		0.06464058	1520
0.2916688	405		0.15416929	965		0.06442021	1525
0.29082613	410		0.15284341	970		0.06420648	1530
0.28997404	415		0.15152256	975		0.06399915	1535
0.28911248	420		0.15020691	980		0.06379794	1540
0.28824144	425		0.14889666	985		0.06360255	1545
0.28736087	430		0.14759197	990		0.06341271	1550
0.28647078	435		0.14629302	995		0.06322813	1555
0.28557113	440		0.145	1000		0.06304849	1560
0.28466192	445		0.14371308	1005		0.06287349	1565
0.28374315	450		0.14243243	1010		0.0627028	1570
0.28281481	455		0.14115824	1015		0.06253612	1575
0.2818769	460		0.13989066	1020		0.06237309	1580
0.28092944	465		0.13862987	1025		0.06221339	1585
0.27997244	470		0.13737604	1030		0.06205667	1590
0.27900591	475		0.13612934	1035		0.06190257	1595
0.27802988	480		0.13488993	1040		0.06175072	1600
0.27704436	485		0.13365797	1045		0.06160076	1605
0.27604939	490		0.13243364	1050		0.06145231	1610

0.27504501	495		0.13121708	1055		0.06130498	1615
0.27403125	500		0.13000845	1060		0.06115839	1620
0.27300815	505		0.12880792	1065		0.06101212	1625
0.27197576	510		0.12761564	1070		0.06086576	1630
0.27093413	515		0.12643175	1075		0.0607189	1635
0.26988331	520		0.12525641	1080		0.06057112	1640
0.26882336	525		0.12408977	1085		0.06042198	1645
0.26775434	530		0.12293197	1090		0.06027103	1650
0.26667632	535		0.12178316	1095		0.06011782	1655
0.26558936	540		0.12064347	1100		0.0599619	1660
0.26449354	545		0.11951305	1105		0.05980279	1665
0.26338893	550		0.11839203	1110		0.05964003	1670
0.26227562	555		0.11728054	1115		0.05947313	1675
0.26115368	560		0.11617872	1120		0.05930159	1680
0.2600232	565		0.1150867	1125		0.05912491	1685
0.25888427	570		0.1140046	1130		0.05894258	1690
0.25773699	575		0.11293254	1135		0.05875408	1695
0.25658145	580		0.11187065	1140		0.05855889	1700
0.25541775	585		0.11081904	1145		0.05835647	1705
0.25424599	590		0.10977782	1150		0.05814626	1710
0.25306628	595		0.10874712	1155		0.05792773	1715
0.25187872	600		0.10772703	1160		0.0577003	1720
0.25068343	605		0.10671767	1165		0.0574634	1725
0.24948053	610		0.10571913	1170		0.05721645	1730
0.24827012	615		0.10473152	1175		0.05695887	1735
0.24705234	620		0.10375494	1180		0.05669004	1740
0.2458273	625		0.10278947	1185		0.05640936	1745
0.24459513	630		0.10183521	1190		0.05611621	1750
0.24335596	635		0.10089223	1195		0.05580997	1755

Characteristic curve Zeolite NaMSX:

$$W_{ad} = a \cdot A^5 + b \cdot A^4 + c \cdot A^3 + d \cdot A^2 + e \cdot A + f$$

with: $a = -1{,}43 \cdot 10^{-16}$ $b = 6{,}24 \cdot 10^{-13}$ $c = -8{,}32 \cdot 10^{-10}$

$d = 3{,}04 \cdot 10^{-7}$ $e = -1{,}51 \cdot 10^{-4}$ $f = 3{,}43 \cdot 10^{-1}$

valid range: $83 < A_{Dub} < 1760$ [J/g], $R^2 = 0{,}997$

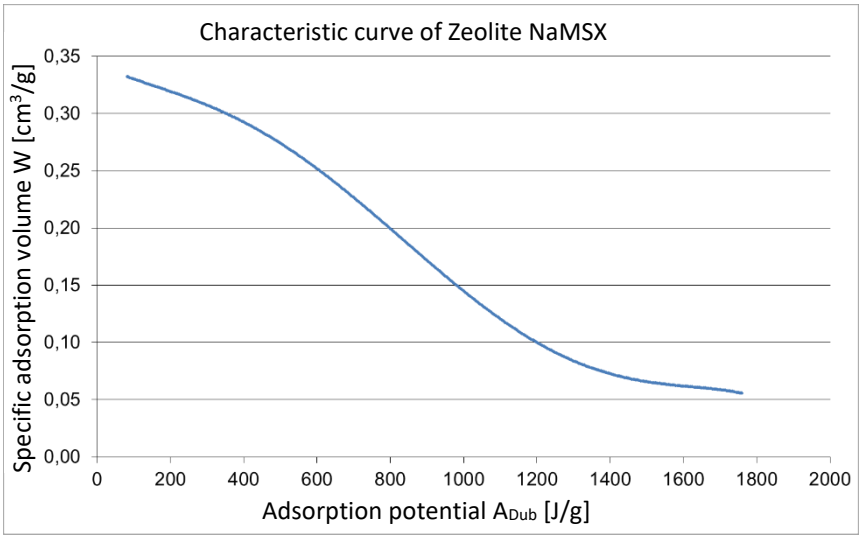

Figure 9.1: Characteristic curve of Zeolite NaMSX

Differential Adsorption enthalpy Zeolite NaMSX:

$$\Delta h_{ad} = a \cdot \Theta^4 + b \cdot \Theta^3 + c \cdot \Theta^2 + d \cdot \Theta + \mathrm{e}$$

with: a = 169086 b = -270581 c = 115005

d = -22116 e = 4973,9

valid range: $0{,}078 < \Theta < 0{,}36$ [kJ/kg]; $R^2 = 1$

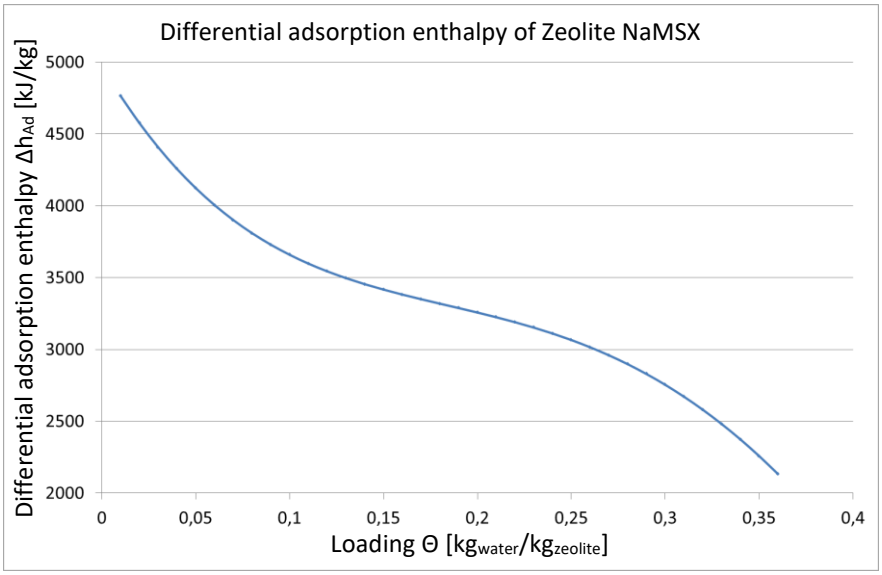

Figure 9.2: Differential Adsorption enthalpy as a function of Zeolite NaMSX loading

Equipment of the test set-up

a. Reactor

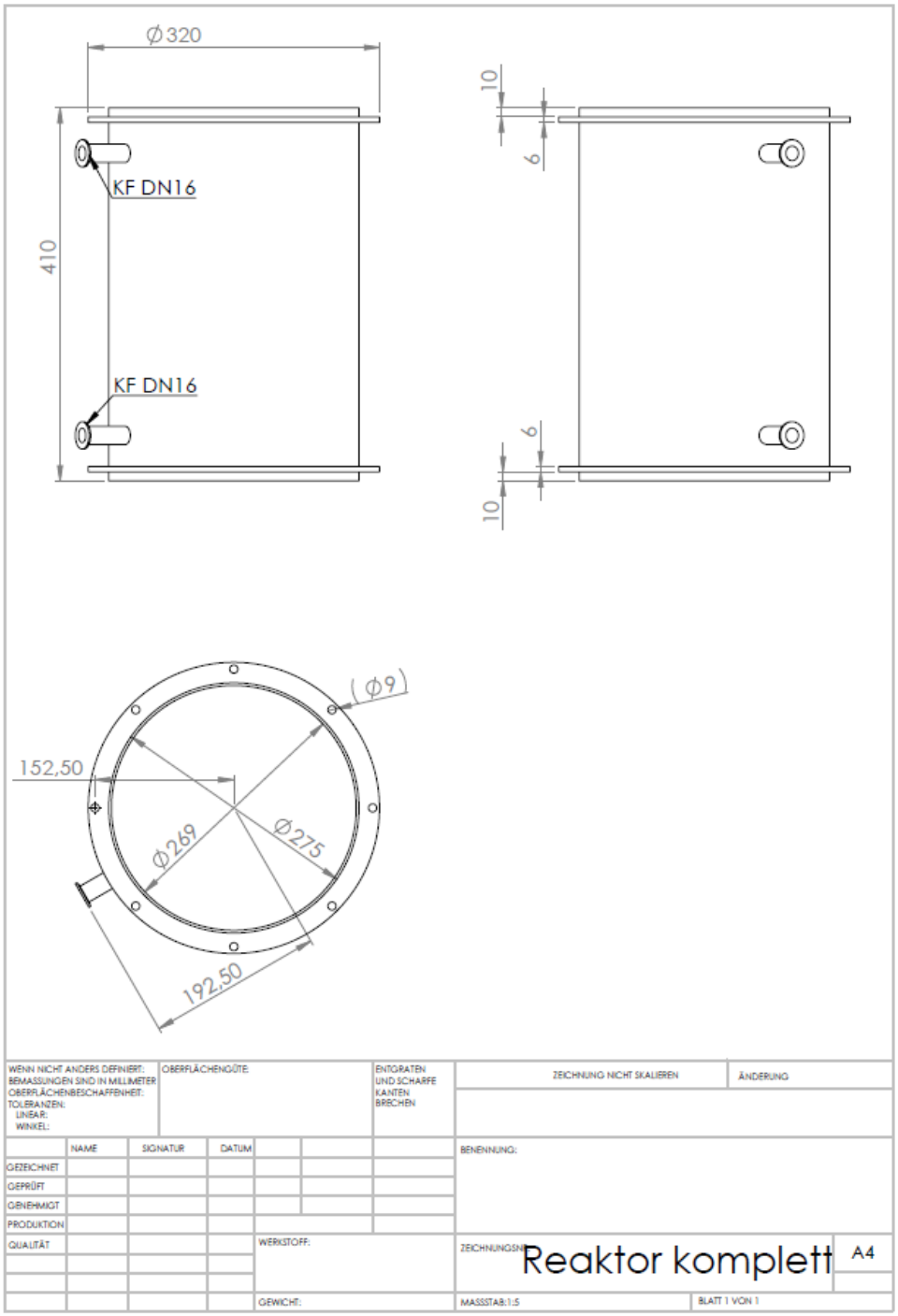

b. Heat exchanger inside reactor

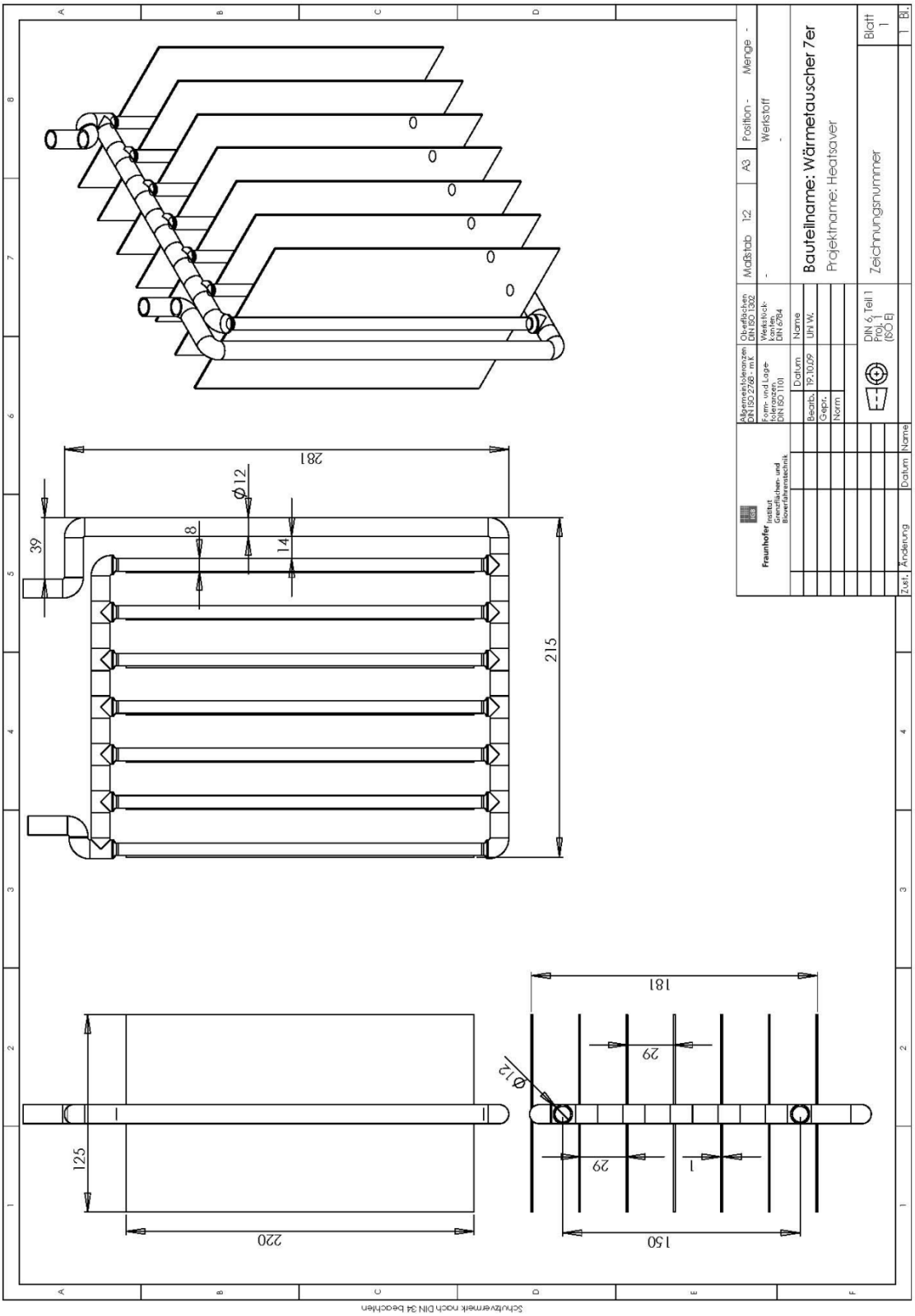

c. Location of temperature sensors inside packed bed

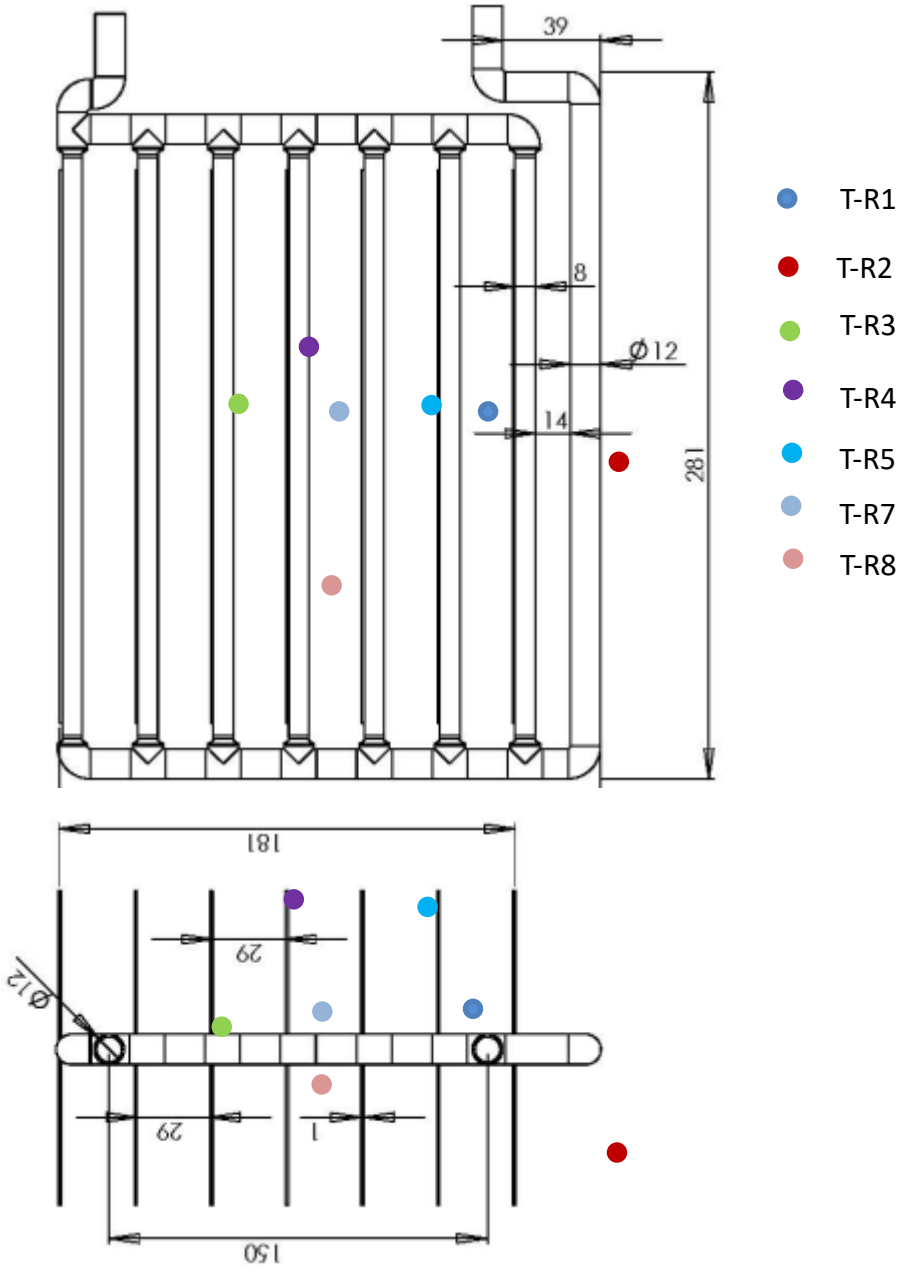

d. Overhead condenser

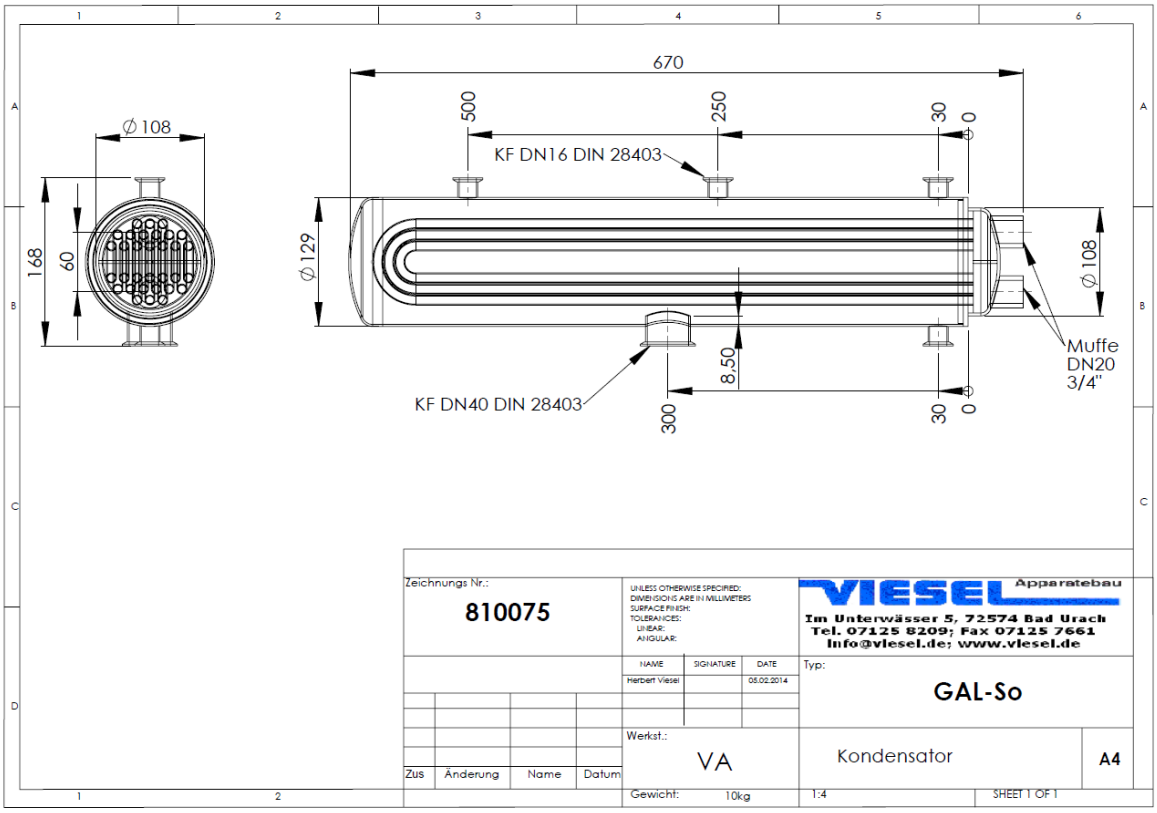

Datasheet					
Heat duty	kW	2			
Heat transfer coefficient	W/(m²·°K)	519,3			
LMTD	°K	5,87			
Heat transfer area	m²	0,8			
		Shell side		**Tube side**	
Flow rate	kg/h	3		719	
Vapor (in/out)	kg/h	3	-		
Liquid (in/out)	kg/h	-	3		
Temperature (in/out)	°C	27,30	27,1	20	22,4
Density	kg/m³	997,2		998	
Viscosity	mPa·s	0,848		0,9727	
Specific heat capacity	J/(kg·K)	4179,6		4183,8	
Thermal conductivity	W/(m·K)	0,6107		0,6015	
Latent heat	J/kg	2436600			
Inlet pressure	bar	0,04		2	
Velocity	m/s	5,89		0,2	
Length	mm	700		600	
Inner diameter	mm	104		-	
Outer diameter	mm	108		10	
Perimeter	mm	-		12,8	
Number	mm	1		40	

e. Evaporator

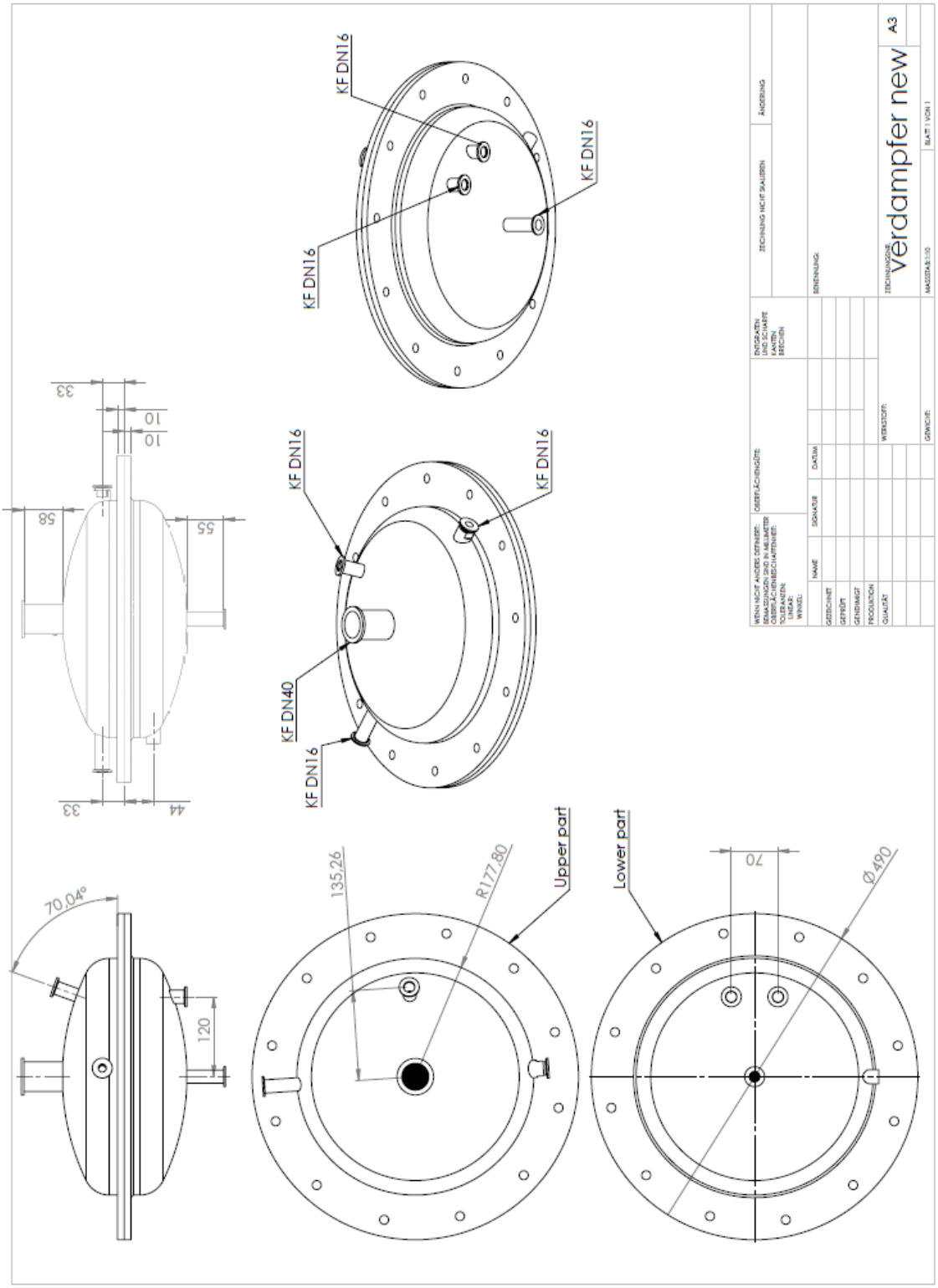

f. Heat exchanger inside evaporator

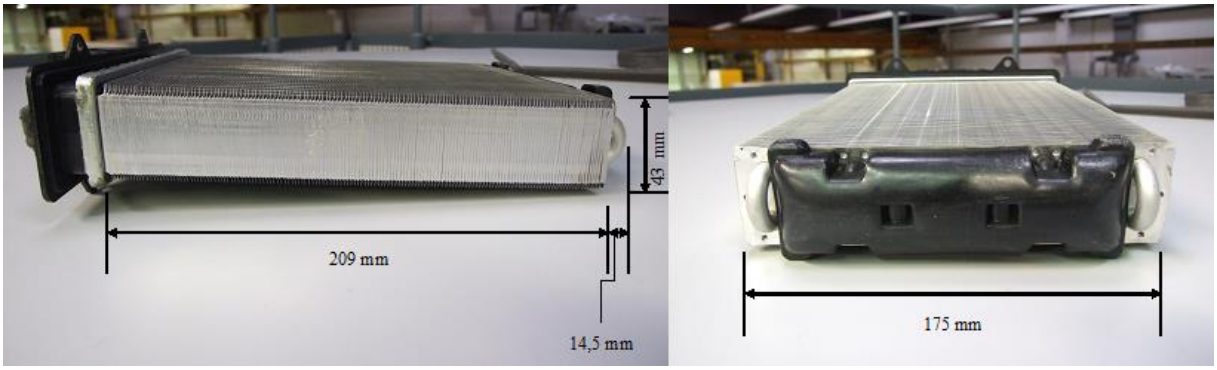

Heat duty max	kW	2
Fins		
Total number	-	151
Length	mm	175
height	mm	43
Width	mm	0.21
Distamce between fins	mm	1.3
Tubes		
Total number	-	9
Outer diameter	mm	8.3

g. Condensate tank

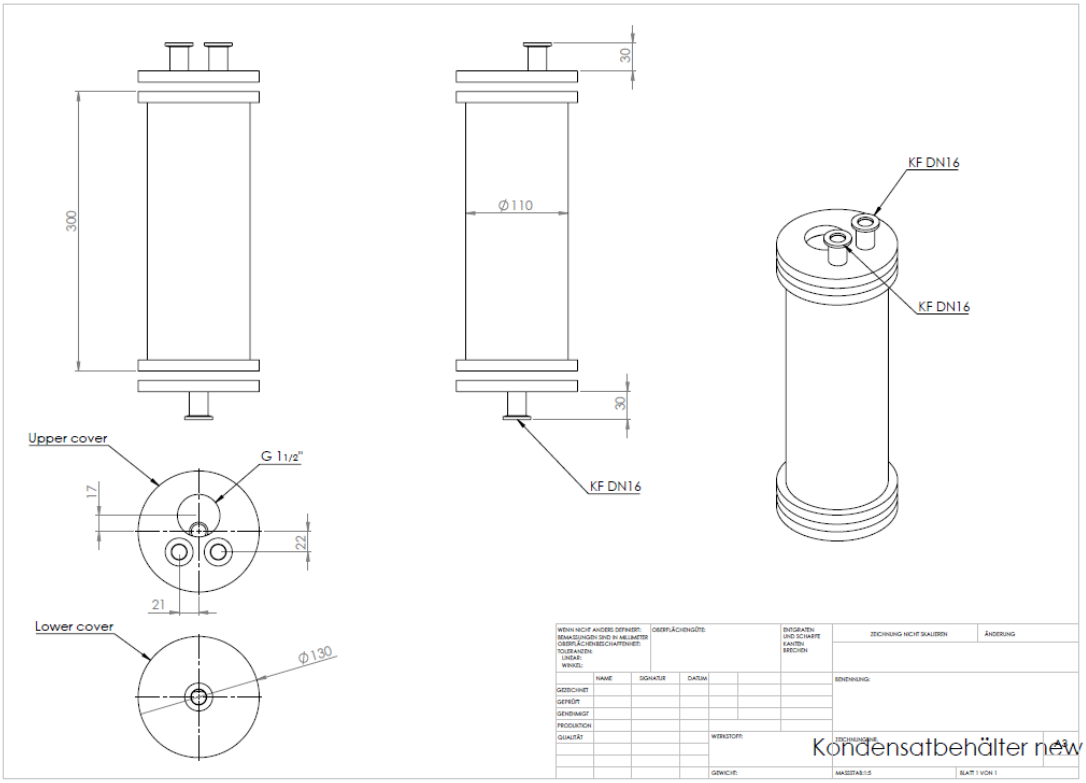

h. Water tank

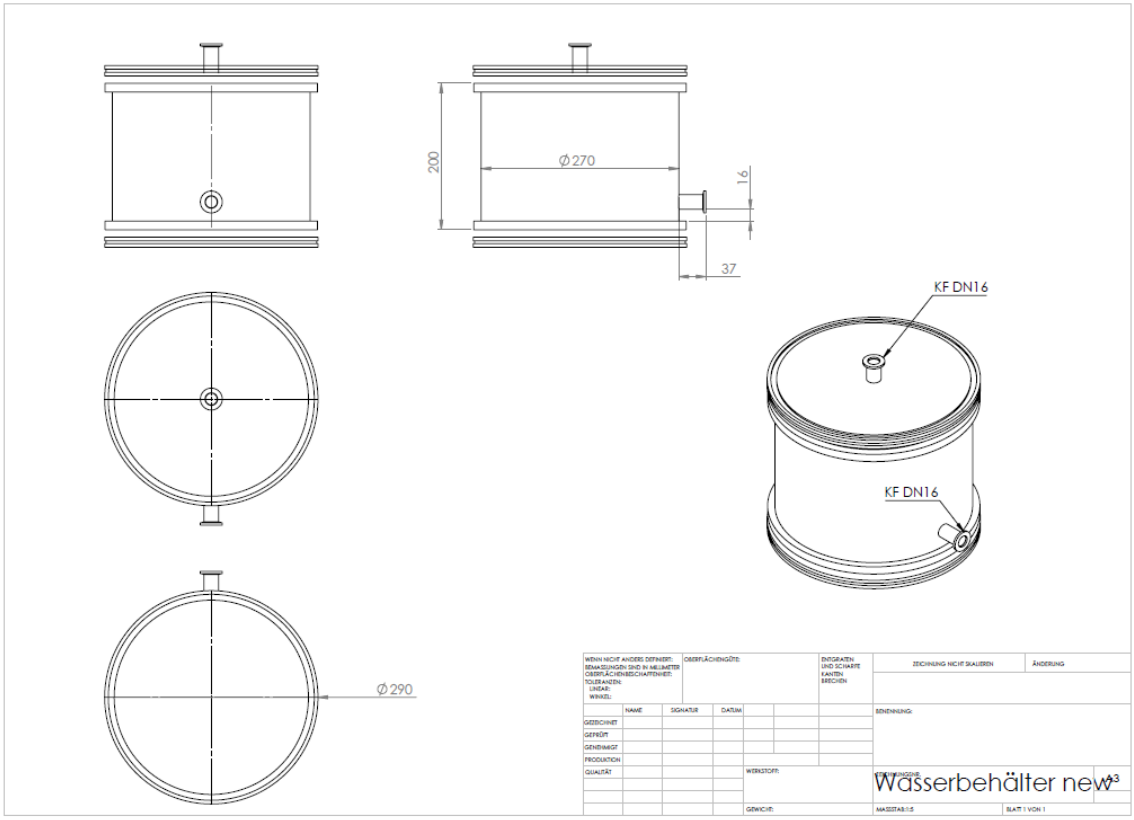

i. Heat exchanger (new design)